Politecnico di Bari

LIBERATORIA PER L'ARCHIVIAZIONE DELLA TESI DI DOTTORATO

Al Magnifico Rettore
del Politecnico di Bari

Il sottoscritto **IRIO DE FEUDIS** nato a **CANOSA DI PUGLIA** il **18/09/1990**

residente a **BISCEGLIE (BT)** in via **MOLFETTA, 2** e-mail **irio.defeudis@gmail.com**

iscritto al 3° anno di Corso di Dottorato di Ricerca in **Ingegneria Elettrica e dell'Informazione** ciclo **XXXIV**

ed essendo stato ammesso a sostenere l'esame finale con la prevista discussione della tesi dal titolo:

ENABLING TECHNOLOGIES FOR HUMAN-CENTERED INDUSTRY 4.0 AND HEALTHCARE 4.0

DICHIARA

1) di essere consapevole che, ai sensi del D.P.R. n. 445 del 28.12.2000, le dichiarazioni mendaci, la falsità negli atti e l'uso di atti falsi sono puniti ai sensi del codice penale e delle Leggi speciali in materia, e che nel caso ricorressero dette ipotesi, decade fin dall'inizio e senza necessità di nessuna formalità dai benefici conseguenti al provvedimento emanato sulla base di tali dichiarazioni;
2) di essere iscritto al Corso di Dottorato di ricerca **Ingegneria Elettrica e dell'Informazione** ciclo **XXXIV**, corso attivato ai sensi del "*Regolamento dei Corsi di Dottorato di ricerca del Politecnico di Bari"*, emanato con D.R. n.286 del 01.07.2013;
3) di essere pienamente a conoscenza delle disposizioni contenute nel predetto Regolamento in merito alla procedura di deposito, pubblicazione e autoarchiviazione della tesi di dottorato nell'Archivio Istituzionale ad accesso aperto alla letteratura scientifica;
4) di essere consapevole che attraverso l'autoarchiviazione delle tesi nell'Archivio Istituzionale ad accesso aperto alla letteratura scientifica del Politecnico di Bari (IRIS-POLIBA), l'Ateneo archivierà e renderà consultabile in rete (nel rispetto della Policy di Ateneo di cui al D.R. 642 del 13.11.2015) il testo completo della tesi di dottorato, fatta salva la possibilità di sottoscrizione di apposite licenze per le relative condizioni di utilizzo (di cui al sito http://www.creativecommons.it/Licenze), e fatte salve, altresì, le eventuali esigenze di "embargo", legate a strette considerazioni sulla tutelabilità e sfruttamento industriale/commerciale dei contenuti della tesi, da rappresentarsi mediante compilazione e sottoscrizione del modulo in calce (Richiesta di embargo);
5) che la tesi da depositare in IRIS-POLIBA, in formato digitale (PDF/A) sarà del tutto identica a quelle **consegnate**/inviate/da inviarsi ai componenti della commissione per l'esame finale e a qualsiasi altra copia depositata presso gli Uffici del Politecnico di Bari in forma cartacea o digitale, ovvero a quella da discutere in sede di esame finale, a quella da depositare, a cura dell'Ateneo, presso le Biblioteche Nazionali Centrali di Roma e Firenze e presso tutti gli Uffici competenti per legge al momento del deposito stesso, e che di conseguenza va esclusa qualsiasi responsabilità del Politecnico di Bari per quanto riguarda eventuali errori, imprecisioni o omissioni nei contenuti della tesi;
6) che il contenuto e l'organizzazione della tesi è opera originale realizzata dal sottoscritto e non compromette in alcun modo i diritti di terzi, ivi compresi quelli relativi alla sicurezza dei dati personali; che pertanto il Politecnico di Bari ed i suoi funzionari sono in ogni caso esenti da responsabilità di qualsivoglia natura: civile, amministrativa e penale e saranno dal sottoscritto tenuti indenni da qualsiasi richiesta o rivendicazione da parte di terzi;
7) che il contenuto della tesi non infrange in alcun modo il diritto d'Autore né gli obblighi connessi alla salvaguardia di diritti morali od economici di altri autori o di altri aventi diritto, sia per testi, immagini, foto, tabelle, o altre parti di cui la tesi è composta.

Luogo e data **21/07/2022** Firma 

Il/La sottoscritto, con l'autoarchiviazione della propria tesi di dottorato nell'Archivio Istituzionale ad accesso aperto del Politecnico di Bari (POLIBA-IRIS), pur mantenendo su di essa tutti i diritti d'autore, morali ed economici, ai sensi della normativa vigente (Legge 633/1941 e ss.mm.ii.),

CONCEDE

- al Politecnico di Bari il permesso di trasferire l'opera su qualsiasi supporto e di convertirla in qualsiasi formato al fine di una corretta conservazione nel tempo. Il Politecnico di Bari garantisce che non verrà effettuata alcuna modifica al contenuto e alla struttura dell'opera.
- al Politecnico di Bari la possibilità di riprodurre l'opera in più di una copia per fini di sicurezza, back-up e conservazione.

Luogo e data **21/07/2022** Firma 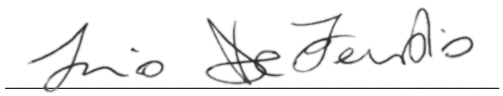

Department of Electrical and Information Engineering
ELECTRICAL AND INFORMATION ENGINEERING
Ph.D. Program

SSD: ING-INF/06 - ELECTRONIC AND INFORMATION BIOENGINEERING

Final Dissertation

Enabling technologies for Human-centered Industry 4.0 and Healthcare 4.0

---

by

Irio De Feudis

Supervisor:
Prof. Vitoantonio Bevilacqua, Ph.D.

Coordinator of Ph.D. Program:
Prof. Mario Carpentieri, Ph.D.

Course n°34, 01/11/2018 - 30/04/2022

Department of Electrical and Information Engineering
ELECTRICAL AND INFORMATION ENGINEERING
Ph.D. Program

SSD: ING-INF/06 - ELECTRONIC AND INFORMATION BIOENGINEERING

Final Dissertation

Enabling technologies for Human-centered Industry 4.0 and Healthcare 4.0

---

by

Irio De Feudis

Referees:
Prof. Leandro Pecchia, Ph.D.
Prof. Eros Pasero, Ph.D.

Supervisor:
Prof. Vitoantonio Bevilacqua, Ph.D.

Coordinator of Ph.D. Program:
Prof. Mario Carpentieri, Ph.D.

Course n°34, 01/11/2018 - 30/04/2022

Abstract

Industry 4.0 has transformed manufacturing industry into a new paradigm causing numerous changes in the models of business and process automation. The profound change in the context production has brought the issue of efficiency. Some of the key technologies emerged to tackle this issue are Big Data, Internet of Things (IoT), Digital Twins, Artificial Intelligence, Machine Learning, Augmented Reality and Additive Manufacturing.

This revolution has not remained in the borders of manufacturing field but it pushes changes in a lot of fields; in particular, it has introduced health care delivery to the dawn of a foundational change into the new era of smart and connected health care, referred to as Healthcare 4.0.

Although automation and assistance technologies are becoming more prevalent in production and logistics, there is consensus that humans remain an essential part of operations systems bringing to the definition of Human-centered Industry 4.0. Nevertheless, human factors are still underrepresented in the research stream resulting in an important research and application gap.

This Ph.D. thesis proposes a set of innovative work-flows for real systems based on enabling technologies of Industry 4.0 and Healtcare 4.0 that can enhance and complement the human in manufacturing and healthcare. The work is trying to fill a portion of the gap between research and application concerning the Human factor in Industry 4.0 and propose new solutions that increase efficacy, flexibility and cost-effectiveness of healthcare services focusing especially on movement disorders rehabilitation.

This thesis is composed by four chapters. The first Chapter provides an introduction about the reference context. Chapter 2 describes the state of the art of Industry 4.0, its challenges and technologies with a focus on the Human factor and reports the contribution about the usage of Industry 4.0 enabling technologies to provide new solutions for maintenance training, process quality assessment and bio-mechanical risks detection. Chapter 3 introduces the Healthcare 4.0 going into details of new rehabilitation protocols for movement disorders; it shows a work for signal processing, focusing on the application of undercomplete autoencoders for surface electromyography analysis and evaluation of cueing technique efficacy for Parkinson

Disease rehabilitation. The study cases and the contributions reported in this thesis were always compared with standard techniques. Finally, the conclusions about the research works and future research proposes.

Contents

List of Figures

List of Tables

Chapter 1

Introduction

1.1 Objective and Research Question

The World Economic Forum said the first Industrial Revolution used water and steam power to mechanize production, the second one created electrical mass production, and the third used electronics and IT to automate production systems. The fourth Industrial Revolution blurred the lines among the physical, digital, and biological spheres. This latest industrial revolution gave birth to Industry 4.0 and the next-generation of smart factory, in which autonomous systems internet-connected are completely digitalized to produce data-driven personalized products.

Industry 4.0 is causing numerous changes in the models of business and process automation. The profound change in the context production has brought the issue of efficiency. Some of the key technologies emerged to tackle this this issue are Big Data, Internet of Things (IoT), Digital Twins, Artificial Intelligence, Machine Learning, Augmented Reality and Additive Manufacturing.

Although automation and assistance technologies are becoming more prevalent in production and logistics, there is consensus that humans remain an essential part of operations systems bringing to the definition of Human-centered Industry 4.0. Nevertheless, human factors are still underrepresented in the research stream resulting in an important research and application gap[1]. As stated in this European Commission report [2],the real Human-centered industry is still not born and closing the gap will converge in the next industrial revolution Industry 5.0. It is required a strong contribution in research field to make Industry 4.0 enabling technologies not only powerful tools for production but also strong assistant to support, enhance and take care of the Human component.

Industry 4.0 has transformed manufacturing industry into a new paradigm and in similar way has introduced health care delivery to the dawn of a foundational change into the new era of smart and connected health care, referred to as Healthcare 4.0 [3].

A wide range of possibilities for using Industry 4.0 technologies to improve healthcare as it lays out a new and innovative vision for the health sector. The objective is to provide patients with better, more value-added, and more cost-effective healthcare services while also improving the industry's efficacy and efficiency. We can speculate that Healthcare is one of the most anticipated areas in the 4.0 revolution to achieve great results. Today's industry is more computerised than in previous decades, with x-rays and magnetic resonance imaging giving way to computed tomography and ultrasound scans, as well as electronic medical data. As Healthcare 4.0 enhances the healthcare experience, it successfully improves the quality, flexibility, productivity, cost-effectiveness, and dependability of healthcare services. The Internet of Health Things, medical Cyber-Physical Systems, health cloud, health fog, big data analytics, machine learning, and smart algorithms are all integrated and used for providing innovative services that include remote medical assistance, automated medical production, healthcare robotics, intelligent diagnosis systems and new rehabilitative protocols based on human–robot symbiosis. There are some limitations, however, to keep in mind. Building and using healthcare software that matches the Health 4.0 paradigm is doable, but a difficult and time-consuming task and often requires niche specialists.

1.2 Contribution

The aim of this work thesis is to propose a set of innovative work-flows for real systems based on enabling technologies of Industry 4.0 that can assist the human in manufacturing and healthcare. The basic idea is giving a contribution to fill the gap between research and application concerning the Human factor in Industry 4.0. The first part of the thesis focuses on the usage of low-cost devices and enabling technologies like AR/VR, gesture detection and Deep learning for biomechanical risks evaluation, process quality assessment and maintenance training. At the end my activity during the visiting period of 6 months I spent at Toyota Motor Europe Technical Centre in Bruxelles is presented. During this period as Digitalization Engineer, I was involved in different projects about digital transformation of vehicle production processes and I was the responsible of a proof-of-concept concerning maintenance training digitalization. The second part of this thesis focuses on machine learning and deep learning for physiological and kinematic signals processing; a particular neural model for surface electromyography analysis has been proposed for the evaluation

of complex muscle activation patterns, useful in the rehabilitation field. At the end a study about the efficacy of cueing technique for Parkinsonians rehabilitation have been presented.

The developed solutions were compared with literature standards and, if possible, a personalized pipeline has been proposed and customised to face each challenge.

1.3 Part Outline

This thesis is composed by four chapters. The first and current Chapter 1 provides an introduction about the reference context. The following Chapter 2 describes the state of the art of Industry 4.0, its challenges and technologies with a focus on the Human factor and reports the contribution about the usage of Industry 4.0 enabling technologies to provide new solutions for maintenance training, process quality assessment and bio-mechanical risks detection. Chapter 3 introduces the Healthcare 4.0 going into details of new rehabilitation protocols for movement disorders; it shows a work for signal processing, focusing on the application of undercomplete autoencoders for surface electromyography analysis and evaluation of cueing technique efficacy for Parkinson Disease rehabilitation. The study cases and the contributions reported in this thesis were always compared with standard techniques. Finally, the conclusions about the research works and future research proposes.

Chapter 2

Enabling technologies for Industry 4.0

2.1 State of the Art

This chapter describes the background and literature of Industry 4.0 challenges and enabling technologies focusing on the human factors.

2.1.1 Introduction

Industry 4.0, also known as 'The Fourth Industrial Revolution', affects entire industries by transforming the way goods are designed, manufactured, delivered and paid. Due to the techniques and technologies introduced by this revolution, the manufacturing industry is not the only industry enduring this transformation; the service industry is changing the way services are designed and provided. The fourth industrial revolution, different from the previous industrial revolutions, was predicted a priori and not ex-post [4]. This a priori prediction allows companies and research institutes to actively shape the future. In 2011, Germany was the first to introduce an initiative, called Industrie 4.0, as part of its high-tech strategy to establish the idea of a fully-integrated industry [5]. In contrast, Italy waited until 2015 to present a national plan for Industry 4.0.

The main factor causing the fourth revolution is the rapid technological progress that introduces a range of new business potentials and opportunities: Internet of Things (IoT), Internet of Services (IoS), cyber-physical systems (CPS) and smart factories are becoming more relevant and changing the existing approaches of value or service creation. In particular, in [6] the authors explain the IoT and IoS in the manufacturing processes causing the fourth industrial revolution. While the IoT allows objects (e.g., sensors, actuators, mobile phones, wearable devices) and 'things' (i.e., interactions and collaboration with people) to reach the

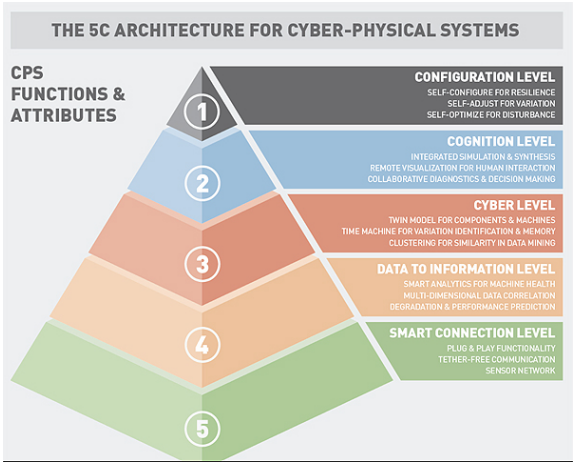

Figure 2.1 The 5C architecture for Cyber-Physical Systems.

common goal, the IoS enables companies that provide services to offer their products via the internet. Another critical component of Industry 4.0 is the CPS. The system allows the physical world to fuse with the virtual world (made of thinking objects or intelligent services) and humans who interact both with the physical and virtual world. In [7] the authors propose a five-level CPS structure, the 5C architecture, which provides a step-by-step guideline for developing and deploying a CPS for manufacturing applications.

As presented in Figure 2.1, the architecture proposed consists of the following:

- **Smart connection layer** (condition-based monitoring): represents the first step for developing a CPS and concerns the accurate and reliable processes for acquiring data from machines, humans and resources (the players of a complex industrial environment);
- **Data-to-information conversion level** (prognostics and health management): concerns the second level of a CPS architecture that creates smart machines using data acquired from the previous level and by applying inferred algorithms to evaluate the machines' health value;
- **Cyber level** (cyber-physical system, self-compare): this level uses the information from every connected machine to form the machine network and to perform specific analytics used to extract additional information that provides better insight over the status of each machine. Therefore, the cyber level is useful to predict the future behaviour of the machinery;
- **Cognition level** (decision support system): displays the correct information derived from previous levels to expert users. Proper presentation of the acquired knowledge to expert users supports correct decisions;

- **Configuration level** (resilient control system): the feedback from cyberspace to physical space. This level acts as a general control to make a machine self-configure and self-adapt.

Finally, the smart factory is the main feature of Industry 4.0. As the authors [8] explain, in a smart factory, people and machines interact to execute a task due to a system working in the background that can consider context information, like the position and status of objects. A system should support people and machines obtaining information both from the physical world (e.g., position of an object) and the virtual world (e.g., simulation model, electronic documents) to be context-aware. Therefore, considering the definitions of CPS, IoT and IoS, the smart factory, as a complex workplace in which humans and machines interact to reach goals, can be defined as a factory in which CPS and IoT and IoS systems communicate to efficiently and effectively support people and machines in the execution of their tasks. Without a clear definition of Industry 4.0, companies face several difficulties when trying to develop ideas or take actions. Therefore, with regard to the previous considerations, Industry 4.0 could be defined as a set of technologies, techniques and concepts of a value chain organisation. In a modular smart factory of Industry 4.0, a CPS monitors physical processes, creates virtual copies of a physical world and makes decisions in cooperation with people and machines in real time over the IoT system. Via the IoS system, both internal and decentralised services could be offered and utilised both by people and machines. Therefore, to support companies and academic researchers in identifying possible Industry 4.0 pilots, in [4], the authors try to derive six design principles from the Industry 4.0 components (**??**).

Interoperability In Industry 4.0, companies rather than in an intelligent workplace in which people and machines interact with a CPS able to manage thinking object use, also, IoS services the interoperability plays a crucial role. Each module of a smart factory should operate with the others to assist people and machines during their work. **Virtualisation** Using sensors data from the IoT infrastructure, with the virtualisation, the CPS creates a virtual copy of the physical world to manage the cooperation between people and machines. **Decentralisation** The central control of several systems that communicate and interact with each other is replaced, in an Industry 4.0 context, with decentralised control. The decentralisation principle allows a smart factory to train CPS to make correct decisions considering all the features coming from the modules of the entire systems. However, to avoid uncontrollable situations, the systems able to make decisions on their own must be designed to support people in their work and not replace them. This aspect is crucial in the healthcare field. For example, in a context in which a CPS can make decisions based on a patient's vital parameters, it is necessary to design and implement an alert system to

Table 2.1 Principles of Industry 4.0 components

	Cyber-Physical Systems	Internet of Things	Internet of Services	Smart Factory
Interoperability	**O**	**O**	**O**	**O**
Virtualisation	**O**			**O**
Decentralisation	**O**			**O**
Real-Time Capability				**O**
Service Orientation			**O**	
Modularity			**O**	

notice an expert domain decision. **Real-Time Capability** For the forth competent, real-time capability, an intelligent system is defined as a system able to analyse, in real-time, considerable information from several sources. It is important to avoid delays in crucial decisions that could compromise the efficiency and efficacy of the entire process. **Service Orientation** Service Orientation allows the entire smart factory to be a workplace in which each module is connected and interacts with the others; only an IoS system could be utilised. Since modules are often not internally reachable, the IoS system must offer the services both internally and across company borders. **Modularity** A factory could be defined as smart if it is flexible and adapts itself to change requirements. A modular system is the only way to reach the goal. Therefore, only a smart factory, consisting of several modules, could adjust itself to improve product characteristics, for example.

Overall, the following are the abilities with which an Industry 4.0 scenario must be provided:

- the ability of machines, devices, sensors and humans to interact with each other via IoT and IoS;
- the ability of the CPS to create a virtual copy of the physical world via an aggregation of raw sensor data or higher-value context information;
- the ability of support systems to help people by aggregating and visualizing information for making informed decisions and solving urgent problems;
- the ability of CPS to support people by conducting a range of tasks;
- the ability of CPS to make a decision on its own and to perform its tasks as autonomously as possible.

2.1.2 Challenges

As described in the previous paragraph, the core of the Industry 4.0 strategy is based on intelligent manufacturing or, in general, on intelligent systems using CPS technology to decentralize production, to personalize products or services and to increase people's participation. In this way, each part of the system (people and machines) can interact to efficiently and effectively create products and services. In [9] the Germany strategic plan to implement Industry 4.0 is described. In particular, are highlighted the main points of this plan. **Building a network** The core of the foundation of Industry 4.0 is the CPS. This system implements the connection between thinking objects and incorporates several functions, such as computing, communications, precision control, interaction, coordination and autonomy. The CPS can implement these functions only by creating a virtual copy of the physical world.

Researching two major topics The first topic is the smart factory, which is key to future intelligent infrastructure. The smart factory is focused on intelligent systems and processes and the implementation of networked distributed production facilities. However, the intelligent production is focused on human-computer interaction and advanced technologies. The main goal of the intelligent production is the use of innovative techniques and technologies, which can be applied to a process to create a highly flexible, personalized and networked industrial chain. In general, not just the human-computer interactions can be applied; thing-tothing interactions are also necessary to create better services to meet customers' needs. Therefore, the common concept between smart factory and intelligent production is the combination of smart devices with information communication technology (ICT).

Realization of three integration Horizontal integration aims to achieve the cooperation between enterprises for providing real-time products and services. Horizontal integration is possible by applying integration between a resource and an information network. Vertical integration refers to a network of intelligent factories to update the traditionally fixed production processes, such as assembly-line production. Finally, end-to-end integration refers to the design and the implementation of the interconnected CPSs, each of which is implemented at a terminal and has a digital value chain that communicates and interacts with other CPS terminals. In general, a terminal can be a man, a machine, or a service. These interconnections allow the entire system to achieve complete horizontal, vertical and end-to-end integration.

Against these backdrops, the challenges of Industry 4.0 can be summarized in eight planning objectives:

1. System standardization and implementation of a reference architecture: a set of standards needs to be designed and developed to create a network between different infrastructures and companies that must be connected and integrated;

2. Efficient management: with the introduction of large and complex systems, appropriate plans need to be made and an efficient model needs to be designed and developed to optimize the management;

3. Implementation of a broadband infrastructure to enforce strict criteria on communications networks that must be reliable, comprehensive and high quality;

4. Safety and security: the interactions between people and machines in these new scenarios have not posed a threat to people and the environment; on the contrary, the introduction of intelligent systems needs to be designed and implemented for the improvement of working conditions regarding safety, health and security;

5. Organization and design of work to achieve humane, automated, green production and management;

6. Staff training and continuing professional development: with the introduction of these technologies, staff training and continuing professional development need to be fast and accurate. For example, new technologies such as virtual reality could be useful for training operators in a virtual safe place;

7. Establishing a regulatory framework: the introduction of the new technologies introduces new issues, such as in enterprise data, liability, personal data and trade restrictions. Therefore, appropriate means of control need to be actuated;

8. Improving the efficiency of resource use while reducing and balancing resource utilization on the environment caused by pollution and destruction.

The interaction between people and machines must be implemented in every step of the production process assuming that, in the future, the individual worker will have more responsibility and a larger operating area. Therefore, the role of the worker will be to creatively solve issues and problems inside the CPS [10]. **??** provides a representation of the interaction between human and intelligent system in a typical production process.

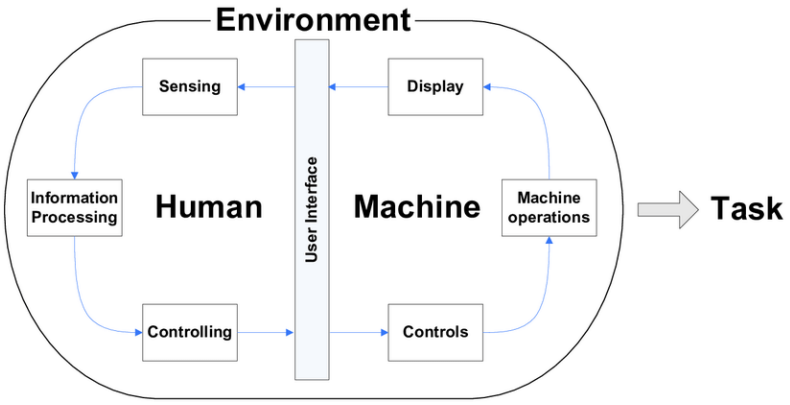

Figure 2.2 Human machine interaction representation of a production process.

2.1.3 Enabling Technologies

There is yet no consensus as to whether we are observing the onset of a Fourth Industrial Revolution and whether this coincides with the Industry 4.0 paradigm. They are not synonyms. Industry 4.0 is the qualification of the "factory of the future", shaped by policy interventions that have fostered the adoption of smart manufacturing technologies in Europe, and resulting from the convergence of a new wave of operational technologies with Internetdriven IT (Kagermann et al., 2013). This might be a fundamental component of a Fourth Industrial Revolution, but does not coincide with it because of its still relatively limited scale and scope. A similar difference exists, as Teece (2018) points out, between the notions of general purpose technology vis-a'-vis enabling technology. Contrary to the concepts of technological paradigm (Dosi, 1982, 1988) and general purpose technology (Helpman, 1998), the concept of "enabling technology" has not been well defined in the academic literature because it has emerged in the policy arena to profile groups of technologies that can contribute to innovation and productivity growth in many sectors of the economy (Commission of the European Communities, 2009), and are therefore identified primarily as industrial policy targets (European Commission, 2017). Technologies are defined as "enabling" when they bear high transformative potential for the productive system in which they are deployed for a variety of uses (Teece, 2018). Paradigm changes and GPTs are much rarer than enabling technologies, but some enabling technologies can become GPTs and trigger paradigmatic change over time. This may happen, but has arguably not yet happened, with the diffusion, convergence and recombination of Industry 4.0 technologies associated with increased digitization, automation and interconnection. This article provides an in-depth examination of the enabling technologies underpinning the "factory of the future" as profiled by the Industry 4.0 paradigm. It contains an exploratory comparative analysis of the technological

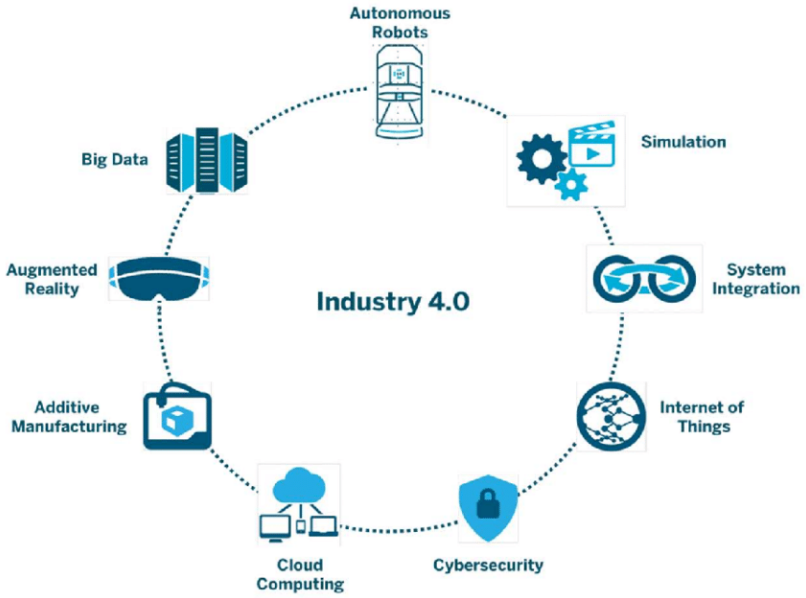

Figure 2.3 Enabling technologies of Industry 4.0.

bases and the emergent patterns of production and use of Internet of Things (IoT), big data, cloud, robotics, artificial intelligence and additive manufacturing.

Industry 4.0 is not a single technology but rather a cluster of different technologies that are de facto agglomerated together by technological leaders, pivotal users, system integrators and government policy makers. **??** synthetizes the concept by illustrating the core technologies of Industry 4.0, with cloud manufacturing connecting industry devices through sensors and digital twins, and manufacturing execution systems (MES) keeping control of the whole factory streams through manufacturing analytics. It is clearly a complex architecture characterized by old technologies paired with new ones, all interconnected by cloud-based Internet.

In more detail, the most interesting technologies are:

Additive Manufacturing Additive manufacturing is a technique introduced in recent years and applied as a production technology [11–14]. Also known as rapid prototyping, additive manufacturing is used in several applications and business models for direct part production. The application fields are the aerospace industry [15], the medical industry [16], and the engineering industry [17**?** , 18]. The Industry 4.0 paradigm introduces the customisation of products and real-time monitoring of engineering systems to gain lifecycle data. Intelligent systems, such as sensors and actuators connected to build a system to support humans in several tasks, are key enablers for smart control of an industrial value chain. Therefore, additive manufacturing contributes to the success of the application of

Industry 4.0 principles through its layer-by-layer fabrication methodology for enabling the production of smart structures. The integration of sensors and actuators through additive manufacturing suggests a great potential to improve process performances in many fields of application for many products. For example, to satisfy the requirements for the centralisation of the patient in the medical field, it is possible to create biomechanical devices for a specific patient's anatomy. These devices would be equipped with several sensors connected in a body area network [19–22]. Furthermore, additive manufacturing has applications in the machine tool industry to predict maintenance [23] and in metal forming tools to monitor the process temperature and wear [23].

Mixed, Augmented and Virtual Reality Among the enabling technologies used to implement an Industry 4.0 scenario in several application fields, augmented reality (AR) and, in particular, mixed reality (MR) have proven to be suitable tools in recent years [24–32]. The main goal of systems that use these technologies is to enable workers to collaborate, to interact with information collected and interpreted using an intelligent system or decision support system and to monitor and control part of or an entire physical system.

The advantage of AR over virtual reality (VR) is that the worker or the operator perceives the instructions without needing to change from a real context to a virtual one. The main application concerns the support of workers in maintenance, repair, and control tasks through instructions with textual, visual or auditory information. However, in conjunction with the introduction of the Industry 4.0 paradigm, the set of application fields had increased and is clearly of great interest in the medical field [33–39]. The benefit of using this technology is both in remote and in local assistance. Companies that have machines installed in remote locations need to monitor, operate and repair those machines with the minimum number of people on-site. Therefore, AR or MR can help by allowing collaboration between workers in different places [40**?** –42]. Likewise, these technologies could help support workers in the decision machining in real scenario, combining their experience with information extracted in real time from databases and overlapping opportunely in the real world.

The last described scenario concerns the quick access to documentation, like manuals, drawings or 3D models, both for training an operator by giving step-by-step instructions to develop specific tasks [43–46] and for reducing the time and effort dedicated to manually checking the well-trained operators [42]. Most of the AR solutions in literature employ head mounted displays (HMDs), which have several drawbacks, including ergonomics, cost, limited field of view, low resolution, encumbrance and weight. The use of spatial (or projected) augmented reality systems (SAR) is the key to solving this issue.

SAR is based on digital projectors that superimpose virtual data (e.g., text, symbols, indicators) directly onto the real environment [47]. However, projected AR, like all new technologies, requires feasibility studies and optimisation processes before it can be introduced into the industrial environment. One of the most important issues is the correct visualisation of technical information. In particular, in [25] the authors evaluated the possibility to project text directly onto workbench surfaces (without the need to calibrate the scene), comparing users' performance with that of a normal LCD monitor [48] because, in a real working environment, the operator stands in front of the workbench and is currently assisted by instructions on monitors usually placed on their workbenches or tool carts.

The design of an AR-based system should include the following aspects [49]:

- The final application must provide added-value services;
- Functional discontinuities in the operating modes should be avoided;
- Cognitive discontinuities between the old and the new operating practice must be reduced;
- If the operator wears an HMD or similar technology, the system should be designed to reduce physical side-effects, such as headaches, nausea or visual loss acuity;
- The systems should be designed to avoid unpredicted effects of the devices used by operators, such as distractions, surprises or shocks;
- The designer must consider the user's perception regarding ergonomics and aesthetics;
- The user interaction must be natural and user-friendly.

Finally, Virtual Reality (VR) [50]. The updates in computing technology allow VR to be used for both professional and public applications, such as for car [51–54], design and construction, in architecture and civil engineering [55, 56] and for educational purposes [57].

In manufacturing, the use of VR technologies can reduce the time necessary for developing machine tools. Machine prototypes built in this way can support human validation of the designed solution's functionality and evaluation of the results of simulations such as stress analysis, kinematics and dynamics [58]. In particular, the concept of a virtual factory, with the introduction of Industry 4.0, is the natural consequence of VR use in manufacturing. A virtual factory is a simulated model consisting of several sub-models. Each sub-model represents a production cell of a factory. In this way, a simulated model for testing a manufacturing system can be designed and controlled [59]. The goal of this simulation is to find a

problem to fix and thus improve the layout of sub-models in the context of the virtual factory. Another application of VR in manufacturing is training workers.

The main goal is to avoid the risk of use for both humans and machines [60]. Moreover, in the medical field, there are several studies in which VR is applied for training in surgery, for treating mental health problems and for analysing human movement and muscle function. For example, in [61] the authors used VR for visualising muscle activation. The system analysed human movement and muscle functions by computing, in real time, kinematic joints and kinetics for full body models and dimensions and force evaluation in muscle elements. With the introduction of VR, the software can create interactions between humans and biomechanical data during patient examination or treatment.

Moreover, for surgery training []delorme2012neurotouch, a virtual environment with a stereovision system and haptic interfaces can help users acquire technical skills involved in craniotomy- based procedures. However, in this particular field, several studies are presented on the different state-of-the-art areas of surgery [62–67]. Several studies addressed treating mental health problems as well [68]. In particular, in [69] four patients with diagnosed claustrophobia were tested. In this study, a reduction of claustrophobia symptoms after three-month treatment was observed. Moreover, the same virtual treatment for other types of phobias was positive [70–73].

Industrial Internet The Industrial Internet of Things (IIoT) is a collection of technology used in an Industry 4.0 scenario, specifically in smart manufacturing [74]. Born from a convergence of industrial systems with ICT, sensors and communication systems, IIOT is derived from a more abstract idea, called IoT, which integrates computing and communications technology, and is expanded to include the many 'things' used both in the home [75] and at work [76]. The IoT started with the idea of tagging and tracking 'things' using low-cost sensors. However, with the introduction of smartphones, this paradigm evolved due to the perfect union between low-cost computing and pervasive broadband networking. Technically, the IoT consists of several physical artefacts that contain embedded systems of electrical, mechanical, computing and communication technologies that enable internet-based communication, using several well-known communication protocols, such as Internet Protocol and data exchange. A consequence of the application of the IoT paradigm in industrial processes is the launch of IIoT. Although IIoT follows the same core definition of IoT, the 'things' and goals are different. The IIoT, for example, consists of sensors, actuators, robots, milling machines, 3D-printers, assembly line components, chemical mixing tanks, engines, healthcare devices, planes, trains and automobiles. An important part of IIoT is the operational technology that refers to hardware and software systems found within the industrial

environment. [77]. These systems, such as a programmable logic controller, distributed control systems and human-machine interfaces are also known as industrial control systems [78–80], and the main goal is to control the several processes and procedures that occur in an industrial environment. However, these are traditional systems that with the introduction of the internet-based communication technologies, can be integrated into manufacturing organisations' information technology systems and infrastructures. Only with the union between operational technology and information technology (the core of the IIoT) will an Industry 4.0 scenario answer the needs of future systems in every application field [81].

Cloud Manufacturing Cloud-based manufacturing (CBM) [82] is a new paradigm that contributes to the success of Industry 4.0. The goal of this paradigm in an Industry 4.0 scenario is to design networked manufacturing for enhance efficiency in a cyber-physical production line, reduce product lifecycle costs and optimise the resource allocation in response to variable- demand customer-generated tasking [83]. The features of CBM are networked manufacturing, scalability, agility, ubiquitous access, multi-tenancy and virtualisation, Big Data and IoT. With these characteristics, a CBM system could be meant as an everything-as-a-service (infrastructure-as-a-service, platform-as-a-service, software-as-aservice) system [84–86]. A consequence of CBM is the Cloud-based Design and Manufacture (CBDM) [87] which focuses on the product realisation processes using an integrated cloud computing model. In other terms, the goal of a CBDM system is to enhance a CBM system by integrating it with cloud-based design concepts along with social product development.

Big Data Analytics and DSS Several companies in different application fields understand it is crucial to have data analytics capabilities of driving digital transformation. Therefore, skills concerning the development of algorithms for interpreting data must be required. In particular, in the manufacturing field, big data analytics (BDA) and technologies allow the support of real-time collection of data from several sources, for comprehensive analysis of the data and for real-time decision making to improve manufacturing flexibility, product quality, energy efficiency and maintenance processes [88–92]. Currently, healthcare organisations involving both single-physician offices with multi-provider groups and large hospital networks with accountable care organisations stand to realise significant benefits by using big data for effectively digitising or combining them [93, 94]. It seems that existing analytical techniques can be applied to the vast amount of existing (but currently unanalysed) patient-related medical data to reach a deeper understanding of outcomes to be applied at the point of care. Potential benefits could include following up on specific diseases. In general, BDA in healthcare could contribute to evidence-based medicine. The goal is the analysis of much structured and unstructured medical data to match treatments with outcomes, device

and remote monitoring for capturing, in real-time, large volumes of fast-moving data from several devices placed at home or in hospital and, finally, patient profile analytics for applying several analyses to patient profiles to improve care and lifestyles.

In general, a big data system (BDS) for healthcare, and for other application fields, consists of four main parts:

- Big data sources generally involve web and social media data, machine-to-machine data, big transaction data, biometric data, human-generated data related to clickstream and interaction data from Facebook, Twitter, LinkedIn, blogs, and health plan websites, smartphone apps, data read from remote sensors, meters, and other vital sign devices. Moreover, data types and sources include health care claims and other billing records increasingly available both in semi-structured and unstructured formats, fingerprints, genetics, handwriting, retinal scans and other medical images, blood pressure and other similar types of data. Finally, data types and sources encompass unstructured and semi-structured data such as physician's notes, paper documents and e-mail.

- Big data transformation is a component that consists of a data warehouse able to store several types of data. To properly cluster and analyse the data stored in the data warehouse, a data transformation process should be applied. For this scope, the open-source Apache Foundation project, Hadoop, should be used to analyse data and to create N datasets used as input in an Ensemble Support Vector Machine (ESVM). Hadoop has two primary components: Hadoop File System and MapReduce programming framework. The main feature of Hadoop is that the file system and MapReduce co-deploy such that a single cluster is produced and the storage system is included in the processing system [95].

- Big data tools and platforms are a component that uses structured or semi-structured data from the big data transformation component as input. In general, this component performs the implementation of an ESVM [96], which implements a DSS based on several datasets collected in a proper data warehouse.

- Big data analytics is the core of the entire system and allows a result aggregation to comprehensively describe the analyses performed using the previous components of the system. These components include an interface to interact with humans who must make decision based on the results of BDS.

The main features of a BDS are volume, velocity, variety and veracity. In detail, a big data system creates and accumulates an incredible amount of several types of data over time.

Advances in data management, particularly virtualisation and cloud computing, are currently facilitating the development of platforms for more effective capture, storage and manipulation of large volumes of data. Moreover, data are accumulated and analysed in real-time and at a rapid pace, or velocity. In many situations, the application of these features in a big data system could be the difference between success and failure. For example, in the medical field, the ability to retrieve, analyse, compare and make decisions based on output values could help physicians create a diagnostic report in a brief period due to the MapReduce ESVM approach used to predict the disease severity of patients. Big data is extensive because the information comes from several different sources. The recent exploiting of these sources for analytics means that structured data (which previously held unchallenged dominance in analytics) is now joined by unstructured data (text and human language) and semi-structured data (XML, RSS feeds). There is also data that is hard to categorise, as it comes from audio, video, and other devices.

Moreover, multidimensional data can be drawn from a data warehouse to add historical context to big data. Multidimensional data is a far more eclectic mixture of data types than analytics has ever involved. Therefore, with big data, variety is just as wide as volume. Also, variety and volume tend to fuel each other. The quality of data acquired from different sources is highly variable, and success or failure decisions depend on having accurate information. Unstructured data imply all often incorrect. The veracity hypnotises a scaling up in the performance of techniques and technologies to use in a big data management system. Big data analytics could be executed across several servers, or nodes, in distributed processing and by considering the use of the paradigm of parallel computing and of the approach called 'divide and process'.

Moreover, models and techniques need to consider the characteristics of BDA. Traditional data management hypnotises the warehoused data is certain, precise, and clean. High-quality data enable improving the coordination of processes in different application fields, avoiding errors and reducing costs.

Simulation and prototype The main goal of simulation and prototype technologies and techniques is to mirror the physical world in a virtual one. This feature is crucial for a CPS implemented in an Industry 4.0 scenario. In general, a physical world includes machines, products and humans. The virtualisation of the world allows workers to test and optimise processes in a simulated manner and apply the changes in the physical world. There are several simulation studies used for observing the behaviour of machines and operators in manufacturing: movements [97, 98], connectivity with robotic arms [99, 100], real-time tracking [101, 102], energy efficiency [103, 104], deadlock prevention [105, 106], and the use

of virtual engineering objects for industrial design and manufacturing [107–109, 109, 110]. Also, in this case, the application fields are many, and since there is great interest in the medical field, the practical knowledge of these techniques from manufacturing is shifted to bioengineering to reach the same goal [111–114].

Robotic Systems This complex system in which machines and humans interact to reach a common goal consists of modern robots characterised by autonomy, flexibility and cooperation. Currently, robots interact with one another and work safely with humans, even learning from them [115, 116].

In general, the use of robots in a system offers cost advantages when performing most of the processes in an intelligent environment. For example, the use of the programmable dual-arm robot is proposed in [11] for material distribution in the assembly line. This study focused on the safe operation of the robot through monitoring the environment while the robot was working. Several procedures were implemented to avoid unsafe behaviour. For example, if any disturbance, such as humans or equipment, enters the robot's virtual space (safety eye), the system stops the robot's movement with a sound anticipating some complicity [117, 118]. At this point, an operator could remove obstacles before the robot resumes working. Since manufacturing tasks are becoming individualised and flexible, robots in the smart environment should perform tasks collaboratively without reprogramming. The way is a ubiquitous interaction between robot and robot and human and robot as described in [119, 120].

Cyber Security A CPS consists of millions of embedded sensors and communications devices. This type of infrastructure is weak regarding risks associated with the increasing use of data or concerning systemic breaches [121]. Therefore, a cyber-physical manufacturing systems may face the threat of cyber-attacks. Generally, malicious software affects and spreads from one machine to another through communication systems to modify the manufacturing processes or destroy data, leading to product quality defects or a complete shutdown. Therefore, the implementation of an intelligent algorithm to avoid these situations is critical in an Industry 4.0 scenario because industrial data is highly sensitive, encapsulating various aspects of the industrial operation, such as information about products, business strategies and companies [89].

Artificial Intelligence It concerns the knowledge and techniques developed to make machines "intelligent," that is to say able to function appropriately also through foresight in their environment of the application. Industrial AI refers to the computer science-based technologies which, coupled with machine learning, are used to generate intelligent sensors, edge computing, and smart production systems.

2.1.4 Human Factor

The centrality of the human factor The Industry 4.0 pushes to a rethinking of the logic of human-machine interface, from touch displays, to wearable devices and augmented reality. The question is what role the human factor should play in this epochal change in the way of doing industry.

In an interesting research, the "Osservatorio Industria 4.0" suggests that to maintain the centrality of the human factor within the new contexts 4.0 it is necessary that companies increase their skills, both in terms of human resources selection and training in general. The "Skills 4.0" are necessary for the management of new technologies for data administration, for privacy, for cybersecurity and much more.

The workforce has to evolve in order to maintain its role within the evolving productive contexts that can potentially make the human presence obsolete. Many aspects and activities in the industrial environment still need the contribution of people, provided that they are able to improve their skills to intercept these "blind spots" in the production chain, where machines' capabilities are not yet sufficient.

First attempts to structure these interactions are made, for example, by Romero et al. (2016), Ruppert et al. (2018) and Fantini et al. (2020), where the operator is interpreted in different roles, depending on the technologies used. As described by Romero et al. (2016), augmented reality used by an operator leads to the "augmented operator", who is presumably capable of making more informed decisions when maintaining a machine, for instance. These works, however, still focus on technological possibilities for the worker without analysing their influences on HF demands and operator experience in depth. Moreover, the "Operator 4.0" as proposed by these works is merely analysed in isolation, without consideration of the organizational, processual, psychosocial, and technological environment of the humans in the system.

This article discusses how failure to attend to HF in previous industrial system generations has had negative consequences for individual employees, production organisations, and for society as a whole. We further show that there has also been a lack of attention to HF aspects in research and development in I4.0, and present and discuss a framework for the systematic consideration of HF in the design and evaluation of I4.0 technologies and technology-assisted workplaces. Addressing these aspects, this paper pursues two research objectives (ROs): RO1: To identify which HF aspects have been considered to what extent in the scientific literature on I4.0.

RO2: To provide a framework that includes foundational theories of HF to support the incorporation of HF aspects into corporate I4.0-system development efforts.

The remainder of this paper is structured as follows. A content analysis of research dealing with I4.0 is performed in Section 2, which highlights the definite lack of considering HF in this research area. In Section 3, concepts of HF in engineering design are discussed that are relevant for understanding the role of HF for system performance. In Section 4, an analysis framework is derived based on the discussed concepts to highlight how HF can be considered systematically in I4.0 research and development. In addition, an example application of the framework to a typical I4.0 use case is presented. The framework's implications are discussed in light of the insights obtained from the content analysis and theory section, and limitations as well as future perspectives of HF in I4.0 for researchers and managers are outlined in Section 5. Fig. 1 illustrates the outline of the paper and the research steps.

2.1.4.1 Human-Computer Interfaces for Industry 4.0

Following the Industry 4.0 principles, each player of an intelligent environment consists of modules to interact with other players. A player is not only a machine, but can be a resource or a human or, in general, intelligent objects.

An intelligent environment can be described as a cyber-physical structure in which humans should be integrated to realise their individual skills and talents fully. Therefore, a cyber-physical structure can be described as a network of relationships between humans and CPS consists of physical and virtual components [122]. The interaction between humans and physical or virtual components of CPS occurs both by direct manipulation of the virtual of physical components and by means of human-computer interfaces. In this contest, the role of the worker is to dictate a production strategy and supervise the implementation of the self-organising production processes. Therefore, the classic workplace becomes less significant due to extensive networking and mobile realtime information availability. The result of the application of this type of paradigm is that the workers assume more responsibility on a larger operating area since that their decision and monitoring processes can be executed on site or from afar. In this way, the worker takes on the role of the creative problem solver and his/her work is characterized by constructive planning activities or mental work. The novel role of human workers must be combined with the implementation of organisational and technological material and methods. Firstly, the need to fit qualifying strategies creates a need to find a resource that solves problems with an interdisciplinary approach that is necessary for an Industry 4.0 scenario. On the other hand, the need of human-technology solutions provides the creation of a networked and decentralised manufacturing system, the main result of the implementation of Industry 4.0 principles.

The CPS implementations with their abilities to gather, exchange and process data are leading to increasing the requests for managing information in every application fields of Industry 4.0. The result is an emerging need for requirements concerning the acquisition, aggregation, representation and re-use of data. In order to control and manage processes in these innovative systems, human workers must easily interact, in a distrusted manner, with all the necessary interfaces for visualising current production processes and the resulting data. On the other hand, each component of CPS must be able to collect data originate from a multitude of different data sources by means of standardised and platform-independent interfaces. Human workers must be able to interact with this component using mediating interfaces such as VR or AR. In particular, as described in Mixed, Augmented and Virtual Reality paragraph, VR allows the user to simulate and explore the behaviour of the CPS-based production system. On the other hand, the AR, which represents the computer-aided enhancement of human perceptions by means of virtual objects placed in the real world, allows the user to interact with CPS directly or to view information to make a decision on a specific process. There is a lot of information that could be visualised in the field of view of the human's works. Therefore the CPS must have such component able to evaluate information with which the human workers have to interact to make an intelligent decision. These components, also called, Decision Support Systems (DSS) are necessary components in a CPS, as described in paragraph 1.1. To implement these types of interactions, the IoT or IoS parts of an Industry 4.0 scenario, must be designed on a network in which each intelligent object has to be able to interact with each other following a precise standard for information access and exchange. By implementing the network of thinking objects and the interfaces for the interaction between data and human workers, the aggregated and preprocessed information can be directly accessible by human workers by means of mediating interfaces [123]. Therefore, several scenarios can be designed:

- maintenance by providing interactive and virtual instructions [124–126];
- quality control monitoring or, in general, production processes monitoring by means of an intelligent retrieval and allocation of information, such as the status of a CPS [127–129];
- planning and simulation of production processes to understand and optimise the behaviour of the CPS. In this scenario, the objectives must be both the design of information and virtual objects handling to be as user-friendly as possible and the implementation of the scenario by following specific requirements especially concerning robustness and security [130–132].

In general, interaction must be intuitive. This means that the same experiences gained while dealing with real objects can be transferred to the virtual/digital world. Tradition user interfaces are characterised by an unimodal interaction, in which the user, by means of several input devices such as a keyboard, mouse, joystick, etc., can give a command to the system that replies with the visualisation of the command result (generally, on a screen). The use of innovative multi-touch and voice control devices allows for improved ease of use, which will be updated by users personal experience [133]. However, the need to introduce innovative user interfaces collides with the strictly specific requirements of the environment in which the interfaces have to be used (industrial environment, operating room, etc.). For example, the most important form of interaction is the touchscreen interaction. However, only with the introduction of the Dispersive Signal Technologies (DST) [134], smartphones or tablets have been introduced in an industrial field since DST allow the human worker to interact with the touch screen when wearing gloves. Other problems such as dust and water splash must be solved to introduce smartphones or tablets in an industrial environment but already exists some hardware solutions. Voice control is another type of interaction that allows human workers to interact with systems even if their attention or haptic capabilities are fully busied [135]. Moreover, natural gestures interfaces are like voice control interfaces since it is particularly intuitive and immediate. Recognizing hand position and movements, natural gestures interfaces could be image or device based. In the device-based version, wearable sensors, such as acceleration or position sensor, have to be worn to record users' movements. On the other hand, image-based systems use camera sensors object recognition and image processing techniques to recognise the gesture, posture, hand position, etc..

Natural User Interface (NUI) is a goal of the Human-Computer Interface (HCI). The true meaning of what NUI is has evolved along with the introduction of the new technologies. For example, the Graphic User Interfaces (GUIs) are considered an NUI compared to command-line interface and Gesture UI, by means of technologies such as Kinect, is considered an NUI advanced over GUI [136]. A meaning of NUI could be gestures, touch, speech and haptics that support user interaction with a system via the human body [137, 138]. For example, in [139] the authors described the concepts regarding touch, tap and swipe on a flat screen with the disappearance of buttons. The new technologies, such as AR, VR and voice commands produce a new definition of NUI. Nowadays user interfaces are based on vision, hearing and tactility.

However, to improve the experience new technologies are implemented by enabling thermal, wind and pressure stimuli based on the sense of touching. For example, in [140] the authors demonstrate how the addition of thermal and wind stimuli in a virtual reality scenario

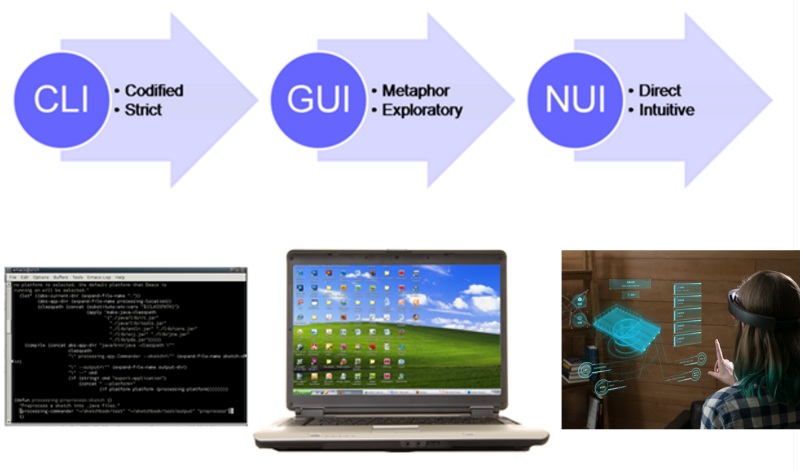

Figure 2.4 The evolution of interfaces, from CLI to NUI.

improves the sense of presence for a specific simulation. Moreover, in [141, 142] the authors design thermal and pressure feedback for mobile devices to reach haptic interfaces. The common goal of these studies is the extension of user interfaces with peripheral modalities beyond vision and hearing. Other senses such as olfaction and gustation 22 are also important for a human to interact with the world since that plays an important role in human emotion, memory and social interaction [143]. However, there are few works in the state of the art that explore the interfaces to support olfaction and gustation. For example, a study that demonstrates how people could use smell to tag photos compare with text label is presented in [144]. Another study designs and built an olfactory display system that distributes spatially on the touch screen several types of odours [145]. Finally, a team of researchers present an olfactory display based on biometric data in [146]. However, the most important study concerning olfaction is [147] in which Obres et al. identified 10 categories of smell experience that are useful to encourage the HCI community to design and implement devices for the improvement the simulation of olfaction in a simulated world. The research in the olfactory interfaces has encouraged the design and implementation of devices to simulate the sense of taste [148–150]. The common goal of these studies is to investigate the implications of gustatory experience by designing and implementing devices to allow users to taste dispensed flavours by touching the tongue to the screen or by developing a digital taste interface that simulates several tastes on the tongue via thermal or electrical stimuli. However, these types of interactions are still limited [151].

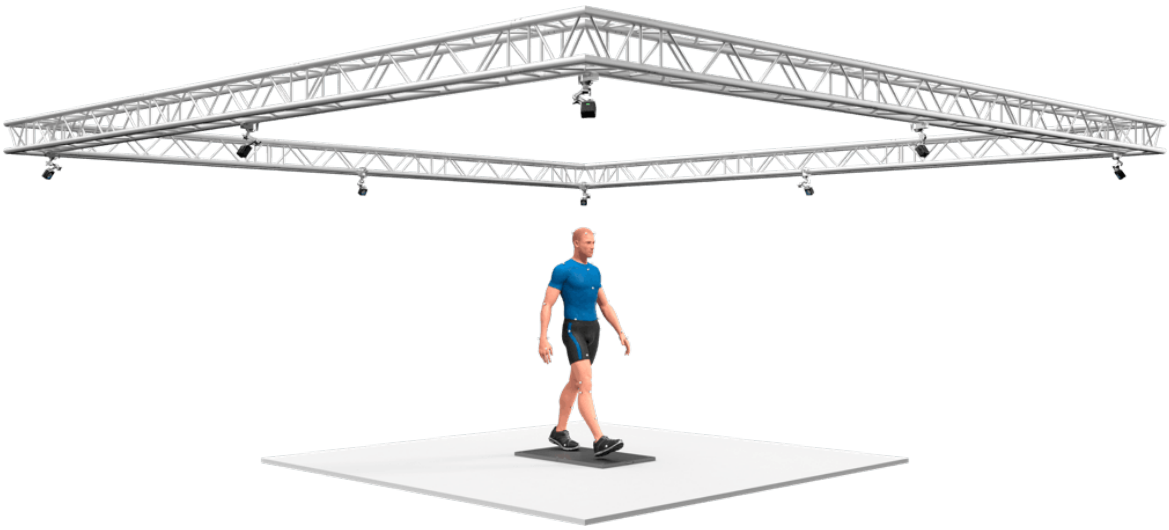

Figure 2.5 A representation of the Optitrack system: infrared cameras (top of the room), force platforms (segments on the floor on which the human is walking), human model, optical-markers (white spots on the human model).

2.1.4.2 Ergonomics and Motion Analysis

The applications of human motion analysis are growing fast in the areas including but not limited to healthcare [152, 153], virtual reality [154], sport [155], etc. [156], over the past decades. Human motion tracking systems generate real-time data that represent human movement and posture. The tracking system can be classified according to the motion capture techniques as optical and non-optical. Non-optical systems, or sensorbased systems, include the inertial, magnetic and mechanical motion capture techniques. These systems have the disadvantage of being intrusive, which can affect the performance of the system and limit its application. Optical-based systems utilize data captured from one or more cameras (infrared or video camera) to triangulate the threedimensional position of a subject according to marker-based or markerless techniques. Systems such as Optitrack (http://optitrack.com/ 2.5), VICON (http://www.vicon.com/), and BTS (www.btsbioengineering.com/) are vision-based tracking systems with markers. Instantaneous bone position and orientation and joint kinematic variable estimations are accurately addressed in the framework of rigid body mechanics.

In particular, by using a combination of several markers in a specific pattern, the software can identify rigid bodies or skeletons. By putting at least 3 markers on the rigid body in a unique and non-symmetric pattern, the motion capture system is able to recognize the object and determine its position and orientation. A skeleton is a combination of rigid bodies and/or markers, and rules for how they relate to each other. Several predefined skeleton

models for the human body exist in the motion capture software, but it is possible to set up user-defined skeletons or models depending on the needs of the researchers. Commercial systems available offer the combination of hardware and software to: acquire the position of the passive markers placed on the body segments (capture), reconstruct the trajectories of each marker (tracking) and - if required - elaborate the three-dimensional data (analyse) according to a specific medical protocol [157, 158].

The posture analysis field is really crucial in an industrial environment in which the human workers are undergone to repetitive movements during work tasks. Therefore, several observational methods used by experts are introduced to avoid posture problems. However, observational methods like OWAS, NIOSH, OCRA, and EAWS, even if supported by depth cameras user data, still require a heavy intervention by a field expert to estimate the required parameters (e.g. forces, loads, static/repetitive muscular activity etc.). The ISO standard 11228-3:2007(E) suggests the use of a simplified method in the early stage of the analysis and, if critical conditions are detected, provides the OCRA method to be applied for additional investigation. Among the simplified methods for rapid analysis of mainly static tasks, the RULA, acronym of Rapid Upper Limb Assessment, is one of the most popular [159]. The main weakness of RULA is related to the inter-rater reliability. In [160] the authors found just "fair" inter-rater reliability of the RULA grand-score (ICC<0.5) among four trained raters. Dockrell et al. [161] proposed an investigation of the reliability of RULA that demonstrated higher intra-rater reliability than inter-rater reliability implying that serial assessments would be more consistent if carried out by the same person. Bao et al. [162] showed that, if a "fixed-width" categorization strategy is used when classifying the angles between body segments, the inter-rater reliability grows with the amplitude of the width. Moreover, larger body parts as shoulder and elbow, allow better estimation than smaller ones, as wrist and forearm [163].

The introduction of low-cost and calibration-free depth cameras, such as the Microsoft Kinect v1 sensor, provided easy-to-use devices to collect data at high frequencies. Several authors studied the accuracy of kinematic data provided by the Kinect v1 device in various application domains [164–166]. The results showed that Kinect v1 is accurate enough to capture human skeletons in a workplace environment. The accuracy and robustness of the provided joint positions (skeleton tracking) are promising for applications that require to fill in an ergonomic assessment grid [167]. Patrizi et al. [168]patrizi2016comparison compared a marker-based optical motion capture system with a Kinect v1 for the assessment of the human posture during work tasks. However, three main technical problems arose in the works using Kinect v1: the lack of wrist joints tracking, the influence of the environment

lighting conditions, and the self-occlusions (in postures such as crossing arms, trunk bending, trunk lateral flexion, and trunk rotation). The Kinect v2, presented in 2013, uses a different technology (time-of-flight), and according to the specifications, it outperforms the previous version. It tracks 25 body joints including wrists; it is more robust to artificial illumination and sunlight [169] and more robust and accurate in the tracking of the human body [170]. Conversely, a study [171] found the non-trivial result that Kinect v1 outperforms v2 as regards average error of joint position (76 mm vs 87 mm) in seated and standing postures. These results feature the Kinect v2 sensor to be a promising tool for postural analyses, especially for the metrics whose calculation is based on angular thresholds that tend to minimize the effect of joint angle errors.

2.1.4.3 Training and Operations Performance

The Industry 4.0 revolution has affirmed the centrality of the human operator, proposing a new way to automate production processes based on human and robotic expertise synergy. The impact of new technologies, such as collaborative robots (co-bots), virtual reality (VR) and augmented reality (AR) [172], wearable devices, Internet of Things (IoT) and artificial vision [173, 174], allows the companies to streamline their processes, ensuring better quality and enhancing the flexibility of their production potential [175, 176]. From this perspective, the human-centered approach has once again been reaffirmed in the automotive sector in the era of electric vehicles [177]; as an example, the technological processes of battery pack assembly require several manual procedures, especially in the completion of electrical connections.

The continuous evolution of production processes, not only in the automotive industry [178] but in the whole world of automation, together with the problem of employee turnover, has led to a progressive and ceaseless need to train novel operators on new techniques and to assess the quality of their job. The assembly and maintenance of industrial assets are complex tasks that require a large number of training hours in classrooms and hands-on sessions. Furthermore, especially in times of restrictions related to the pandemic, only a few trainees can access training on a physical asset at the same time, and their availability is always a trade-off with production line efficiency. Training all the operators of a plant on a piece of new equipment in a reasonable lead time is a huge challenge.

In addition to the personnel training, one of the key factors of success in the new industry is the traceability of manual operations to ensure product quality [179]. Indeed, in most of the manufacturing processes, it is important to collect data from the manual assembly and maintenance interventions and to store these data in a centralized data management

system for subsequent analysis of the performance of the plants [180]. In this scenario, the companies that can accurately understand workers' behaviors and evaluate their performance in real-time will outperform their competitors.

Smart industrial workstations for training and evaluating the performance of the workers are drawing attention as an innovative approach to facing the problem. These systems are designed to guide a non-experienced operator in achieving the same level of precision and performance as the expert [181, 182]. In addition, they ensure that procedures are carried out in the right way while collecting anonymous real-time data that can be used to verify technical parameters and to improve the working efficiency where needed.

The market proposes some commercial solutions for virtual guidance, such as Bosch's Active Assist system (https://www.boschrexroth.com/en/xc/products/product-groups/assembly-technology/news/activeassist-assistance-system/index/, accessed on 20 January 2022), Arkite HIM (https://arkite.com/product/, accessed on 20 January 2022), Rhinoassembly Light Guide System (https://www.rhinoassembly.com/en/catalog/product/-Light-Guide--LGS--LGS/, accessed on 20 January 2022) and Vir.GIL (https://www.comau.com/it/competencies/digital-initiatives/technologies/vir-gil/, accessed on 20 January 2022) (Figure 2.6). They are powerful and flexible systems that are able to guide the operator during the training of a new assembly, inspection or maintenance procedure by means of digital information projected on a workbench or directly on the asset to be manipulated. However, such innovative products do not implement algorithms that are able to accurately track the pose of a hand tool that might also be partially occluded by the operator's hands. In fact, in the best case, these industrial solutions roughly track the position of the hand center and assume that a certain task has been performed if the hand center position is enough close to a specified area. This can clearly lead to a rough performance evaluation and the learning of bad habits. In order to make a difference, it is fundamental to track, with high accuracy, the pose of the tools the worker handles during the learning session of the procedure [183]. As an example, if a worker is required to tighten several screws in sequence, an evaluation of whether the screws were tightened following the correct sequence without missing any screws might be requested.

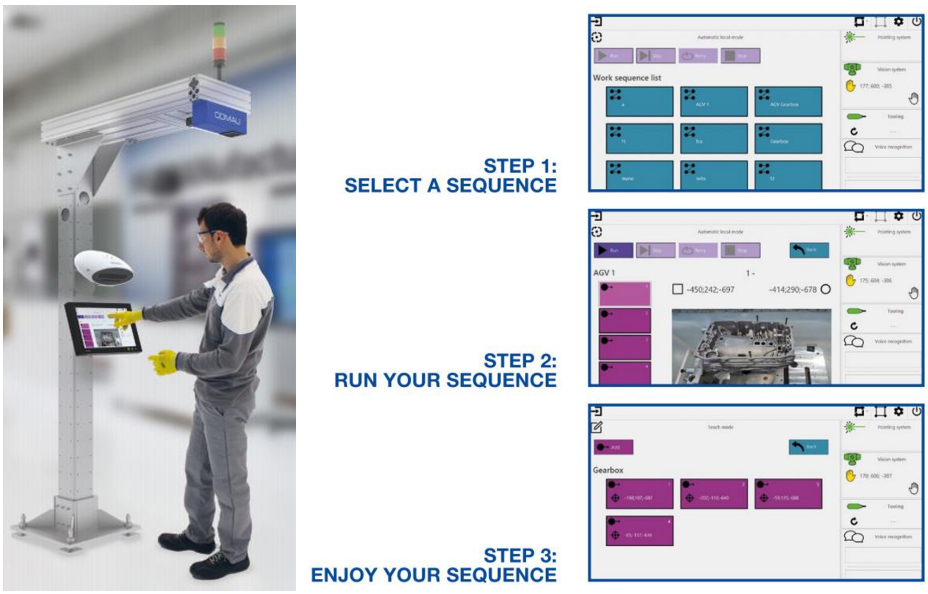

Figure 2.6 Vir.GIL virtual guidance system: (**Left**) hardware setup of the system; (**Right**) application UI workflow for starting a new procedure.

2.2 A Nonlinear Autoencoder for Kinematic Synergy Extraction

How the human central nervous system (CNS) copes with the several degrees of freedom (DoF) of the muscle-skeletal system for the generation of complex movement has not been fully understand yet. Many studies in literature have stat-ed that likely the CNS does not independently control DoF but combines few building blocks that consider the synergistic actuation of several DoF. Such building blocks are called synergies. Synergies have been defined both at muscle level, i.e. muscle synergies, and at kinematic level, i.e. kinematic synergies. Kinematic synergies consider the synergistic movement of several human articulations during the performance of a complex task, e.g. a reaching-grasping task. The principal component analyses (PCA) is the most used approach in literature for the kinematic synergy extraction. However, the PCA only considers linear correlations among DoFs which can be considered as the most-simple model of inter-joint coupling. In the following study, synergies were extracted from kinematics data (five upper limb angles) acquired during 12 different reaching movements with a tracking system based on the HTC Vive Trackers. After the extraction of the upper-limb joint angles with the OpenSim software, the kinematic synergies have been extracted using nonlinear undercomplete autoencoders.

Different models of nonlinear autoencoders were investigated and evaluated with R^2 index and normalized reconstruction error.

2.2.1 Materials and Methods

Participants Three healthy male subjects between 28-30 years old were involved in this study. They were all right handed with normal or corrected-to-normal vision and with no known motor deficit. Participants were informed about experiment of the study and gave their consent.

Experimental Setup Each subject was asked to perform reaching/grasping task in a 3D virtual environment while wearing the HTC Vive Headset and a low-cost tracking system. The virtual reality scenario was developed using the Unity 3D framework and the virtual reality HTC Vive platform. The HTC Vive trackers have been used to track the upper limb movement and accordingly control a virtual hand in the VR. The Leap Motion device has been used to detect the opening and the closing of the user's hand, thus allowing the interaction with the virtual objects placed in the virtual scenario.

Virtual Reality Scenario The virtual reality scenario implements and simulates the interaction between the human upper limb and virtual books. In the scenario the user is sitting close to a table in front of two bookshelves. He is asked to retrieve some books that randomly appear at six possible positions (see Figure 2.7a) with two different orientations (see Figure 2.7b). The different height of the shelves, the positions and orientations of the books modulate the complexity and variability of the action. The experimental session was composed of 12 independent trials (six positions by two orientations) that were randomly repeated three times. Each trial considers the interaction with a book that must be moved from the bookshelf to the top of a desktop. Each trial is composed of a sequence of sub actions as follows:

1. The user moves his hand at the starting position ("START" button as in Figure 2.7a), then, a book located at a random position and orientation on the bookcase appears.

2. Then, the user is asked to reach and grasp the book by closing his hand (the book will be "grabbed" only if the hand closes on the book).

3. Once the book is grabbed, a light spot is activated in correspondence of the re-turn position (the same for starting).

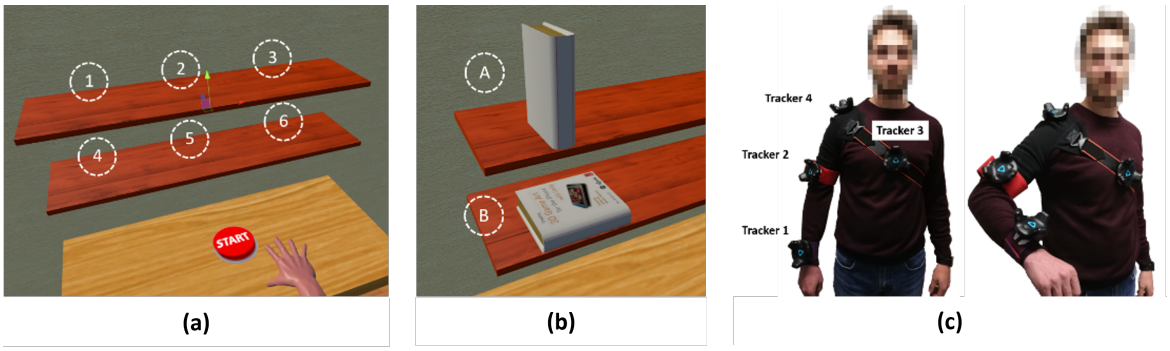

Figure 2.7 **(a)** The Virtual Reality Scenario. Numbers from 1 to 6 indicate the possible book position on the shelves. **(b)** The Virtual Reality Scenario. A e B indicate the two possible book orientation. **(c)** A participant of the study wearing the accessories of the tracking system.

4. The user must place the book at the right location and open the hand.

5. Finally, the patient goes back in the rest position to trigger both the end of the current trial and the start of a new one.

The tracking system based on the HTC Vive trackers The low-cost tracking system was developed using the HTC Vive platform but in particular by means of HTC Vive Trackers. Such system has been used to track the position and the orientation of four Vive trackers placed at specific positions of the user's upper limb, thus allowing the interaction with the VR and reconstruction of the complete movement in terms of joint angles. The low-cost tracking system has been designed for the acquisition of the angles of the shoulder, elbow and forearm joints, i.e. the three shoulder rotation angles defined as in the work of Holzbaur et al. [184], the elbow flexion/extension angles and the prono-supination angle. The system is based on the virtual reality HTC Vive platform and, in particular on, the Vive Tracker device (Figure **??**c) that is a battery-powered tracking device that allows the acquisition of the full pose (position and orientation) of a rigid body on which it is fixed. The tracking system employs four HTC Vive trackers, elastic belts with plastic supports for the trackers and a metallic stick with a known length (Figure **??**c). The four markers are positioned at the wrist, the arm, the sternum and above the acromion. The stable positioning of the trackers is ensured by means of elastic bands and ap-propriate 3D printed plastic supports. A calibration procedure is needed to individuate the relative position of 8 land-mark points of the skeletal system respect to the markers: ulna styloid process, radio styloid process, medial epicondyle, lateral epicondyle, xiphoid process, sternal extremities of the two clavicles and acromion. After

positioning the trackers 1, 2 and 3, the tracker 4 is fixed to the stick (Figure **??**c) to identify the relative positions of the landmark points respect to a specific marker. In particular, the ulna styloid process and the radio styloid process are referred respect to the tracker 1; the medial epicondyle and the lateral epicondyle are referred respect to the tracker 2; the xiphoid process and the sternal extremities of the two clavicles are referred to the tracker 3. The acquisition of the relative positions is performed by placing the extremity of the stick (that has a known position respect to the tracker 4) above the landmark points. Finally, the tracker 4 is positioned with a plastic support above the acromion at a defined distance. After the calibration phase, the subjects of the study, wearing the markers accessories (Figure **??**c) and HTC Vive headset, were immerged into the virtual scenario where they execute the task explained in the previous paragraph.

Joint angles extraction During the entire experiment session, a custom-made software is used to record the pose of all trackers at 90 Hz rate. Then, it was possible to reconstruct the trajectory of each land-mark point given its relative position to the specific tracker. Finally, the articulation angles are extracted by running an inverse kinematic procedure on a scaled version of the upper limb model developed by Holzbaur et al. [185] using the OpenSim software [186]. For each participant of the study, was built a dataset of joint angles extracted during the execution of the trials over the experiment. More in detail, having:

1. 5 joints angles (ϕ_1,ϕ_2,ϕ_3 three shoulder rotation angles, ϕ_4 elbow angle and ϕ_5 prono-supination angle);
2. t = [20000 - 25000] number of samples recorded during the action at 90 Hz;
3. m = 12 reaching-grasping-pulling actions.

The result was a matrix D as in 2.1.

$$D = \begin{bmatrix} \varphi_1^1(1) & \cdots & \varphi_5^1(1) & \cdots & \varphi_1^1(t_{max}) & \cdots & \varphi_5^1(t_{max}) \\ \varphi_1^2(1) & \cdots & \varphi_5^2(1) & \cdots & \varphi_1^2(t_{max}) & \cdots & \varphi_5^2(t_{max}) \\ \vdots & \vdots & \vdots & \ddots & \vdots & \vdots & \vdots \\ \varphi_1^m(1) & \cdots & \varphi_5^m(1) & \cdots & \varphi_1^m(t_{max}) & \cdots & \varphi_5^m(t_{max}) \end{bmatrix} \tag{2.1}$$

Furthermore, trigger system implemented in the virtual scenario label automatically the samples basing on action phases (reaching – pulling).

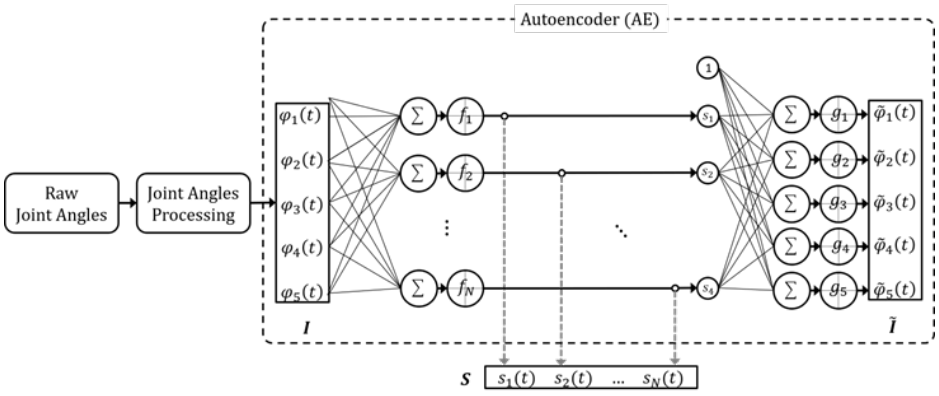

Figure 2.8 Undercomplete Autoencoder Topology.

Nonlinear Autoencoder for Kinematic Synergy Extraction Autoencoder is an artificial neural network designed with the purpose of coding the input variables into a latent-space from which reconstructing them as accurately as possible. This unsupervised learning technique is mostly used for dimensionality reduction. An autoencoder (AE) has a hidden layer that generates a coded representation h of the input x. AE is composed of two main parts: an encoder that codifies the input into the code (h=e(x)) and a decoder that reconstruct it, (r=d(h)). There are different kinds of AE that differ for internal structure of the network and training modalities [187]: undercomplete AE, regularized AE, sparse AE and denoising AE. An undercomplete autoencoder is an AE able to extract the most representative features contained in the input data. Such property is ensured by setting the dimension of the code h to a value smaller than the size of the input x. Such network's bottleneck should force the AE to learn some sort of structure that exists in the input data, e.g. correlation among input signals. In this study, different models of nonlinear undercomplete autoencoders were investigated in order to extract the spatial kinematic synergies of the human upper limb from joint angles while executing a reaching task in a 3D space. After that, the result was compared with the most used technique in dimensionality reduction, Principal Component Analysis. The general structure of the autoencoder is shown in Figure **??**. All designed models, had one hidden layer and N neurons, $N \in [1,\ldots,4]$ that produce the synergy activations named s_i with $N \in [1,\ldots,4]$ depending on the number of neurons. Neurons' activation functions ($f = g$) were chose between log sigmoid and tan sigmoid. The performance of all possible autoencoders generated from these specifics were evaluated. In the design of the autoencoder linear neurons were avoided because a linear autoencoder would have provided only a linear transformation that would have been equivalent to Principle Components Analysis. The output layer of every model had the same dimension as the input layer as a typical AE.

A pre-processing phase composed of the following 4 steps was needed to prepare the dataset of each subject: (1) outliers' removal to remove some bad samples; (2) low-pass filtering (0.01 Hz with Kaiser window) to remove the noise on the data, (3) segmentation of the samples that encoded reaching phases, (4) normalization in joint angles' range. The pre-processed datasets were used to train, validate and test all autoencoders. The AE networks have been implemented in MATLAB and trained using a gradient descent with momentum and adaptive learning rate algorithm and considering 1000 training epochs. Given a train set, the AE training was repeated 20 times with different initial weights. Then the best one among the 20 AEs featuring the minimum correlation index among the synergy activations was chosen. Such index was computed as the sum of the elements of the absolute upper triangular matrix extracted by the correlation matrix of s_1(t),...,s_n(t). The multivariate R^2 index and Normalized Root Mean Square Error (E_{RMS}) were computed in order to evaluate the synergy extraction performance of every model of autoencoder. The multivariate R^2 index is the fraction of total variation accounted by the synergy reconstruction and then is an indicator with E_{RMS} of the goodness of reconstruction ability of the autoencoder.

Autoencoder vs PCA Since the autoencoders are typically used for dimensionality reduction, the designed autoencoders models were compared with the most used technique in literature for kinematic synergies extraction, Principal Components Analysis (PCA) [188]. PCA is a linear transformation that projects a set of multivariate data on a new orthonormal coordinate system with unity vectors aligned with the directions of largest variance. These vectors are so called Principal Components (PCs). Although the number of PCs is equal to the number of variables often only the first few components are needed to explain most of the variance of the data set [189]. It was applied PCA on dataset of each subject; cumulative explained variance and Normalized E_{RMS} by PCs were computed in order to compare the PCA with Autoencoders.

2.2.2 Results

Encoding ability of nonlinear autoencoder models were evaluated and compared in terms of the multivariate R^2 index computed between the input joint angles dataset of each subject (see Figure 2.9) and the reconstructed one and Normalized Reconstruction Error (E_{RMS}) (see Figure 2.10).

Table 2.2 report that 3 synergies were enough for describing the 0.942±0.013 (R^2 index of log sigmoid model) and 0.936±0.015 (R^2 index of tan sigmoid model) of the movement variance for the entire experiment with respectively a Normalized Reconstruction Error

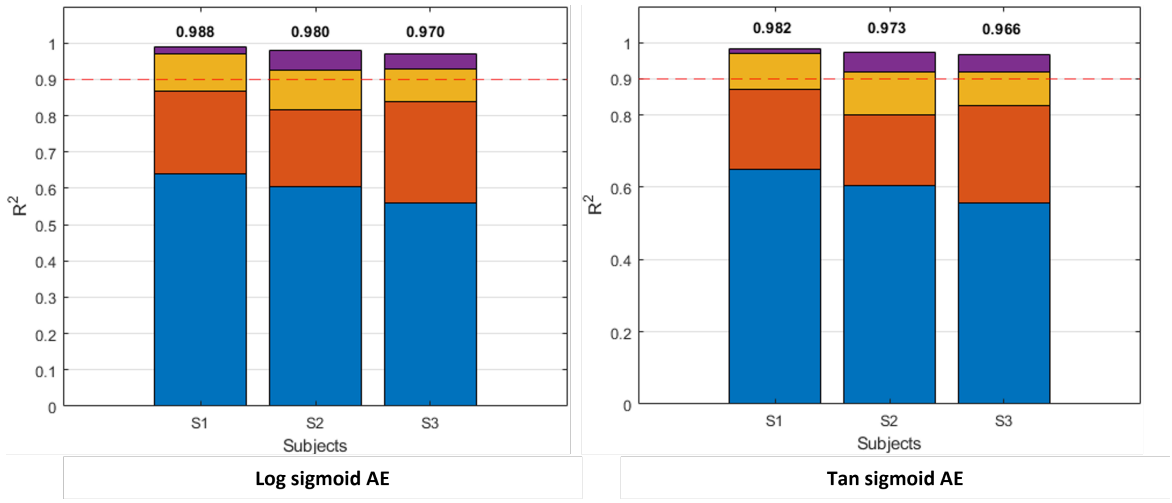

Figure 2.9 R^2 index of Log sigmoid and Tan sigmoid AE models calculated for each subject.

(E_{RMS}) of 0.05±0.011 and 0.053±0.012. They applied the PCA to the same dataset to extract kinematic synergies with a linear transformation and calculated the Explained Variance % and the Normalized Reconstruction Error (E_{RMS}) of each principal component.

The results of PCA are reported in Figure 2.11 with cumulative explained Variance percentage of PCs across the 3 subjects and Normalized Reconstruction Error (E_{RMS}). They show that 3 components are needed to represent task data; an index threshold of 90% variance is enough.

Table 2.2 reports the performance comparison between autoencoder models and PCA in term of mean of the Normalized explained variance (NEV) and mean Normalized Reconstruction Error on the three subjects. In order to have a fair comparison, the NEV percentage was normalized in range 0-1 then it is a matter of fact that number of synergies are represented by hidden neurons in autoencoders and principle components in PCA. The result shows how nonlinear autoencoder models are accurate as PCA in term of reconstruction of the input never overcoming it.

2.2.3 Discussion and Conclusions

The same complex reaching movement can be executed with several arm trajectories due to the high redundancy of the arm skeletal system. This redundancy can be simplified into kinematic synergies. Synergies from kinematics data of 12 different reaching movements were extracted by means of nonlinear autoencoder obtaining accurate performances. Different models of AE were investigated and evaluated with two metrics, R^2 index and Normalized E_{RMS}. The results show that 3 synergies were enough for describing the 0.942±0.013 (R^2

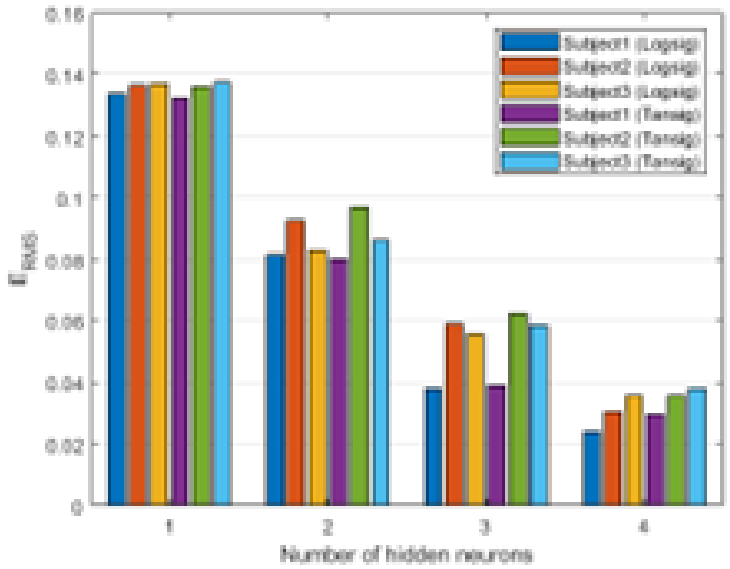

Figure 2.10 Normalized Reconstruction Error of the two AE models calculated for each subject.

Table 2.2 R^2 of autoencoder models compared with Normalized Explained Variance of PCA. Reconstruction Error (Normalized E_{RMS}) of autoencoders models and PCA comparison.

# Syn	R^2 /Normalized Expl Variance			Normalized Rec Error (E_{RMS})		
	AE (*Log sigmoid*)	AE (*Tan sigmoid*)	PCA	AE (*Log sigmoid*)	AE (*Tan sigmoid*)	PCA
1	0.601±0.026	0.603±0.029	0.604±0.037	0.136±0.002	0.135±0.003	0.135±0.001
2	0.841±0.014	0.833±0.019	0.841±0.018	0.086±0.006	0.088±0.008	0.086±0.005
3	0.942±0.013	0.936±0.015	0.945±0.021	0.05±0.011	0.053±0.012	0.05±0.009
4	0.979±0.005	0.974±0.004	0.986±0.009	0.03±0.006	0.034±0.004	0.025±0.001

index of log sigmoid model) and 0.936±0.015 (R^2 index of tan sigmoid model) of the movement variance for the entire experiment with respectively a Normalized Reconstruction Error (E_{RMS}) of 0.05±0.011 and 0.053±0.012. The AE reconstruction ability was compared with the PCA and results showed that the AE commit a low reconstruction error comparable with PCA but never overcoming its performance. The PCA results show that 3 components were enough for describing the 94.48 % ±2.1% of the movement variance for the entire task with a reconstruction error of 0.05 ± 0.009. A linear transformation of the dataset was enough to extract accurately synergies to describe the entire experiment. It is possible that nonlinear autoencoders can have better performance that PCA for kinematic synergy extraction from data of more complex movements with more than 5 joint angles tracked. More investigations are needed. In the future works, the tracking system will be improved considering more

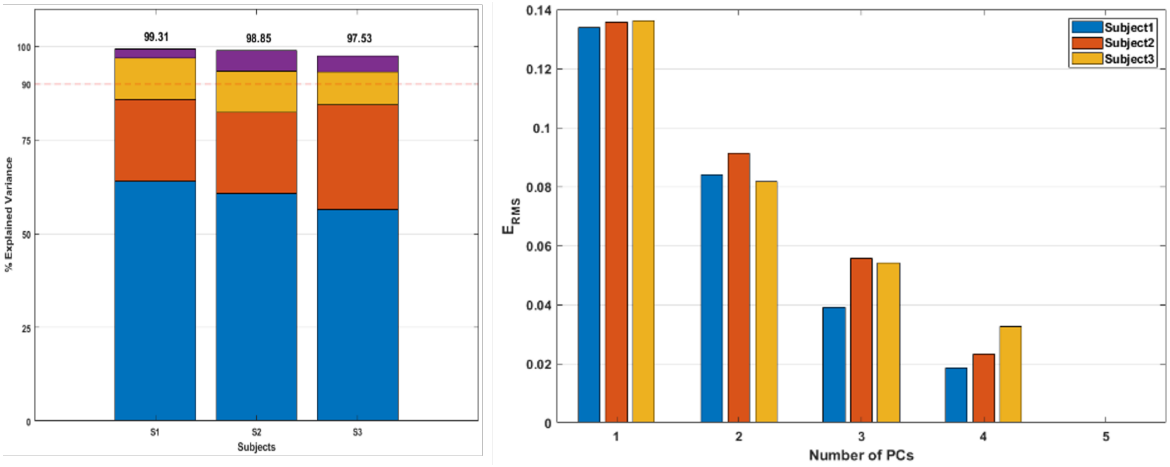

Figure 2.11 Cumulative explained variance by PCs and Normalized Reconstruction Error of PCA for each subject.

joint angles, virtual scenarios with involving complex movements will be implemented, number of test subjects will be increased, other AE models will be investigated and they will be used also for movement prediction. Furthermore, future studies will investigate the use of synergies as performance index of the motor activity in neurodegenerative disorders [190–194].

2.3 Vision-Based Hand Tool Tracking

The problem of the pose estimation of 3D objects, including the hand tool for allowing autonomous manipulation [195], has been studied for years and is an open and debated problem. The approaches that allow for high accuracies rely on a 3D model of the object that has to be detected within a 3D point cloud [196]. However, such methods are time consuming and may not be applicable due to the unavailability of the 3D model [196]. The unstoppable rise of deep learning in recent years has pushed the pose estimation research out of the the boundaries of classical computer vision techniques, and new approaches based on deep neural networks have been exploited [197]. Novel methods require minimal human intervention, improve the performance of 3D data-based approaches [198, 199] and, in some cases, avoid the usage of 3D models for estimating the pose of an object [200, 201]. Even if the problem has also been extended to the general situation of occluded objects, hand tool pose estimation and tracking in the industrial environment during assembly and maintenance procedures has not been extensively investigated.

Detecting and tracking a tool handled by an operator performing an assembly or maintenance procedure is not easy, mainly because of the tool's occlusion due to the operator's hands. The problem of hand tool pose estimation can be solved with a direct or indirect approach. In a direct approach, the tool is detected and then tracked using some robust features that are visible even if it is occluded. In an indirect approach, body joints of the operator and their hands are detected and tracked; the tool pose is derived assuming a unique handling pose of the tool. In order to investigate both paradigms, four artificial vision-based systems have been design, implemented and compared. Each developed system has been evaluated with a set of experiments replicating real industrial scenarios, and their performances have been compared to analyze the pros and cons according to the task properties. Even though general methodologies are proposed, the developed systems have been tested with a specific use case considering the estimation of the 3D position of a cordless power drill.

This study has the ambition to identify the best method(s) to integrate in the next cutting-edge workstations for training and assessment in Industry 4.0. Such systems will be designed with the following objectives:

- Training an operator on assembly and maintenance procedures with a recorded sequence of actions;
- Tracking an operator activity to validate each manual operation and certify the quality of the job;
- Detecting risky actions and behaviors in time and alerting the operator;
- Ergonomics monitoring during the procedure for always proposing to the operator the less stressful posture to perform the operations.

The main constraints of these solutions should be:

- Real-time execution;
- High accuracy.

The real-time execution is a key factor of a virtual guidance system because it has to be ready to warn the operator as soon as possible when their safety is compromised, when ergonomics guidelines are not respected [174, 202] or when the process is going to be completed in the wrong way. On the other hand, a high level of accuracy is required to control the operator's movement in the assembling process to avoid errors.

2.3.1 Materials and Methods

Systems for Hand Tool Tracking In this work, four different systems based on either open-source or commercial solutions have been developed and compared:

1. The first system is a marker-based solution using the ArUco markers [203, 204];
2. The second system is based on a deep learning model engineered for 2D detection problems and is called YOLO v4 [205, 206];
3. The third system is based on the Azure Kinect Body Tracking (AKBT) service [207, 208]
4. The fourth system considers the use of the OpenPose [209–212] library.

Each system has been designed to estimate a single interesting point of a hand-held tool, even though three out of four systems have the intrinsic capability of estimating the entire pose of the tool. It is worth citing that all four systems are based on RGBD camera, except for the method based on Aruco, which does not need the depth information. For this reason, the new Kinect Azure camera has been used either for acquiring RGBD data or estimating the human skeleton configuration with the Microsoft SDK "Azure Kinect Body Tracking".

ArUco-Based SYSTEM The system based on ArUco marker considers the possibility of applying a 2D planar marker on the hand tool that must be always visible by a RGB 2D camera. The main benefit of this approach is that a single marker provides enough correspondences to obtain the camera pose and, from that, a tracked object pose can be derived. Once the position of the tracked tool's point within the marker reference frame is known, the path of such a point can be reconstructed by the marker frame pose. Such an approach is the most invasive one since it considers the introduction of a new object, i.e., the marker, within the scenario. The strength of this approach is that it can determine a robust 3D pose estimation using a simple 2D camera and some printed markers, keeping computational costs low and therefore saving hardware resources for other essential tasks. On the other hand, it is an invasive way to track an object because markers have to be installed on it. Furthermore, if the marker is not visible, it is not possible to detect the object and, as a consequence, to establish the correct pose.

ArUco [203, 204] is a popular opensource library for detection of square fiducial markers and camera pose estimation mostly used in augmented reality applications. An ArUco marker is a synthetic square marker composed of a wide black border and an inner binary matrix

that determines its identifier (id). The black border facilitates its fast detection in the image, and the binary codification allows for its identification and the application of error detection and correction techniques. The marker size determines the size of the internal matrix. For instance, a marker size of 4×4 is composed of 16 bits. The ArUco decoding algorithm can locate, decode and estimate the pose in realtime of any ArUco markers in the camera's field of view, as shown in Figure 2.12. It is based on the knowledge of the matrix encoded in the square. Multiple matrices are encoded in a group of markers, identified in dictionaries. It is possible to choose among several predefined dictionaries or by generating one yourself.

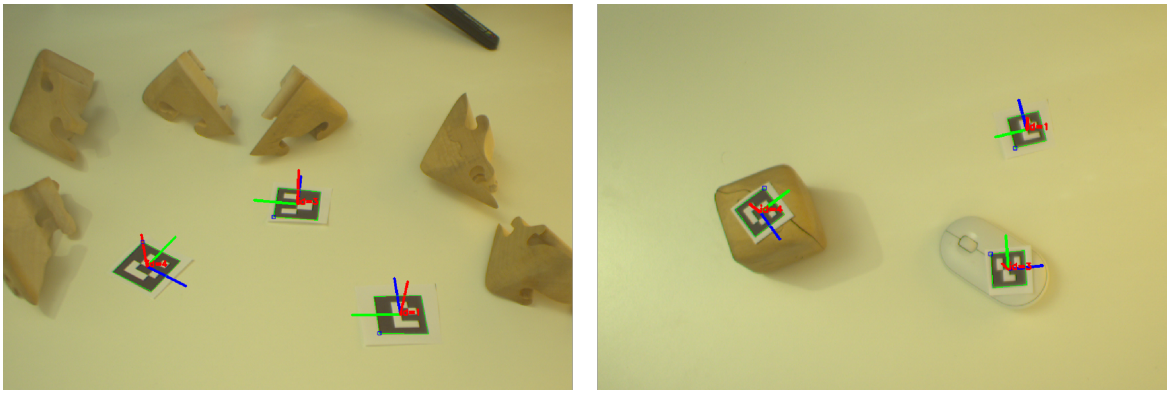

Figure 2.12 Example of ArUco markers pose estimation: (**Left**) three markers placed on a desk in different poses; (**Right**) three markers placed on three different objects.

For the sake of simplicity, in this study, a wooden support for the power drill was realized and three ArUco square markers with 5 cm side were stuck on it. Usage of a group of markers was preferred to a single marker in order to provide a more robust pose estimation: a single marker being visible but not recognized quickly in the scene, or not recognized at all because of an occlusion, could occur. When more markers of the group are detected in the same frame, only one marker's pose needs to be chosen as reference for the power drill chuck pose estimation. The area in pixels of a marker was used as selection criteria for the best marker because it is a matter of fact that AruCo algorithms have better performance the bigger the detected marker appears in the frame.

System Based on Deep Detection Model (YOLO) The system that uses a deep neural network, i.e., YOLO, is based on two subsequent steps: (1) a deep neural network is trained to localize within a 2D RGB image the specific tool's area (or point) that has to be tracked, and (2) the 3D position of the tracked tool's point is estimated by computing the spacial centroid of the point cloud underlying the ROI found in the previous step.

You Only Look Once (YOLO) [205, 206] is a family of convolutional neural networks (CNN) that achieve near state-of-the-art results with a single end-to-end model that can perform object detection in real-time. Compared to the approach taken by previous object detection algorithms, YOLO proposes the use of an end-to-end neural network that makes predictions of bounding boxes and class probabilities all at once (Figure 2.13). Starting from YOLO's pre-trained models, it is possible to re-train the last layers to introduce new classes that are not available in the original dataset to fit the object detector capabilities to new objects. In the re-training process, it is also possible to tune settings of the net and to adjust accuracy over performance, training time and batch iterations, choosing the best weight candidate. YOLO's performance has improved over time, starting from the v1 version. The original YOLO v1 was born as the first object detection network to combine the problem of drawing bounding boxes and identifying class labels in one end-to-end differentiable network. YOLO v4 outperforms most of the other object detection models [213] by a significant margin, keeping frame-rate high and making it the best opportunity to detect objects in real-time.

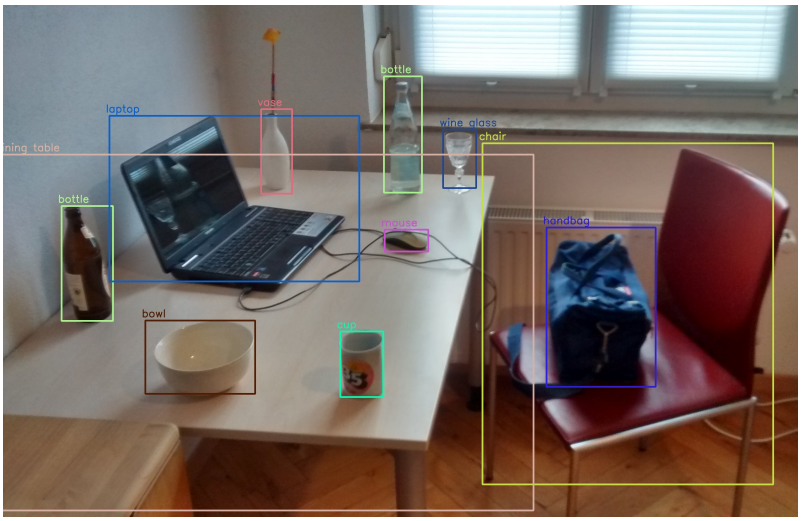

Figure 2.13 YOLO object detection output for office scene (from MTheiler, CC BY-SA 4.0, via Wikimedia Commons).

In this study, YOLO was implemented in its fourth version. The last layers of the model were re-trained to recognize the power drill chuck as a new class, and then the performance of the model inference was evaluated. In order to train the model, a dataset consisting of 735 images was created. The images were acquired by Azure Kinect RGB camera with the power drill in different poses, with heterogeneous light conditions and in different environments. Considering the objective of study, the model was trained with images containing only the particular power drill used for our experiment, leading the net to recognize only the chuck of

this tool and not that of other power drills. Data augmentation was performed in order to improve the performance of the model using flip upside-down, flip left-right, rotation and Gaussian blur. The training process was based on transfer learning and the CNN model was initialized with the weights retrieved from the GitHub page of YOLO v4 based on darknet framework. The net was trained with images of 512x512 resolution and max batches set to 2000. The starting weights were obtained from the training on the COCO dataset, containing 80,000 images and 80 different object classes.

The trained model was able to recognize the power drill chunk in every frame of real-time acquisition, returning the pixel coordinates x and y of the top-left corner of a box that contains it, the width and the height of the box and the confidence as the probability that the object was classified correctly. In order to estimate the 3D pose of the power drill chuck, the center point (x,y) of the box returned by YOLO model was calculated and the 3D coordinates of that point in the scene were computed by using the functions of Azure Kinect SDK.

System Based on Azure Kinect Body Tracking The system based on the Azure Kinect Body Tracking exploits the 3D body configuration estimation performed by the AKBD SDK of Microsoft. The system is based on the tracking of the upper link main segments to estimate a specific tool's point if the relative position of such a point, with respect to the hand reference system, is known.

The Azure Kinect from Microsoft is a cutting-edge spatial computing developer kit with sophisticated computer vision and speech models, advanced AI sensors and a range of powerful SDKs. It is equipped with several sensors in order to sense the surrounding environment; the device integrates a 12-megapixel RGB camera supplemented by 1-megapixel depth camera, a 360-degree seven-microphone array and an orientation sensor. The main modules of the SDKs are the Sensor SDK and Body Tracking SDK. The first one is designed for the interface with sensors and for managing data provided by them, automatically handling the problem of RGB and depth camera data alignment; the Body Tracking SDK is based on a complex deep learning model that supports body segmentation, human skeleton reconstruction, human body instance recognition and body tracking in real-time. The model recognizes 31 joints of the human body, each joint with its own reference system organized in a hierarchical structure, as shown in Figure 2.14. The deep learning model is able to reconstruct the entire human body model, where the higher the accuracy, the better the visibility of the body; the model has a good tolerance to the occlusions only for the highest joints of the hierarchical structure.

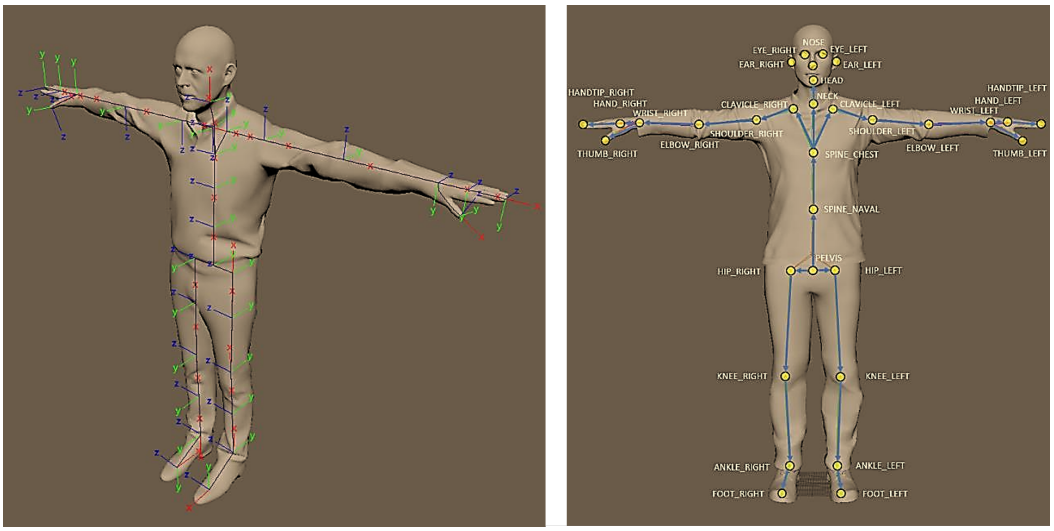

Figure 2.14 Azure Kinect Body Tracking detectable joints: (**Left**) joints with reference systems; (**Right**) joints' hierarchy.

Body Tracking SDK is able to detect and track all joints of a human body in the scene, returning position and orientation (in quaternion form) for each of them [207, 208].

Intuitively, the kinect hand joints, i.e., n.8—left hand and n.15—right hand, should be the most useful to estimate the power drill chunk pose. Unfortunately, several tests led to exclude the above-mentioned joints because experimental trials proved the poor quality of the orientation prediction. In fact, most of the time, the model predicted the power drill in the scene as part of the hand of the operator. Thus, the joints of the wrists (n.7—left and n.14 right) have been considered. The downside of this choice is that the tool pose changes relative to the wrist flexion/extension, and wrist radial–ulnar deviation movements are not considered.

System Based on OpenPose This system, like the one based on the AKBT, uses the information of the operator upper limb pose to obtain the tool's point position. In detail, it relies on the 3D position of some hand's keypoints. OpenPose [209–212] can be considered as the state-of-the-art approach for real-time human pose estimation. It is the first framework that can jointly detect human body, hand, facial and foot keypoints on single images. OpenPose is a multi-stage CNN that uses a bottom-up approach to find every instance of a key point and then attempts to assemble groups of key points into skeletons of distinct humans. The deep learning OpenPose model is based on a CNN and follows a precise pipeline: in the first step, the model computes confidence maps for every body part detection; in the second part, it predicts part affinity fields (PAF) in order to associate every

key point of every person in the frame; in the third step, bipartite matching is computed, so a several-graph connection is evaluated in order to choose the best performing PAF; in the last step, results are parsed and the skeleton is reconstructed. A confidence map is the 2D representation of the belief that a particular body part can be located. A single body part will be represented on a single map. Therefore, the number of maps is the same as the total number of body parts, and is a number that depends on the dataset the model is trained on. Instead, PAF is a set of 2D vector fields that encode the location and orientation of limbs over the frame domain. The framework integrates three different trained models for body, hands and face keypoint estimation. They return, respectively, 25 keypoints for the body, 21×2 keypoints for hands and 70 keypoints for the face (135 keypoints).

This study was focused on OpenPose capability to track up to twenty keypoints of the hand, consisting of wrist, finger's knuckles and phalanges. The adopted configuration for the framework has the following characteristics: Body Network input size equal to 160×160, Hands Net input size equal to 368×368 and Face Net disabled. The keypoints are just recognized in the 2D frame and the output is expressed in pixel coordinates within the image. Hence, a registered 3D point cloud is used to obtain the 3D position of the keypoints.

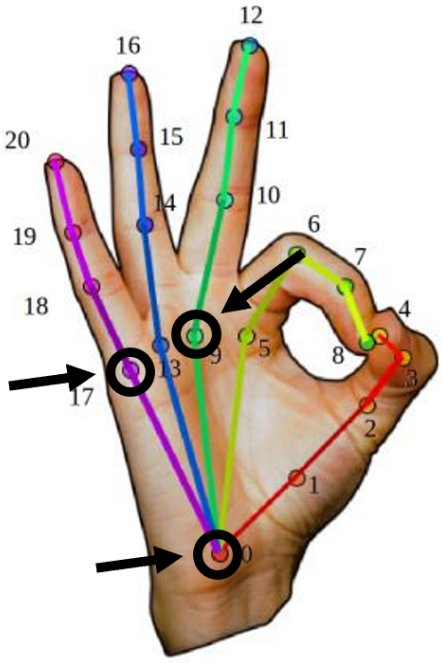

Figure 2.15 OpenPose keypoints for the hand, where the ones used for the calculation are highlighted. (Keypoint n.9) Middle finger knuckles; Keypoint n.0) wrist; (Keypoint n.17) little finger knuckles.

Three out of all detected keypoints of the hand have been considered to compute the estimated hand's pose (Figure 2.15):

- Keypoint n.0 (wrist);
- Keypoint n.9 (middle finger knuckles);
- Keypoint n.17 (little finger knuckles).

The reference frame of the operator's hand was computed as follows. First, two vectors are computed: one from the wrist point (kp_0) to the middle finger knuckle point (v_1) (Equation (2.2)) and one from the wrist point to the little finger knuckle point (v_2) (Equation (2.3)). The cross-product between v_1 and v_2 returns v_3, as shown in Equation (2.4); it is an orthogonal vector to v_1 and v_2 with a direction given by the right-hand rule outgoing from the back of the hand. Then, it was possible to calculate the vector whose direction is toward the thumb (v_4) as cross-product between v_1 and v_3 (Equation (2.5)).

$$\bar{v}_1 = [kp_{9x} - kp_{0x} \ , \ kp_{9y} - kp_{0y} \ , \ kp_{9z} - kp_{0z}] \tag{2.2}$$

$$\bar{v}_2 = [kp_{17x} - kp_{0x} \ , \ kp_{17y} - kp_{0y} \ , \ kp_{17z} - kp_{0z}] \tag{2.3}$$

$$\bar{v}_3 = \bar{v}_1 \times \bar{v}_2 \tag{2.4}$$

$$\bar{v}_4 = \bar{v}_1 \times \bar{v}_3 \tag{2.5}$$

with

$$x \equiv v_1 \ , \ y \equiv v_3 \ , \ z \equiv v_4 \tag{2.6}$$

Calibration of the Proposed Systems All of the proposed methodologies consider the estimation of the 3D position of a specific point of interest of the hand tool. The system based on YOLO is the only one that directly estimate such a position. The other three systems are based on the knowledge of the position (that can be considered fixed) of such a point with respect to the estimated reference system. A specific calibration procedure is thus needed to acquire the position of such a point that, in this work, has been experimentally found by positioning the tool's point (while it was hand-held by the operator) in correspondence of a known position. However, other model-based techniques might be investigated.

Experimental Validation In order to evaluate and compare the proposed systems, it was selected a specific scenario that considered an operator holding a cordless power drill; then,

its mandrel was considered as the point of interest to be tracked. As will be deeply discussed below, the pose of the power drill and the position of the mandrel were also acquired with an accurate system in order to quantitatively evaluate the performance of each system.

Evaluation System Setup The experiment environment was set up with the Azure Kinect positioned at approximately 1.8 m from the ground and two meters from a wall, tilted 15 degrees downwards with respect to the horizon. The distance of the operator from the Kinect camera could be in a range between 0.80 m and 2 m, compatible with the range defined in the official documentation of the device.

In order to evaluate the performance of the four frameworks under investigation, a highly accurate tracking of the power drill chunk pose was needed as reference. The HTC Vive (Figure 2.16) was selected as benchmark for the experiment since the precision of its tracking technologies has been tested to be around RMS 1.5 mm, and its accuracy around RMS 1.9 mm [214–216].

The HTC Vive system is used for rendering 3D virtual reality and it is developed by HTC in partnership with Valve. The headset (Figure 2.16—Top-left) uses room scale tracking technology (Lighthouse, as shown in Figure 2.16—Middle) for virtual reality experiences that allow users to freely move around a play area, accurately tracking the position and orientation of the user's head-mounted display and controllers, reflecting all real-life movement in the VR simulation environment. The tracking is possible thanks to two infrared signals emitters called base stations (Figure 2.16—Top-right) and special active sensors that cover the surface of the headset, and controllers that intercept the infrared pulses can autonomously track their own position and orientation in the workspace determined by the field of view of the stations. The HTC Vive capabilities can be extended by means of small devices called Vive trackers (Figure 2.16—Bottom) [217] that implement Lighthouse technology too. They allow for a high degree of flexibility, making it possible to track items or body parts if correctly configured [218].

Figure 2.16 HTC Vive components: (**Top-Left**) the VR headset with a controller; (**Top-Right**) front and rear of a base station; (**Middle**) Lighthouse tracking system setup; (**Bottom**) a HTC Vive tracker with details scheme.

HTC Vive base stations were placed in the space between Azure Kinect, delimiting a workspace that completely contained the field of view of the Kinect cameras to ensure the operator movements were in a monitored space. An HTC Vive tracker was placed on the power drill to track its pose. The position of the chunk with respect to the Vive tracker reference frame was found using the calibration procedure described above. The power drill

Vive tracker was installed by means of a wooden support (Figure 2.17—Right) designed for the purpose.

Figure 2.17 (**Left**) The power drill used for the experiment. (**Right**) The wooden support mounted on the power drill with ArUco markers and HTC Vive tracker installed.

It is worth noting that the position of the tool's point of interest estimated by the proposed system is referred to as the reference frame of the kinect camera. Since the accurate measure of the power drill pose is with respect to the reference system of the HTC Vive, it is necessary to know the relative pose between the two reference systems in order to compare the accurate measure with the estimated one. Hence, a second Vive tracker was fixed on the Azure kinect chassis by using a 3D-printed support (Figure 2.18). Such a support designed ad-hoc allowed for the positioning of the Vive tracker with a well-known pose with respect to the camera frame.

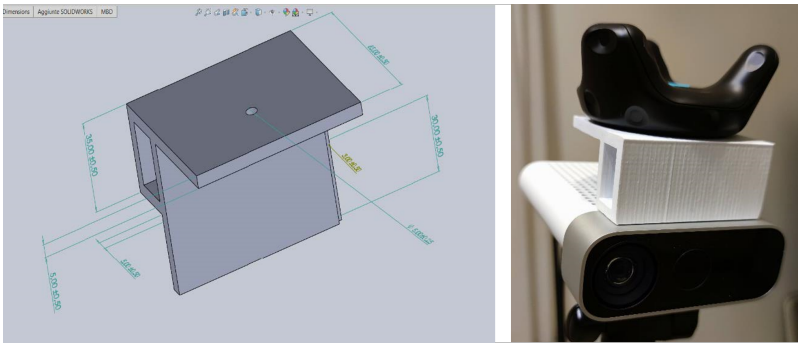

Figure 2.18 The support mounted on the Azure Kinect: (**Left**) the 3D model of the support; (**Right**) the 3D-printed support mounted on the Azure Kinect with the HTC Vive tracker.

Experiment Description In order to evaluate and compare the pose estimation performance of the proposed systems, some experiments reproducing typical manual task performed by a worker were conducted. As already reported, a power drill (Figure 2.17—Left) was selected for the experiment because it is one of the most frequently used tools in industrial assembly/disassembly procedures.

Three different scenarios have been designed:

- In the first scenario, the operator holds the power drill in static position on a workbench (stationary position) (Figure 2.19—Left);
- In the second scenario, the operator follows a trajectory with the power drill on the platform, keeping the speed of the movement low (slow-motion condition) (Figure 2.19—Right);
- In the last scenario, the previous trajectory is considered, but the speed was increased (fast-motion condition).

For the second and third scenario, the trajectory was defined as a path from a starting point A to another point B on a horizontal workbench. Two different velocities were adopted for performing the same trajectory (approximately 4 cm/s for slow-motion condition; approximately 8 cm/s for fast-motion condition). A vision feedback on a monitor was used as a virtual reference to follow. Four users were involved in the experiment. Everyone was asked to perform three trials in each condition, for a total amount of twelve trials.

The execution of all of the proposed systems was performed by a real-time C++ application that both integrated all of the frameworks and synchronized the data acquired by the HTC Vive system with the estimation positions computed by each system (Figure 2.20).

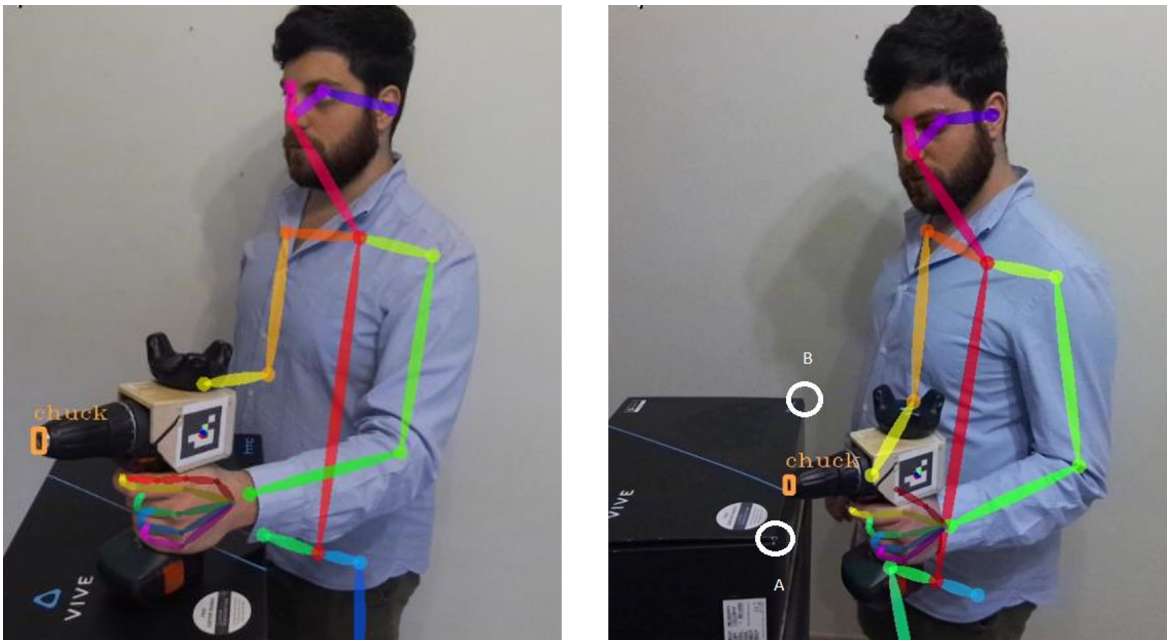

Figure 2.19 A user performing a trial in (**Left**) stationary condition and (**Right**) slow-motion condition.

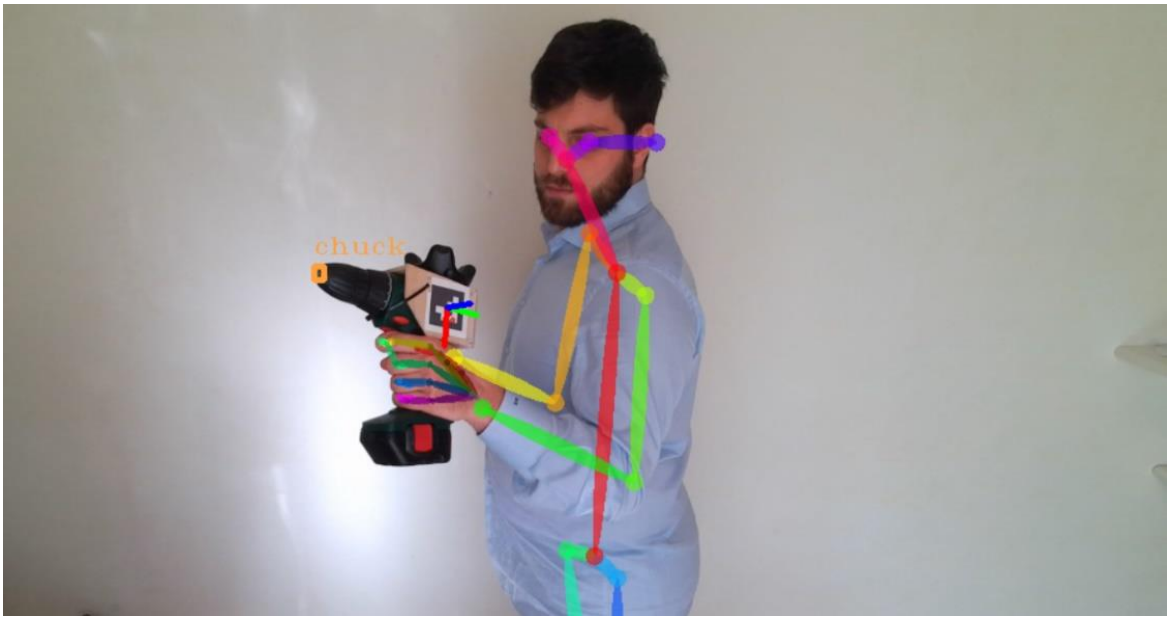

Figure 2.20 Output of the application for a scene with a user holding the power drill.

The application ran on a computer with the following configuration: Intel i7-8750H, GTX 1060 with 6 GB memory and 16 GB RAM. The frame per second (FPS) performance for the frameworks on the machine was the following: YOLO 30+ FPS, AKBT 10 FPS,

OpenPose 10 FPS and ArUco 30+ FPS. The leveling off of all the performances to the lowest FPS (10 FPS) was required. The final performance of the application was under 10 FPS.

Evaluation Metrics The performance of each proposed methodology was evaluated considering both the root mean square point to point distance (D. RMS) and the multivariate R^2 between the estimated and measured tool path. In particular, such metrics have been independently computed for each trajectory of a trial. It is worth remembering that the tool's pose acquired by the HTC Vive system was considered as the measured pose.

The multivariate R^2 index represents how much variability of the estimated path components is explained by the variability of the measured path components. It is then a global indicator of the goodness of the estimation. The R^2 was computed as follows:

$$R^2 = 1 - \frac{SSE}{SST} = 1 - \frac{\sum_{C=X,Y,Z}\sum_{k=1}^{N}\left\|path_C(t_k) - path_C^{est}(t_k)\right\|^2}{\sum_{C=X,Y,Z}\sum_{k=1}^{N}\left\|path_C(t_k) - \bar{path}_C\right\|^2} \tag{2.7}$$

where $path_C(t_k)$ is the value of the measured path component (on the X,Y or Z axis) at the specific sample time t_k, $path_C^{est}(t_k)$ is the value of the estimated path component (on the X,Y or Z axis) at the specific sample time t_k, SSE is the sum of the squared errors and SST is the sum of the squared residuals from the mean $\bar{path}_C$.

Statistics For a deeper look into the difference in the methods, the Friedman test and the Dunn's pairwise post hoc tests with Bonferroni correction on root mean square point to point distance (D. RMS) and multivariate R^2 data were performed for each condition, comparing the four methods. The significance level was set to 0.05. Non-parametric tests were adopted since the assumptions underlying parametric tests resulted in being violated for all sets of data. All the analyses were performed using the SPSS software (Version 21). The correlation data of stationary condition were left out from this analysis, considering it pointless to apply the test in that particular condition because its variability is already explained by standard deviation previously calculated.

2.3.2 Results

For each trajectory estimated by the four proposed systems during the 12 trials, the root mean square point to point distance (D. RMS) and the multivariate R^2 (see Equation (2.7)) between the measured and estimated trajectory were computed.

The results obtained for the stationary, slow-motion and fast-motion conditions are reported in Table 2.3, Table 2.4 and Table 2.5, respectively.

Table 2.3 Mean and standard deviation of root mean square point to point distance (D. RMS) expressed in cm calculated on each trajectory for all methods (stationary condition).

Traj. #	**ArUco**	**AKBT**	**OpenPose**	**YOLO**
1	2.8 (0.4)	6.1 (1.0)	6.1 (0.4)	13.1 (0.5)
2	2.7 (0.4)	8.9 (0.9)	5.3 (0.2)	14.5 (0.4)
3	3.0 (0.4)	6.9 (2.3)	5.6 (0.2)	24.4 (0.5)
4	2.5 (0.5)	5.4 (1.2)	5.9 (0.2)	25.1 (0.4)
5	4.7 (0.1)	2.1 (1.5)	10.1 (0.7)	13.4 (0.1)
6	4.6 (0.8)	11.2 (1.6)	5.1 (0.8)	8.7 (0.4)
7	4.6 (0.9)	10.3 (1.0)	4.1 (0.4)	8.5 (0.3)
8	3.1 (1.3)	7.3 (0.4)	7.6 (0.2)	7.9 (0.1)
9	3.0 (1.0)	9.2 (0.7)	7.4 (0.2)	7.9 (0.1)
10	2.6 (0.4)	8.7 (0.2)	7.2 (0.1)	7.9 (0.1)
11	3.1 (0.3)	8.9 (0.3)	7.1 (0.1)	8.0 (0.1)
12	1.5 (0.1)	15.3 (0.4)	8.1 (0.2)	7.9 (0.1)
	3.1 (1.0)	8.9 (3.8)	6.7 (1.6)	11.9 (6.1)

In order to compare the performance of the methods side by side in the three different conditions, the results were represented in boxplot charts. This is a useful way to visualize differences between groups and to quickly identify information, such as median and data dispersion. The resulting boxplots are shown in Figures 2.21 and 2.22. Then, the Friedman test and the Dunn's pairwise post hoc tests with Bonferroni correction were performed on the data to compare one-to-one the methods and to understand if their distributions were significantly different (Tables 2.6 and 2.7).

Table 2.4 Mean and standard deviation of root mean square point to point distance (D. RMS) expressed in cm and multivariate R^2 calculated on each trajectory for all methods (slow-motion condition).

Traj. #	**ArUco**		**AKBT**		**OpenPose**		**YOLO**	
	D. RMS	R^2	D. RMS	R^2	D. RMS	R^2	D. RMS	R^2
1	7.0 (1.1)	0.99	20.6 (5.3)	0.98	11.2 (1.3)	0.99	14.7 (1.8)	0.99
2	9.0 (3.3)	0.99	23.1 (2.7)	0.97	12.4 (1.3)	0.99	11.6 (1.9)	0.99
3	8.2 (3.5)	0.99	20.0 (1.7)	0.98	11.1 (0.7)	0.99	12.1 (1.2)	0.99
4	9.8 (4.6)	0.99	22.4 (1.5)	0.97	12.6 (0.9)	0.99	13.4 (1.2)	0.99
5	5.0 (2.7)	0.99	18.3 (0.9)	0.92	9.1 (1.9)	0.98	13.4 (3.4)	0.96
6	6.2 (1.9)	0.99	27.5 (15.6)	0.84	10.0 (2.2)	0.98	15.7 (4.9)	0.95
7	9.0 (2.3)	0.98	13.1 (1.4)	0.97	10.7 (1.3)	0.98	12.5 (0.9)	0.97
8	9.7 (4.5)	0.98	15.0 (2.9)	0.97	6.8 (1.5)	0.99	14.9 (6.4)	0.96
9	11.0 (4.7)	0.98	14.1 (3.6)	0.97	6.6 (1.1)	0.99	18.5 (4.5)	0.95
10	8.9 (3.8)	0.98	12.3 (2.3)	0.97	8.1 (1.5)	0.98	13.4 (2.0)	0.97
11	7.4 (2.6)	0.99	31.6 (12.3)	0.83	7.3 (1.8)	0.99	13.0 (1.7)	0.97
12	4.6 (1.9)	0.99	26.9 (2.4)	0.75	8.3 (1.0)	0.97	9.8 (1.4)	0.96
M (SD)	7.8 (2.0)	-	20.0 (6.1)	-	13.3 (2.4)	-	13.3 (2.3)	-

Table 2.5 Mean and standard deviation of root mean square point to point distance (D. RMS) expressed in cm and multivariate R^2 calculated on each trajectory for all methods (fast-motion condition).

Traj. #	**ArUco**		**AKBT**		**OpenPose**		**YOLO**	
	D. RMS	R^2	D. RMS	R^2	D. RMS	R^2	D. RMS	R^2
1	12.5 (6.3)	0.99	25.2 (3.3)	0.97	13.4 (1.8)	0.99	16.6 (2.8)	0.98
2	5.4 (1.7)	0.99	28.7 (1.2)	0.96	11.7 (0.9)	0.99	11.9 (1.1)	0.99
3	12.2 (4.7)	0.99	21.3 (3.1)	0.98	13.1 (2.0)	0.99	14.5 (1.6)	0.99
4	6.3 (1.9)	0.99	21.8 (2.4)	0.97	13.1 (1.8)	0.99	13.5 (2.4)	0.99
5	5.6 (1.0)	0.99	22.6 (0.9)	0.97	11.6 (0.5)	0.99	11.6 (1.7)	0.99
6	13.6 (8.5)	0.98	20.5 (2.9)	0.98	13.0 (1.7)	0.99	15.3 (2.4)	0.99
7	8.7 (6.1)	0.99	18.1 (6.5)	0.98	11.4 (1.6)	0.99	16.3 (4.5)	0.98
8	10.1 (4.0)	0.99	15.5 (5.0)	0.98	11.7 (1.8)	0.99	19.6 (10.1)	0.97
9	9.4 (4.2)	0.99	17.1 (5.6)	0.98	11.6 (1.3)	0.99	14.6 (1.7)	0.99
10	10.7 (6.5)	0.99	15.0 (2.7)	0.99	11.6 (1.4)	0.99	13.9 (2.2)	0.99
11	4.0 (0.6)	0.99	17.4 (4.3)	0.94	10.2 (0.6)	0.98	11.6 (1.8)	0.97
12	5.9 (2.8)	0.99	12.5 (5.4)	0.96	10.0 (0.7)	0.98	10.9 (2.3)	0.97
M (SD)	8.7 (3.2)	-	19.6 (4.6)	-	11.8 (1.1)	-	14.2 (2.5)	-

Table 2.6 p-values of root mean square point to point distance (D. RMS) Bonferroni-corrected post hoc methods comparison for dynamic conditions. Significant results ($p \leq 0.05$) are highlighted in bold.

Pairwise Comparison	**Stationary**	**Slow**	**Fast**
ArUco vs. YOLO	**<0.001**	**0.003**	**0.002**
ArUco vs. AKBT	**<0.001**	**<0.001**	**<0.001**
ArUco vs. OpenPose	0.09	1.00	0.492
YOLO vs. AKBT	1.00	0.772	0.492
YOLO vs. OpenPose	0.41	**0.05**	0.347
AKBT vs. OpenPose	0.201	**<0.001**	**0.002**

Table 2.7 p-values of multivariate R^2 Bonferroni-corrected post hoc methods comparison for dynamic conditions. Significant results ($p \leq 0.05$) are highlighted in bold.

Pairwise Comparison	**Slow**	**Fast**
ArUco vs. YOLO	**0.002**	**0.009**
ArUco vs. AKBT	**<0.001**	**<0.001**
ArUco vs. OpenPose	1.00	1.00
YOLO vs. AKBT	1.00	0.492
YOLO vs. OpenPose	**0.037**	0.106
AKBT vs. OpenPose	**<0.001**	**<0.001**

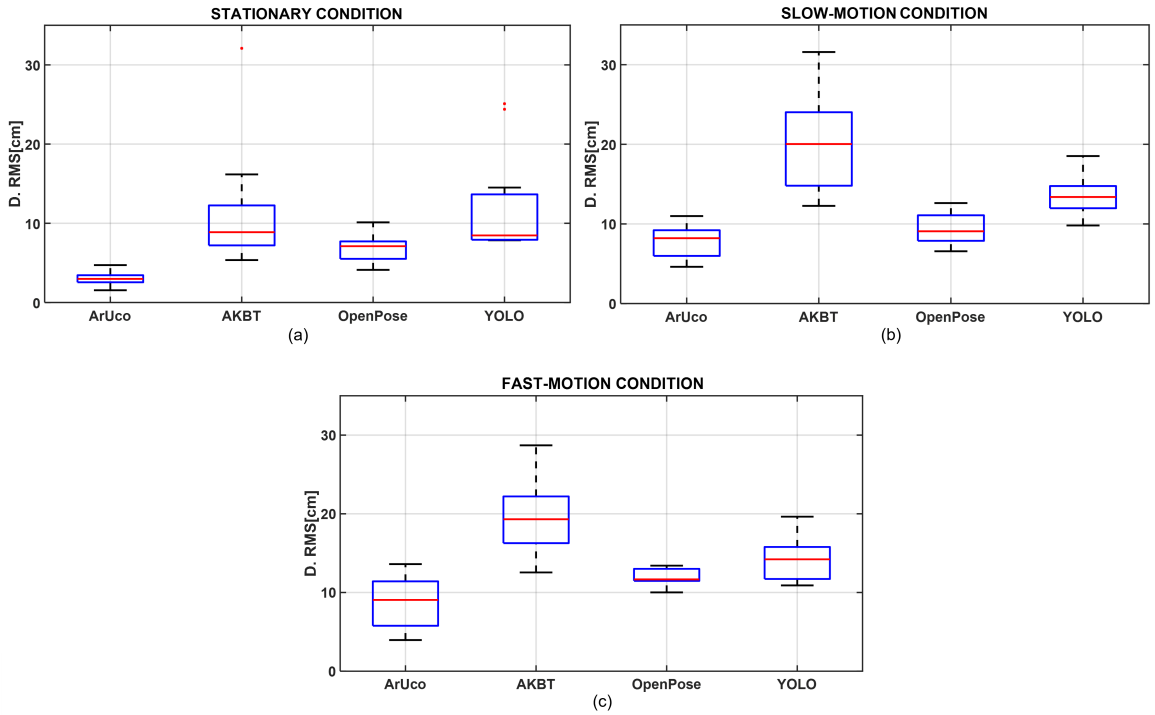

Figure 2.21 Box plots of root mean square point to point distance (D. RMS) expressed in *cm* calculated for (**a**) stationary condition, (**b**) slow-motion condition and (**c**) fast-motion condition.

The results show that, in all of the conditions, the ArUco method has a great performance. Indeed, it shows a significantly lower root mean square point to point distance (D.RMS) than AKBT and YOLO (stationary ArUco vs. YOLO: t-stat = -2.154, p <0.001; stationary ArUco vs. AKBT: t-stat = -2.308, p <0.001; slow-motion ArUco vs. YOLO: t-stat = -1.769, p = 0.003; slow-motion ArUco vs. AKBT: t-stat = -2.538, p <0.001; fast-motion ArUco vs. YOLO: t-stat = -1.917, p = 0.002; fast-motion ArUco vs. AKBT: t-stat = -2.833, p <0.001), but not OpenPose; the ArUco variability increases in dynamic conditions. In addition, OpenPose obtained notable results, showing a significantly lower D.RMS than AKBT and YOLO in the slow-motion condition (OpenPose vs. AKBT: t-stat = 2.077, p <0.001; OpenPose vs. YOLO: t-stat = -1.308, p = 0.05) and only AKBT in the fast-motion condition (t-stat = 1.917, p = 0.002). It appears to be the most reliable in terms of variability compared to all of the methods. On the other hand, the multivariate R^2 results (Figure 2.22, Table 2.7) show that the ArUco performance is significantly better than YOLO and AKBT (slow-motion ArUco vs. YOLO: t-stat = 1.846, p = 0.002; slow-motion ArUco vs. AKBT: t-stat = 2.462, p <0.001; fast-motion ArUco vs. YOLO: t-stat = 1.667, p = 0.009; fast-motion ArUco vs. AKBT: t-stat = 2.583, p <0.001) but is comparable with OpenPose in dynamic

conditions, and also confirm the difference between OpenPose and Kinect (slow-motion OpenPose vs. YOLO: t-stat = 1.385, p = 0.037; slow-motion OpenPose vs. AKBT: t-stat = -2.0, p <0.001; fast-motion OpenPose vs. AKBT: t-stat = -2.167, p <0.001).

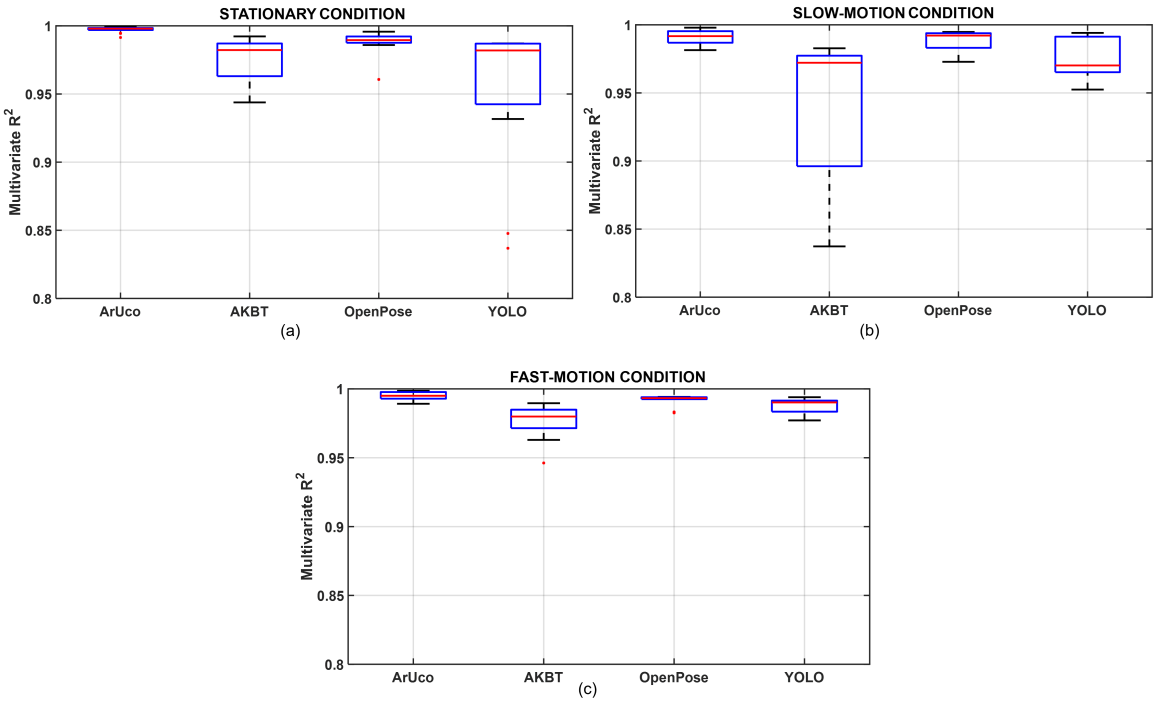

Figure 2.22 Box plots of multivariate R^2 index values calculated for (**a**) stationary condition, (**b**) slow-motion condition and (**c**) fast-motion condition.

2.3.3 Discussion and Conclusions

In order to evaluate and compare ArUco-, OpenPose-, YOLO- and AKBT-based methods, a system composed of an Azure Kinect device, HTC Vive tracking system (the benchmark) and an application with all of the frameworks in one was designed and runt on a computer with this configuration: Intel I7-8750H, GTX 1060 with 6GB memory and 16 GB RAM.

The frame per second (FPS) performance for the frameworks on the machine were the following: YOLO 30+ FPS, AKBT 10 FPS, OpenPose 10 FPS and ArUco 30+ FPS. The leveling off of all performances to the lowest FPS (10 FPS) was required. The final performance of the application was under 10 FPS because it was subjected to the overhead of the post-processing phases and the simultaneous execution of the methods.

An experiment in which a user handling a power drill simulated three different conditions during an assembly procedure was designed: holding the tool in a static position (stationary

condition) and moving the tool at two different velocities (slow-motion condition, 4 cm/s, and fast-motion condition, 8 cm/s).

The performance of the four methods has been evaluated on two metrics: the root mean square point to point distance (D. RMS) and the multivariate R^2 of a trajectory compared to the benchmark system (HTC Vive tracking system).The results have been reported as boxplot charts and a statistical analysis has been performed.

As reported in Figure 2.21, ArUco resulted in a very accurate method in the stationary condition, showing a D. RMS lower than all the other methods and a low variability. The slow-motion and fast-motion conditions boxplot charts (Figure 2.21) show that the better accuracy of ArUco is also preserved in dynamic conditions, even if the variability increases, becoming comparable with the one of OpenPose and YOLO for the slow-motion condition and even being the worst overall for the fast-motion condition. The correlation boxplots in Figure 2.22 confirm the same situations, and the ranking of the methods seems, globally, the following: ArUco, OpenPose, YOLO, AKBT.

ArUco would be the most accurate of the frameworks because it implements a marker-based technique, unlike the others. It confirms the results of other studies, such as [219]. Nevertheless, it is not enough, because an invasive method cannot be seriously considered in a real industrial application; it is rarely accepted, for safety and ergonomics reasons, to install markers on a hand tool and to handle it in a way that always keeps them visible.

Although OpenPose does not have the best performance in term of D. RMS, it could be considered a valid framework for building a virtual guidance system; the low variability of the D. RMS suggests it is a reliable method if the user can accept a D.RMS of around 10 cm. Furthermore, its non-invasiveness and flexibility make OpenPose a brilliant option to adopt. As a matter of fact, its performance is probably reduced by the limited hardware used for the experiment; a network with a higher resolution should improve its performance.

YOLO v4 did not show an exceptional performance, but it has a good variability of D.RMS for dynamic conditions. The main problem of the framework is that it requires being retrained with many pictures of the hand tool under consideration (735 images were used in this study) in order to make the model able to recognize the point/s of interest. This framework would require a deeper investigation exploiting different points of interest for the selected hand tool to be detected and considering a more effective reinforcement learning for the DL model.

Azure Kinect Body tracking returned the worst results. It is certainly an innovative, compact, lightweight and well-documented framework; its DL model capabilities and accuracy improve with time thanks to continuous support from Microsoft. A study could be designed,

in order to reinforce the model performance, on tracking some interesting points of the upper limb for more accurately deriving the hand tool position.

In this study, a literature review and market research was conducted , looking for studies and out-of-the-box solutions that proposed or implemented methodologies for hand tool pose estimation during assembly and maintenance procedures in the industrial field. They discovered that, even if there are plenty of studies concerning static and dynamic object pose estimation in the literature, the problem of occluded hand tool pose estimation and tracking in the industrial environment is not extensively investigated. Furthermore, it emerged that all of the commercial solutions do not really implement algorithms that are able to accurately track the pose of a tool partially occluded by the operator's hands, but they roughly derive it by the hand pose or by using color matching techniques.

For this reason,four of the most promising computer vision and deep learning frameworks (ArUco, OpenPose, YOLO and AKBT) in the field were selected to evaluate their performance in the task of industrial hand tool detection and pose estimation in real-time during an assembly or maintenance procedure. Two different approaches have been considered: a direct approach, in which the tool is directly detected and tracked using some robust features that are visible, and an indirect approach, in which the body joints of the operator and their hands are detected and tracked, and the tool pose is derived by considering the unique handling pose of the tool. This study is the first that compares the performance of ArUco-, OpenPose-, YOLO- and AKBT-based methods side by side in the task of occluded hand tool tracking.

In order to fairly compare these frameworks, the objective was redefined, reducing the pose estimation problem to only 3D position estimation, because it is intuitive that a method such as YOLO, which only returns a position estimation, requires being complemented with another technique for orientation estimation. A complete pose estimation investigation is worth a further study.

The results of the study suggests OpenPose is the most complete proposal, thanks to its acceptable root mean square point to point distance, D. RMS (approximately 12cm) and low variability in dynamic conditions, even when a limited network resolution is adopted. This framework is worth a dedicated study in order to exploit all model capabilities in extracting the information with a higher accuracy. OpenPose could be used to implement a tool pose estimation module in a smart workstation for training and assessment. A system designed with this feature would have a great impact in the automotive industry, especially for critical procedures that require monitoring, with high accuracy, the movements of the operator and the correct usage of hand tools for battery-pack assembling, engine repairing and overhauling, glue smearing and adhesive and sealant application. Two more topics

are worth of investistigation in future studies: the problem of complete pose estimation (including orientation) and to conduct a deeper study on OpenPose, implementing a pose estimation module based on it and evaluating the performance in experiments that simulate procedures at different levels of complexity.

2.4 Toyota Proof-of-Concept: Maintenance Training Digitalization

During my PhD I had the luck to touch with my hands this culture spending 6 months as Digitalization Engineer of Production Engineering Innovation(PEInno) division in the Toyota Motor Europe Technical Centre (Bruxelles). As Digitalization Engineer, I was involved in different projects related to the digitalization of processes to reduce the lead-time in vehicle production. In particular, I became the responsible of a Proof-of-Concept project concerning the Digitalization of Maintenance Training with enabling technologies.

The objective of this pilot project can be summarized as follows:

- Investigating AR/VR/MR based learning environments for maintenance training efficiency/leadtime improvement;
- Reducing maintenance dojo (training rooms) investment for physical training assets;
- Finding the best way to have a clear visualization of maintenance skills mapping in all the Toyota Manufacturing Plant in Europe.

The Toyota Production System is a production system that has been established based on many years of continuous improvements, with the objective of "making the vehicles ordered by customers in the quickest and most efficient way and deliver the vehicles as quickly as possible". The Toyota Production System (TPS) is based on two concepts:

- JIDOKA (which can be loosely translated as "automation with a human touch") which means that when a problem occurs, the equipment stops immediately, preventing defective products from being produced;
- "Just-in-Time," in which each process produces only what is needed by the next process in a continuous flow.

Based on the basic philosophies of jidoka and Just-in-Time, the TPS can efficiently and quickly produce vehicles of sound quality, one at a time, that fully satisfy customer

requirements. These concepts are part of one of the most important principle in the Toyota culture that is Kaizen or continuos improvement. Kaizen is a daily process whose purpose is the improvement of production efficiency through the humanization of the workplace:

- Designing the production line and the processes connected to it following the needs of the Worker;
- The progressive elimination of heavy and / or repetitive work ("walls") with extensive use of automated processes;
- Continuous training of personnel technological retraining processes and dedicated learning stages;
- Staff training in the use of the scientific method to find and eliminate waste ("muda");
- The involvement and identification of personnel with the company vision.

According to the Kaizen approach, the humanization of the workplace, at the level and involving any business process, leads to an increase in productivity: "the idea is to nourish the human resources of the company by praising them and encouraging them to participate in activities related to Quality[34]". The connection between this principle and Industry 4.0 is intuitive. Indeed, Toyota culture embraces many paradigms of Industry 4.0 even before the trend spread.

2.4.1 Background

The trigger point of the pilot was the situation in Toyota Motor Manufacturing France (TMMF). In this plant overtime and weekend productions were becoming were necessary to catch back the planned volumes. So data were collected from the plant to investigate the phenomen with a focus on the weld shop. It emerged that the Operation Production Ratio (OPR) of the weld shop was lower than expected; in 2019 linestops were around 16825 min. The low OPR was directly connected to a long Mean Time to Repair (MMTR) (average 5.6 min for robots). If a long MTTR for old generation robots breakdown were mostly due to wear and tear and it could be beat only replacing them with new generation ones, new generation robots MTTR were due to low maintenance skills for recovery. In particular, Kawasaki BX robot series was investigated deeper considering that the 60% of the robots adopted in TMMF were this kind and it's a relative new generation. An screening on

maintenance members of TMMF was conducted and it resulted that only 3 on 40 operators were fully trained on all BX Series maintenance procedures.

Maintenance procedures of industrial robots are complex and require a large number of training hours in classrooms and hands-on sessions. Furthermore, especially in times of restrictions related to the pandemic, only a few trainees could access training on a physical asset at the same time, and their availability was always a trade-off with production line efficiency. Training all the operators of a plant in a reasonable lead-time is a huge challenge. Indeed, a maintenance member usually reaches the expertise that makes him independent in all the procedures in almost 10 years. This is really inefficient if you think a robot series obsolescence in the shop is around 20 years.

A radical transformation of maintenance training approach was required to reduce the lead-time and improve the efficiency of the plant, digitalization of the training experience could be the solution.

2.4.2 Proof-of-Concept (POC)

A Proof-of-Concept project was design in order to develop and test the efficacy of an interactive digital experience for training maintenance members and evaluating their learning.

The main requirements identified for the solution were the following:

- Reduce training leadtime (50%) "Train Anytime Anywhere Simultaneously";
- Easy to use (Smartphone/Tablet);
- Training without a trainer;
- Evaluating the trainee without a trainer;
- Reduce vendor support for equipment maintenance(-50%);
- Improve maintenance skill = Lower MTTR in production (-5:10%);
- Increase reuse of maintenance instructions across Europe;
- Digital model (3D, Video & image) based learning to reduce language dependency;
- Training without physical assets;
- Organization know-how management through system based assessment.

Evaluation Criteria	Current (paper)	AR	VR	XR	Expert Video
3D Data Necessity	○	△ (-)	✗	✗	○
Interactivity	△ (-)	△ (+)	○	△ (+)	✗
Evaluation/ Progress Tracking	△ (-)	○	○	○	△ (-)
Easy to edit	○	△ (+)	△ (+)	△ (+)	○

Figure 2.23 Evaluation of digitalization technologies comparing them to classical approaches. The approach is evaluated (**Green Circle**) positive, (**Yellow Triangle**) partially positive, (**Red Cross**) negative based on the criteria.

In order to digitalize the training experience in a comfortable solution, enabling technologies AR, VR and MR (2.1.3) were investigated and evaluated based on the following criteria:

- 3D Data necessity;
- Interactivity;
- Evaluation/Progress tracking;
- Easy to edit.

The results are summarized in the cross-table of Figure 2.23.

AR and MR were selected as effective technology for an interactive maintenance training platform. Mobile devices and tablets were selected as target devices.

BX robot series was selected as Use Case of the POC. The 5 most occurring maintenance procedures were chosen as the maintenance training experiences to be digitalized.

After all, POC specs with details about the experience requirements, technology to adopt and the Use Case were drawn up.

POC specs were issued to 6 identified vendors of digital solutions, some big players on the panorama and some small companies. All the vendors returned a quotation for developing the solutions and details about licensing model. Only four of them were selected for the POC. Each vendor was engaged to implement a different combination of 3 procedures on 5 of BX

robot series in AR. Furthermore, two vendors implemented also 1 additional procedure in MR for HoloLens 2 headset.

All the vendors designed and developed their solutions under the guide of TME, a constant interaction between TME responsible of the project and them was the key of a satisfying result from all vendors. The development required almost 3 months.

2.4.3 Evaluation of POC Output

In order to select the best solution among the ones provided by the vendors, two different levels of evaluation were performed:

- **PEInno Evaluation** - to evaluate the solution against the PEInno initial requirements;
- **EMCs Evaluation** - to evaluate the effectiveness of the solution in the plants.

PEInno Evaluation The output of the POC was evaluated by the members of PE Innovation division. A set of KPIs (Key Performance Indicators) with a scoring system was defined in order to evaluate each solution against the others. The KPI were grouped in three macro-categories and they can be summarized as follows:

- COMPLIANCE WITH REQUIREMENTS

  Completeness - the Vendor has completed XX% of all the Use Cases assigned;

  Supportability – the solution can be used on both iOS and Android devices;

  Data Compatibility – the solution supports Catia, Creo, JT.

- UTILITY

  Usability - the solution is easy to use and implement the common best practices of software Usability;

  Learning/ Evaluation Effectiveness - the solution is effective for the maintenance training and the evaluation of what learnt.

- FUTURE BUSINESS

  Maintainability – the solution admit the update of manuals by Toyota Members.

  Sustainability of the Solution – the solution is reasonable in term of deployment and running costs.

  Interoperability – the solution support PLM platform connection

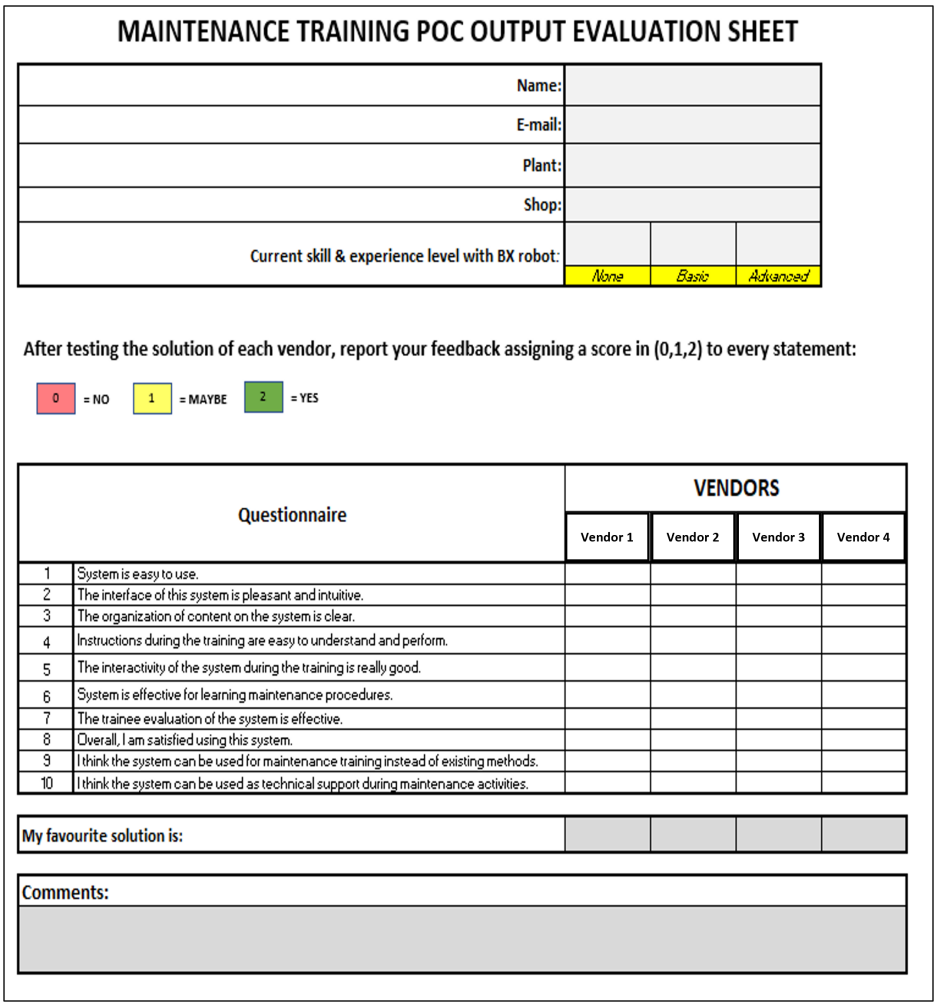

MAINTENANCE TRAINING POC OUTPUT EVALUATION SHEET

Name:			
E-mail:			
Plant:			
Shop:			
Current skill & experience level with BX robot:	None	Basic	Advanced

After testing the solution of each vendor, report your feedback assigning a score in (0,1,2) to every statement:

0 = NO 1 = MAYBE 2 = YES

	Questionnaire	VENDORS			
		Vendor 1	Vendor 2	Vendor 3	Vendor 4
1	System is easy to use.				
2	The interface of this system is pleasant and intuitive.				
3	The organization of content on the system is clear.				
4	Instructions during the training are easy to understand and perform.				
5	The interactivity of the system during the training is really good.				
6	System is effective for learning maintenance procedures.				
7	The trainee evaluation of the system is effective.				
8	Overall, I am satisfied using this system.				
9	I think the system can be used for maintenance training instead of existing methods.				
10	I think the system can be used as technical support during maintenance activities.				
	My favourite solution is:				

Comments:

Figure 2.24 The first page of the questionnaire dispensed to the testers for evaluating the POC solutions.

After the evaluation in PEInno division, Vendor 3 and Vendor 4 solutions obtained the best scores.

EMCs Evaluation The ouput of the POC was evaluated by maintenance operators and trainers across all Toyota Europe Manufacturing plants. A sub group of maintenance operators with all levels of experience and trainers in all Toyota Euope Manufacturing plants (France, Turkey, Czech Republic, United Kingdom, Russia) were selected to take part in the evaluation process. All of them were trained on the basics of each solution through some demonstrations and video tutorials. A different set of KPIs was identified in this case and a questionnaire (Figure 2.24) with a scoring system was generated as a friendly method for the testers to submit their evaluation of the solutions.

The testers evaluated the solutions in a 4 weeks evaluation window, Vendor 4 solution obtained the best score from the EMCs. At the end, Vendor 3 and Vendor 4 were selected for a discussion about potential future business.

2.4.4 Conclusions

As responsible of the POC on Maintenance Training Digitalization, I took part and contributed in all stages of the projects that can be organized in two big sections: Strategy and Budget Approval, POC Execution.

Concerning the Strategy and Budget Approval my contributions can be summarized as follows:

- TMMF problem investigation, data collection and analysis;
- solution design and specs definition;
- technologies evaluation;
- vendors engagement and evaluation;
- business value analysis;
- Ringi (POC Budget Approval request) preparation, presentation and submission.

Instead during the POC Execution my activities were the following:

- vendors agreement;
- Hardware procurement;
- POC execution scheduling definition and agreement;
- weekly review meetings with each vendor;
- stackholders collaboration management;
- vendors output testing and feedback;
- evaluation KPIs definition and sharing;
- vendors output presentation to the panel of maintenance operators and trainers across all Toyota plants.

During my visiting period at Toyota Motor Europe I was a strong contributor in setting the direction for future of Maintenance training in EMC's. My previous experience and knowledge and deep analysis of Customer needs helped to define a beneficial approach towards digital maintenance training. I followed a logical approach to breakdown the problem, evaluate the solutions and propose an approach that is more suited and manageable in the given scenario. I positively received the feedback from various stakeholders during the budget approval process and refined the strategy to ensure the required budgets were signed off and the project kicked off in a timely manner. Corporate experience contributed to connect my research results around Industry 4.0 approaches to the concrete needs of a real industry made by humans.

Chapter 3

Enabling Technologies for Healthcare 4.0

3.1 State of the Art

This chapter describes the paradigms of Healthcare 4.0 focusing on the usage of enabling technologies for develop new rehabilitation protocols.

3.1.1 Introduction

Healthcare 4.0 [220, 221] is a newly coined concept that is developed from Industry 4.0., which represents the fourth manufacturing revolution. Ultimately the concept lies around smart machines that get access to large amounts of data, which allows them to make decisions without human involvement. Many aspects make up Industry 4.0. Cloud computing, Big Data, Internet of Things, various forms of wireless Internet and 5G technologies, cryptography, the usage of semantic database design, Augmented Reality and Content-Based Image Retrieval are all part of the Industry 4.0 Standard. These technologies are now at the heart of the so-called Fourth Industrial Revolution (or Industry 4.0), which sees the digital, physical, and biological worlds converge. When it comes to Healthcare 4.0, it refers to a wide range of possibilities for using Industry 4.0 technologies to improve healthcare as it lays out a new and innovative vision for the health sector. The objective is to provide patients with better, more value-added, and more cost-effective healthcare services while also improving the industry's efficacy and efficiency. Healthcare is one of the most anticipated areas in the 4.0 revolution to achieve great results. Today's industry is more computerised than in previous decades, with x-rays and magnetic resonance imaging giving way to computed tomography and ultrasound scans, as well as electronic medical data. As Healthcare 4.0 enhances the healthcare experience, it successfully improves the quality, flexibility, productivity, cost-

effectiveness, and dependability of healthcare services [222]. The Internet of Health Things, medical Cyber-Physical Systems, health cloud, health fog, big data analytics, machine learning, blockchain, and smart algorithms are all integrated and used. There are some limitations, however, to keep in mind. Building and using healthcare software that matches the Healthcare 4.0 paradigm is doable, but a difficult and time-consuming task and often requires niche specialists. The focus of the thesis is the design and development of innovative rehabilitation approaches for movevement disorders using enabling technologies derived by Industry 4.0.

3.1.2 Upper Limb Rehabilitation with Myo-control and Synergies

The ability to reach, manipulate, and interact with objects has always been a fundamental ability of humans that has defined their survival and ingenuity. It has been shown that in the majority of stroke patients upper limbs are more severely involved than lower limbs, as most strokes occur in the territory of the middle cerebral artery [223]. In fact, it is estimated that up to 80% of stroke survivors have upper limb impairment early after stroke [224–226], with just a small percentage of patients demonstrating complete functional recovery at 6 months post-stroke [227]. Apparently, stroke sub-type could significantly determine the outcome of the recovery [227] leading to mismatches with previous studies, regarding differences between upper and lower limb lesions. In some cases, like impairments deriving from anterior circulation ischemic stroke, the severity of motor impairment and patterns of motor recovery were similar for the upper and lower extremities [228], while other circulation infarcts could advantage lower limb recovery. Generally, upper limb rehabilitation trials, designed to improve recovery rates, have been unsuccessful and, as a result, the burden of upper limb impairment after stroke remains high [229, 230]. Nevertheless, rehabilitation robotics appeared as a breakthrough in trials design, thickening the overall complexity of rehabilitation platforms but promising much better results, under the aegis of a greater involvement, assistance, and continuous motor functions assessment. The way patients interact with the robotic device is of crucial importance, as many research teams constantly pursue the way of a natural and intuitive human-machine interface. Several robot control strategies have been developed, and the one most appropriate to implement strongly depends on patients' residual motor capabilities. These strategies range from being impedance/admittance based, to adaptive control techniques, to exploiting bio-signals [231]. In the latter case, electromyographic and electroencephalographic (EEG) signals can be used to intercept the patients' intention of movement even when residual motor activity is low. EMG-based and

EEG-based strategies can be built on top of an intuitive and natural interaction scheme. The latter greatly suffer the scarce reliability of electroencephalographic signals as a control input and thus struggle to achieve decent performances for clinical or commercial use. EMG signals, however, have been successfully employed in prostheses control and as a biofeedback provider for years. In addition, these same signals could be used to extract co-contraction patterns and muscle synergies, as useful tools for both motor functions assessment and control generalizing modules. Currently, with the help of machine learning it is possible to build functional model-free strategies, simpler than more complex neuromusculoskeletal models, that can be used to estimate motion intentions. Nevertheless, to increase the usability and usefulness of such systems, models should be able to generalize in various poses of upper limbs without requiring strenuous and long-lasting training sessions. This aspect comes from the mean available time for one-to-one patient therapy, and from the overall complexity of use of said clinical systems, concurrently reducing the accessibility costs of rehabilitation. Moreover, therapists should be free to design exercises without being limited by system's constraints, thus avoiding the risk of skipping on using the technology altogether [232]. In this chapter, it's described the main contributions of EMG-based control systems to the field, and highlighting how the myo-controller can be used to estimate users' hand force on the horizontal plane in different upper limb poses. Furthermore, it is presented a way to optimize the myo-control by reducing the recorded muscles without affecting the estimation performance. In the context of using muscles synergies in both control and assessment schemes, both usages have been investigated, as well as an alternative way to extract them using machine learning techniques.

The literature is disseminated with robot control schemes based on electromyography both for rehabilitation and prostheses control purposes. The main advantage of these systems is the ability to decode the movement intention, building a control signal for supporting that movement in the right direction and with the correct intensity. Invasive and non-invasive methods exist to register and action these signals through the measurement of descending driving signals either directly from the muscle fiber with needle electrodes or attaching adhesive electrodes on the skin surface. In the latter case, the measured signal is also called "surface EMG" or, simply, sEMG and aims at monitoring the electrical activity of more fibers on the targeted muscle. Since rehabilitation therapies are, generally, long lasting processes that cover several weeks, non-invasive measurements are preferable, also considering the discomfort caused by the motor impairment itself. When dealing with individuals with low muscular activity, the trade-off between robot support and the involvement in the required task, is of crucial importance. As mentioned in the introduction, in fact, the 'assistance-as-

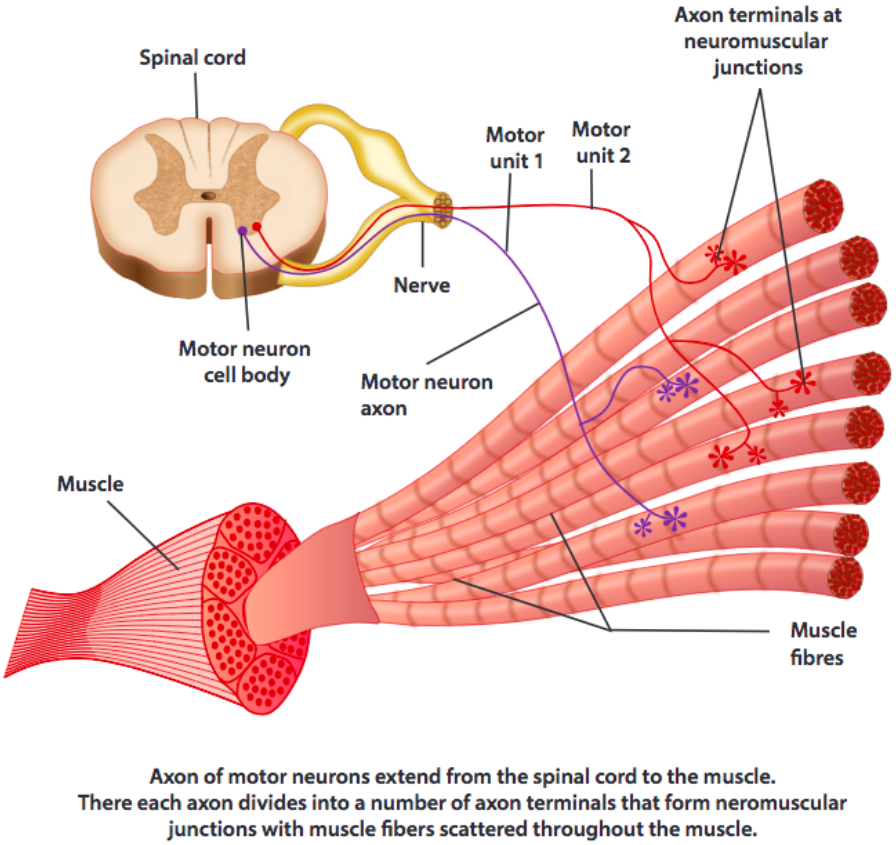

Figure 3.1 Motor units components. Each muscle is a hierarchical structure, organized in concentric bundles, and its inner layer (fiber) gets innervated by the motor neuron.

needed' paradigm takes place and several studies have been conducted trying to find a control signal based on the users' effort or muscular activity. In this paragraph it will be presented an overview of the state-of-the-art EMG-based systems, and it will also be highlighted how some limitations have led to further studies in the field of myo-controllers.

3.1.2.1 The biomechanics of movement

The generation of movements in humans is the macroscopic result of a complex series of biochemicals phenomena that originate in the primary motor cortex of the brain and terminate on a muscle fiber. The intention of movement triggers electrical impulses that travel through the spinal cord down to peripheral nerves, made by a motor neuron and its axons, that innervate a set of muscular fibers. This nervous structure together with the targeted fibers compose a motor unit (MU, **??**).

The macroscopic movement (e.g. of a limb) is the result of multiple contractions of muscles fibers, that start with a depolarization wave, caused by the release of sodium molecules when the impulse hits the fiber (action potential), and ends with micro-shifts between myosin and actin proteins. Contractions can occur with the shortening (concentric) or the stretching (eccentric) of fibers, or with no modifications to the fiber length (isometric). Invasive electromyography aims at precisely understanding the behavior of a particular fiber, by directly measuring the variations in electric potential on the fiber. Surface electromyography aims at measuring the sum of action potentials that elicit in a wider region of the skin, targeted by the electrode, and it is called motor unit action potential. sEMG signals are composed by a "train" of these impulses that can have a negative or positive amplitude. The raw sEMG signal cannot be used in a control scheme and it generally undergoes a series of processing operations for the extraction of the informative content.

Features and processing of electromyographic signals sEMG signals amplitude depends on the specific muscle tone and transversal section, and it ranges in the $\pm 5000\ \mu$V interval. The power spectrum of these signals typically covers a 6-500 Hz band, usually reaching a peak between 20-150 Hz: spectrum features change according to muscle fatigue conditions, enriching low-frequency components due to the recruiting of the biggest motor units. Also, sEMG signals' features strongly depend on the way these are acquired, and several operations are needed for a correct acquisition. "Surface ElectroMyography for the Non-Invasive Assessment of Muscles" (SENIAM) project designed a standardized procedure for the electrodes positioning, maximizing the signal-to-noise ratio [233]. Following signal acquisition, the pre-processing phase takes place for the extraction of the muscle activation profile. As SENIAM project outlined the operations prior to signal measurement, "ISEK Standards for Reporting EMG Data" designed EMG signal processing guidelines. First, any DC offset or low frequency noise should be removed from raw EMG signals. This filtering stage could be either hardware or software and it is usually composed by a 20/30Hz-500Hz band-pass filter and by a 50Hz notch filter. After that, signals can be rectified by taking the absolute value of each temporal sample. Finally, it is applied a normalization and a low-pass (also called envelope) filtering. The rectified EMG signal normalization is achieved by dividing its value by the peak of rectified EMG values, obtained during the maximum voluntary contraction (MVC). The low-pass filtering (1-10 Hz) is applied by using a 2nd or higher order filter and it is used to include the lowpass filtering effect of the muscle, due to muscle force being a low frequency signal. At this point, the sEMG could additionally undergo two more operations that characterize the actual contraction process: the activation

dynamics and the non-linearization. The former includes in a single equation the actual delay that elapses between the action potential elicitation and the contraction start, that is typically very short (10 ms) but could get up to 150 ms in certain conditions [234], and the 2-nd order model of the twitch generation dynamics [235, 236]:

$$u(t) = \alpha e(t-d) - \beta_1 u(t-1) - \beta_2 u(t-2) \tag{3.1}$$

where d represents the electromechanical delay, e(t) the processed sEMG signal, u(t) the so-called neural activation, and α, $beta_1$ and $beta_2$ the coefficients. These parameters should be set under the following constraints:

1. $\beta_1 = \gamma_1 + \gamma_2$;
2. $\beta_2 = \gamma_1 * \gamma_2$;
3. $|\gamma_1| < 1$;
4. $|\gamma_2| < 1$;
5. $\alpha - \beta_1 - \beta_2 = 1$.

Non-Linearization occurs in the event of high-amplitude muscle activations to overcome the non-linear variation in force, generated by muscle contraction, with sEMG. Several studies proposed a non-linear contribution [237–241] given by the following equation:

$$a(t) = \frac{e^{Au(t)} - 1}{e^{A} - 1} \tag{3.2}$$

with the A parameter, that assumes negative values, that regulates the non-linearity effect on the neural activation u(t).

3.1.2.2 EMG-based control strategies

Electromyography has been in use since 1960 to control external devices and dozens of different control strategies have been developed, always pursuing something useful to be delivered for clinical uses. Electromyography can be used as a triggering command for actuated rehabilitation systems or under the paradigm of a “simultaneous and proportional control” (SPC). In SPC-based systems the EMG measures are continuously fed into the torques/forces estimation process rather than triggering a pre-defined actuation after reaching a threshold on the muscular activation. Currently, very few platforms have been successfully tested

in a clinical environment, mostly still being at the laboratory stage with healthy subjects. EMG-based systems can be mainly categorized in two groups: model-based and model-free systems. Model-based approaches comprise of kinematics models, musculoskeletal models, or dynamic models while model-free systems utilize artificial intelligence methods, such as neural network, regression models and factorization algorithms [242]. Model-based algorithms are usually more complex and accurate than model-free systems and, concurrently, require a time-consuming calibration procedure, also bringing a higher computational cost. Kinematics models mainly aims at finding parameters such as positions, orientations, velocities, and accelerations. They employ forward and inverse kinematics, together with the dynamic modeling of upper limbs, and they determine torques or forces by considering the weight and force of the limb as an input to a function of inertia, Coriolis, centrifugal, and gravity vectors [243–248]. Neuromusculoskeletal models instead aims at computing the muscle force by using a muscle contraction model. For example, Huxley-type models employ a complex set of differential equations that need a numerical integration [249–251], gradually replaced by Hills-type models, being simpler and with a lower computational cost and representing a good solution for real-time upper limb torques/forces estimators [252–255, 255, 256]. Model-free algorithms try to bypass the muscle contraction dynamics modeling, building an input/output relation using machine learning techniques. Usually, these algorithms require training/validation phases and rely on generalization capabilities for estimating upper limb muscles torques/forces in unknown conditions. Model-free algorithms have been extensively used in two main applications: patterns or motions classifiers and continuous torques/forces estimators. In the former case, machine learning techniques are employed in training these systems to recognize a finite set of limb or hand poses, using several time-domain or frequency-domain EMG features. In this context, there are many examples of applications with neural networks, linear discriminant analysis, support vector machines, random forest, PCA and hybrid techniques [257–265]. In the latter case, the goal is estimating limbs or fingers torques/forces in every moment, extracting, the same features from EMG signals. The scope of such systems is much broader than the previous ones, since they would allow for a continuous support, if coupled with an end-effector robot or exoskeleton, or even driving a prosthesis. Also in this case, neural networks have been used for estimating joint torques in dynamic conditions [266–269], as well as neuro-fuzzy controllers, proportional controllers, linear, and non-linear regressions [270–275, 275–277]. These systems build the control signal on time-domain features like mean absolute average or root mean square of a pre-defined time window. Also frequency-domain features have been extensively used for the same objectives, mostly concerning the median frequency or

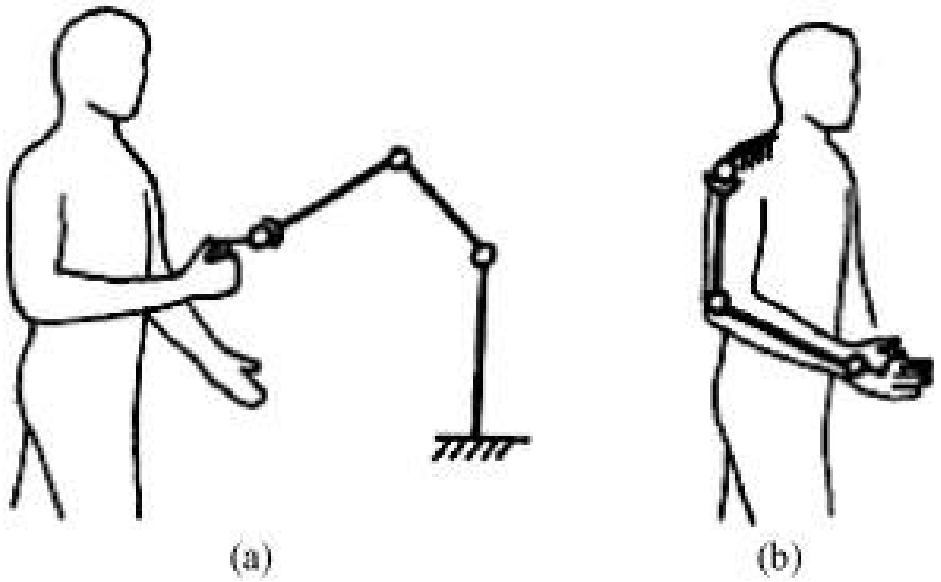

Figure 3.2 End-effector robots (a) vs exoskeletons (b).

mean frequency, extracted from the signal power spectrum. Under the paradigm of SPC systems, most of continuous torque/force estimators are suitable for rehabilitation systems. The therapist can, thus, design several task-oriented movements (e.g. reach and grasp), having a robotic system that continuously support patients' movements, as much as needed for regaining limbs motor control.

Myo-controller in clinical rehabilitation platforms Robotic systems are used in various medical disciplines and different highly specialized applications, for example, in the field of minimally invasive surgery [278]. In addition, clinical use of robots in the rehabilitation field has produced a few examples of robust and intuitive systems, suitable to be involved in large-scale trials. Most systems have been evaluated in laboratory environments only, leaving the robotics rehabilitation efficacy not fully understood. Starting from the 1990s, among robotic devices, two main types have been tested in clinical environments: end-effector robots and exoskeletons [279].

End-effector type devices are simple in structure, easily adjustable as they are attached to only one point to the patient's limb during therapy, mostly allowing only planar motion. Furthermore, end-effector robots have relatively lower cost compared to exoskeletons, and they have hit the market sooner making them the first rehabilitation robots prototypes. Several platforms have been delivered in clinics, obtaining significant motor recovery outcomes with reference to traditional therapies, without aforementioned natural control strategies [280–

289]. They generally employ force-feedbacks or torque controls and automatized exercises without the constant intervention of a therapist. A very limited set of these systems has been tested in clinical trials on stroke subjects with EMG-based control strategies, aiming at the recovery of upper extremities' motor functions. MIT-MANUS device is an example of end-effector robots with a simple EMG-threshold actuation method, supporting planar motion of patients' paretic limb (3.3). Several clinical studies have been conducted using commercial versions of MIT-MANUS, mostly revealing the overall efficacy of robot-aided rehabilitation [290–293].

Upper extremities exoskeletons, on the other hand, started to spread in the first years of the new century, as a new standard for assistive platforms. The advantage of such mechanisms is that they follow the kinematic structure of human limbs, allowing for a coherent support of all anatomical articulations and, thus, granting a joint-specific measurement. Also in this case, a few examples of effective rehabilitation sessions with these devices exist, with the rest of them still exploiting control strategies that are not based on myoelectric controls [294–297]. The Hand of Hope is a rare example of EMG-driven exoskeleton in which electromyography is an active part of the control scheme and not only a way of supplying bio-feedbacks to users. The Hand of Hope has been effectively tested with stroke survivors, showing significant improvements with reference to standard rehabilitation therapies [298, 299].

Limitations The aforementioned overview is a sample of past and present devices and of control strategies in the state of the art. It also highlights important gaps between what happens in lab environments and what is commercially and clinically available, with regards to myo-controlled robots. In particular, the reader can notice how patterns classification algorithms have limited usefulness, especially if framed in clinical trial conditions, since they do not allow for the planning of an exercise framework thus limiting the freedom of the intervention of therapists. Except for EMG-based hand training devices, myo-controlled integrated multi-DoF exoskeleton systems still struggle to appear on the market or in intensive care programs, failing to show significant benefits in clinical trials. The reason for this lag in adoption may rely on the intrinsic difficulty in managing both the highly redundant human arm kinematics and the intention of movement, by only employing simple strategies based on muscular activations. As showed in previous paragraphs, model-based algorithms are complex and difficult to calibrate, suggesting that model-free techniques would be easier to deploy. Even if there is evidence that robotic interventions improve upper limb motor scores and strength, these improvements are often not transferred to performance of ADLs [300]. One of the biggest studies on robotics rehabilitation efficacy, conducted by Albert

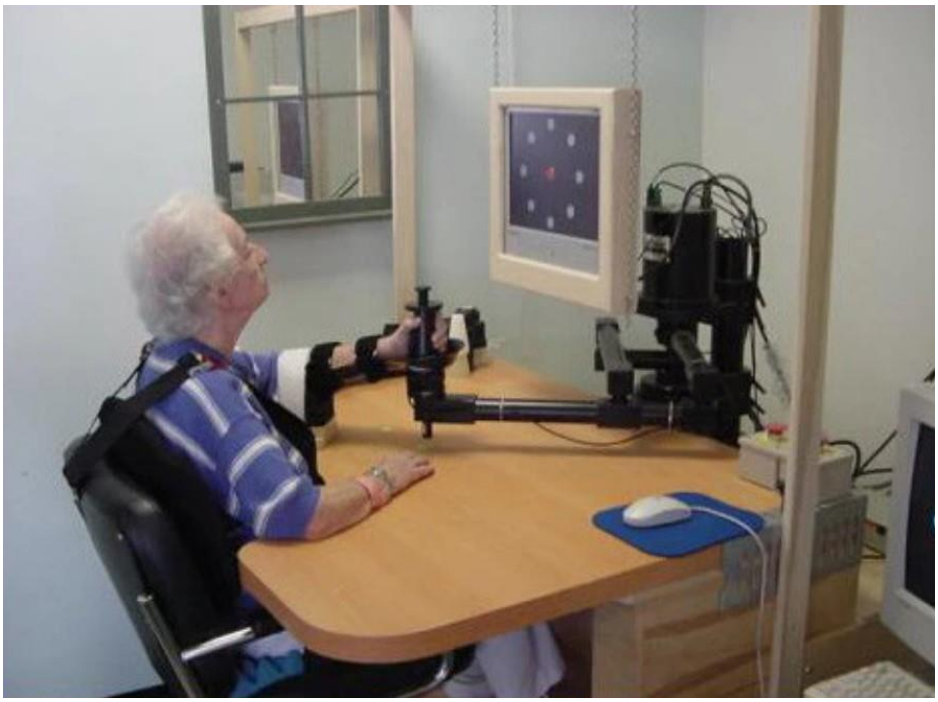

Figure 3.3 Stroke Inpatient during therapy at the Burke Rehabilitation Hospital (White Plains, NY). Therapy is being conducted with a commercial version of MIT-MANUS (Interactive Motion Technologies, Inc., Cambridge, MA).

Lo et al., showed greater improvements on long-term therapies if myo-controlled robotics rehabilitation was carried on, rather than with traditional care programs [301]. However, no significant differences were found when analyzing performances at 12 weeks. Training sessions were divided in single-DoF sub-sessions, significantly extending the duration of any therapy, being less intuitive for the patient and for the therapist, and not suitable for home therapies. Also in another study, robot-aided sessions outcome did not show any significant difference compared to unassisted reaching practice, suggesting that future studies should carefully control the amount of voluntary movement practice delivered to justify the use of robotic forces [302]. The MIT-MANUS example suggests that EMG-driven systems could bring great benefits, to patients with low residual muscle activity, however further efforts are needed, to build more standardized platforms and tailored protocols, alleviating as much as possible the burden of technology off the therapists. In a recent article, Krebs et al. asserted that “there is no magic bullet in rehabilitation” and each patient and lesion is unique in stroke rehabilitation, so there is no reason to believe that a one-size-fits-all optimal treatment exists [303]. To improve current upper limb rehabilitation techniques multi-DoF, SPC EMG-driven platforms can be suitable, adding the advantage of a bio-inspired kinematic of exoskeletons

and, thus, delivering a compact and functional device, adaptable to customized protocols within clinical and home therapies, easily interfaceable with serious games.

3.1.2.3 Muscle synergies

A preponderant issue of motor control is the way the central nervous system (CNS) generates the muscle activity to perform such a wide variety of tasks. The complexity of the musculoskeletal apparatus allows for a dexterous and redundant approach to most of the behaviors but also makes the control problem challenging. Muscle synergies, coherent activations, in space or time, of a group of muscles, have been proposed as building blocks that could simplify the construction of motor behaviors [304]. Since motor control and stroke are strictly related, in the last years the concept of muscle synergies has landed in the rehabilitation robotics field, specifically enriching myo-control features or existing motor functions assessment tools. In this paragraph an overview of the muscle synergies theory will be presented and how they have been used in the last years in robots control schemes or assessment tools. Moreover, an innovative synergies extraction algorithm, based on autoencoders networks, will be described, also highlighting how the informative content of synergies can be specialized involving data coming from the performed task.

Synergy derives from the Greek word "συνεργία" or "συνέργεια" composed by "σύν" that means "together" and "ἔργω", "work, act". Muscle synergy, in brief, is a concurrent activation of different muscle groups with the aim of accomplishing a task. Synergies have been theorized as motor primitives exploited by the CNS to simplify the control of many muscle fibers and to compute a solution for the intrinsic musculoskeletal system redundancy. In other words, synergies have been hypothesized as atomic components of a CNS modular organization for motor control. Evidence has been found after experiments with frogs, cats and monkeys supporting the existence of such "modules" during recurrent or instinctive behaviors [305–312]. Experiments with humans revealed recurrent patterns in muscular activations during repetitive tasks like walking [312–315], cycling [314–316], balance or postural control and reaching [317–321]. All these clues indicate that muscle synergies show up in conditions that are well-known by the brain and with a particular need for performance and efficiency. Nevertheless, many studies hypothesized that synergies features may reflect task biomechanical constraints rather than the underlying neural strategies of motor control [322**?** –325]. In any case, the muscle synergy hypothesis still struggles to be proven or falsified. Meanwhile, muscle synergies have been used in several applications, mainly as components in synergy-based control schemes and markers of cortical damages in motor control assessment [326–331]. Nevertheless, clinical usage of synergies only conceives

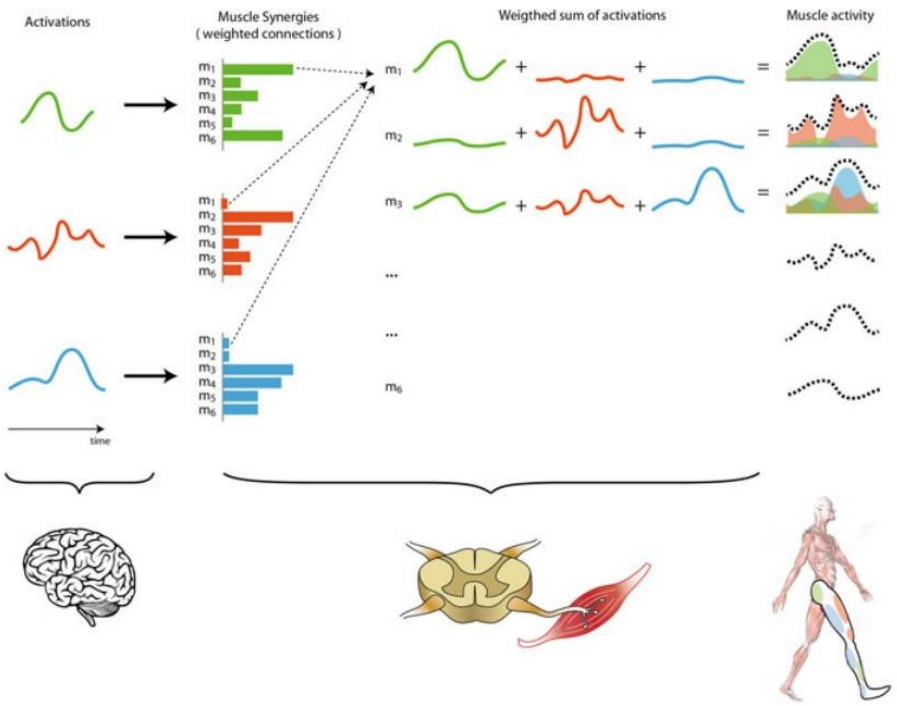

Figure 3.4 Muscle activities result from a combination of a few activation signals mediated by muscle synergies.

them from the point of view of identifying abnormal patterns of movement, comparing them with healthy subjects [332–335], without involving them in an integrated platform with a real-time synergy-task mapping. This aspect still represents a limitation in the context of synergy-based myo-control schemes.

Synergy models Practical synergy implementations have been proposed following three models: spatial, temporal, and spatio-temporal synergies. Each model involves a different way of combining these building blocks together, to obtain, as a macroscopic output, a limb motion. Spatial synergies, also called time-invariant or synchronous synergies, are muscular activation patterns that are all activated at the same time, with different coefficients or contributions **??**.

$$m(t) = \sum_{i=1}^{N} w_i \cdot c_i(t) + \varepsilon_{res} \tag{3.3}$$

with N as the number of samples, m(t) as the multi-channel input of muscular activation signals, wi the spatial pattern vector, ci the pattern coefficient or weight and ε_{res} the residual decomposition error. Spatial synergies have been often used as the simplest method to

represent synergies starting from EMG signals [305, 310]. Temporal synergies are objects that vary over time and they can be obtained through a temporal decomposition as follows:

$$m_m(t) = \sum_{i=1}^{N} c_{m,i} \cdot s_i(t) + \varepsilon_{res} \tag{3.4}$$

where si represents the i-th temporal synergy that is combined with the others using fixed coefficients, to reconstruct the m-th channel of the input. Temporal components based on this definition have been identified in kinematic [334, 335], dynamic [336] and EMG [337, 338] space. A more complex model includes potential activation delays of such temporal synergies, that could be different muscle by muscle:

$$m_m(t) = \sum_{i=1}^{N} c_{m,i} \cdot s_i(t - \tau_{m,i}) + \varepsilon_{res} \tag{3.5}$$

Where $tau_{m,i}$ is the delay time of the i-th synergy.

The last synergy type, called spatiotemporal or time-varying synergies, has been proposed to model muscle activation components that are invariant in both, space and time [188, 339]. Similarly to the more complex "temporal model" version, for each synergy additional temporal delays are admitted. On this base, the following model (referred to as "spatiotemporal decomposition") is described by the following equation:

$$m(t) = \sum_{i=1}^{N} c_i \cdot w_i(t - \tau_i) + \varepsilon_{res} \tag{3.6}$$

The time-varying synergies and the corresponding weights have typically been assumed to be non-negative [304].

Extraction and visualization of synergies Moving the synergies model to a practical computational application, the issue of identifying motor primitives has been addressed and discussed in several experimental contexts. Mostly, synergies have been extracted from a set of EMG signals, recorded from multiple muscles of either upper or lower limbs while performing tasks like walking, reaching or movements of a selected set of degrees of freedom. Since the electromyogram does not include information about the number and features of synergies, their extraction only relies on the supplied dataset. This issue, known as blind source separation, has been mainly addressed with four algorithms: principal component analysis (PCA), factor analysis (FA), independent component analysis (ICA), and non-negative matrix factorization (NNMF or NMF). Each factorization method makes a different assumption regarding the variance of input data and employs a different algorithm to extract

muscle synergies [340]. The NNMF algorithm is implemented using the multiplicative update rule based on Euclidian distance objective function, gradient descent and least square methods, and can be applied to both Gaussian and non-Gaussian datasets. PCA extracts the muscle synergies that best describe the data variance while minimizing the covariance of the basis vectors (i.e. muscle synergy weights), and it works best with Gaussian distributed datasets. ICA is designed to deal with non-Gaussian variation in datasets and finds basis vectors (i.e. muscle synergy weights) that maximize the absolute value of the fourth moment of the data (i.e. kurtosis). Similar to PCA, FA employs eigenvalue decomposition to produce eigenvectors (i.e. muscle synergy weights) of the covariance matrix. Each algorithm allows for the decomposition of the input signal with a certain residual error. In order to evaluate the performance of a factorization or component analysis algorithm, two indexes are recurrent in literature [188]: the coefficient of determination (R2) and the variance accounted for (VAF). Both metrics measure the amount of data variation "explained" by the synergies model. The VAF is computed as follows:

$$VAF = 1 - \frac{SSE}{SST} = 1 - \frac{\sum_S \sum_{k=1}^{k_S} \| m_S(t_k) - m_S^r(t_k) \|^2}{\sum_S \sum_{k=1}^{k_S} \| m_S(t_k) \|^2} \tag{3.7}$$

while the R2 is:

$$R^2 = 1 - \frac{SSE}{SST} = 1 - \frac{\sum_S \sum_{k=1}^{k_S} \| m_S(t_k) - m_S^r(t_k) \|^2}{\sum_S \sum_{k=1}^{k_S} \| m_S(t_k) - \bar{m} \|^2} \tag{3.8}$$

where SSE represents the sum of the squared errors, and SST is the sum of the squared residual from the mean activation vector $\bar{m}$, i.e., the total variation multiplied by the total number of samples $K = \sum_S k_S$. The higher the values of these indexes, the better resulting synergies can describe the input signal. Although all these algorithms have been extensively used with the same aim, several studies assessed that the NMF algorithm is better in reconstructing the probability distribution of muscle activation patterns, also potentially digging into actual physiological outcomes thanks to the non-negativity constraints on both weights and spatial/temporal patterns [340, 341]. In the case of spatial synergies, given the time-invariant property, it is common to highlight how each muscle contribute to each synergy and, thus, to detect abnormal co-contractions patterns. Two main way of visualizing synergies have been employed in literature, one plotting the contribution of each muscle through bars, the other plotting polygons on a radar or spider plot **??**.

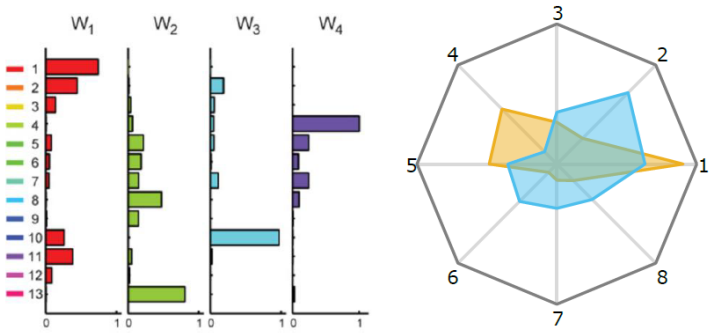

Figure 3.5 Two different ways of visualizing synergies.On the left, an example of synergies depicted with bars in which every row represents a channel or DoF and the bar length is associated to a certain weight. On the right, an example of synergies depicted with radar plots in which each vertex corresponds to a channel or DoF and the length of each colored polygon (i.e. synergy) segment is associated to a certain weight.

3.1.3 Parkinson's Disease Rehabilitation

3.1.3.1 Physiopathology and Risk Factors

Parkinson's disease is mainly characterized by a progressive degeneration of dopaminergic neurons in the "sub stantia nigra", with consequent decrease and limitation of motor functions; however, the presence of non-motor symptoms suggests the implication of other sections of the brain in the degenerative process. The triggering causes of this process are not yet fully understood, so the disease is still considered idiopathic; however, two relevant hypotheses concerning the pathogenesis of the disease, not necessarily exclusive, are reported by literature. The first hypothesis suggests the "misfolding" and aggregation of proteins as the main protagonists of the dopaminergic neurons cell death in the "substantia nigra pars compacta" (SNpc); indeed, these proteins can be neurotoxic and cause damage to cells if the body is not able to recognize and degrade them. A second hypothesis argues instead that the cause of such degeneration is to be found in mitochondrial dysfunction and the consequent oxidative stress: an increased production of reactive oxygen species (ROS) or their defective removal can lead to interactions with nucleic acids, proteins and lipids, causing cellular damage; since dopamine metabolism (DA) makes dopaminergic neurons for the production of ROS, such neurons may be more vulnerable and susceptible to oxidative stress [342]. In addition to the substantial loss of neurons, from 30% to 70% when the motor symptoms are evident, which particularly affects the pars compacta of the sub stantia nigra, another distinctive pathological element of Parkinson's disease is the presence of the so-called Lewy bodies (LBs). Lewy bodies are cytoplasmic aggregates of proteins composed of a circular

body surrounded by fibrils, arranged radially and with a diameter varying between 7 and 15 nm; these agglomerates are found mainly within dopaminergic neurons in the sub stantia nigra and are composed for the most of insoluble synuclein, as filaments, in combination with a series of proteins among which ubiquitin is present, responsible for the "targeting" of proteins to be eliminated. The mechanisms that lead to synuclein aggregation are not completely clear, however the literature suggests that an incorrect functioning of the ubiquitin-proteasome system (UPS), a system that deals with intercellular proteolysis by removing unnecessary proteins to cells, leads to an abnormal aggregation of proteins, including the synuclein [343][344]. In addition to age, a factor that strongly influences the incidence of the disease, ethnicity and gender, specialists believe that the disease may be the result of a network that includes other factors, such as environmental pollution and genetic predisposition. In particular, the incidence of the disease is associated with exposure to pesticides, herbicides and heavy metals. Indeed, some studies have shown that a great exposure to substances such as rotenone and paraquat, respectively a pesticide and a herbicide, increases by 70% the incidence of the disease over the following 10-20 years. Concerning genetic factors, several studies show that familiarity, the presence of a first-degree relative with Parkinson's disease, increases the risk of pathology, mostly at an early stage [345]; specifically, it is estimated that more than 5% of patients are affected by a form of PD, so-called "juvenile" due to Mendelian inheritance. This theory is sustained by the identification of 23 genes, called PARK, whose mutation is strongly related to the pathology; among the most relevant is the mutation of the synuclein gene, which can lead to an autosomal dominant form of PD through point mutation, duplication or tripling of the gene, mutations that are however relatively rare; instead, the mutation with the greater risk is the one of the GBA1 gene that encodes the - glucocerebrosidase. The literature also reports the presence of "protective" factors, which seem to reduce the risk of contracting Parkinson's disease. One of these is being cigarette smoker, a factor that decreases the risk of PD by 39%, probably thanks to the presence of nicotine, which stimulates the release of dopamine and activates neuroprotective receptors against dopaminergic neurons. Another factor that decreases the risk of pathology is caffeine, which, being an antagonist of the adenosine A receptor, also has a receptor that regulates oxygen consumption in the myocardium and blood flow in the coronary arteries.

3.1.3.2 Symptons

Parkinson's disease is primarily classified as a movement disorder. The main symptoms are therefore mainly motor and are due to the constant and progressive loss of dopamine within the neurons; the most frequent motor characteristics are commonly grouped under

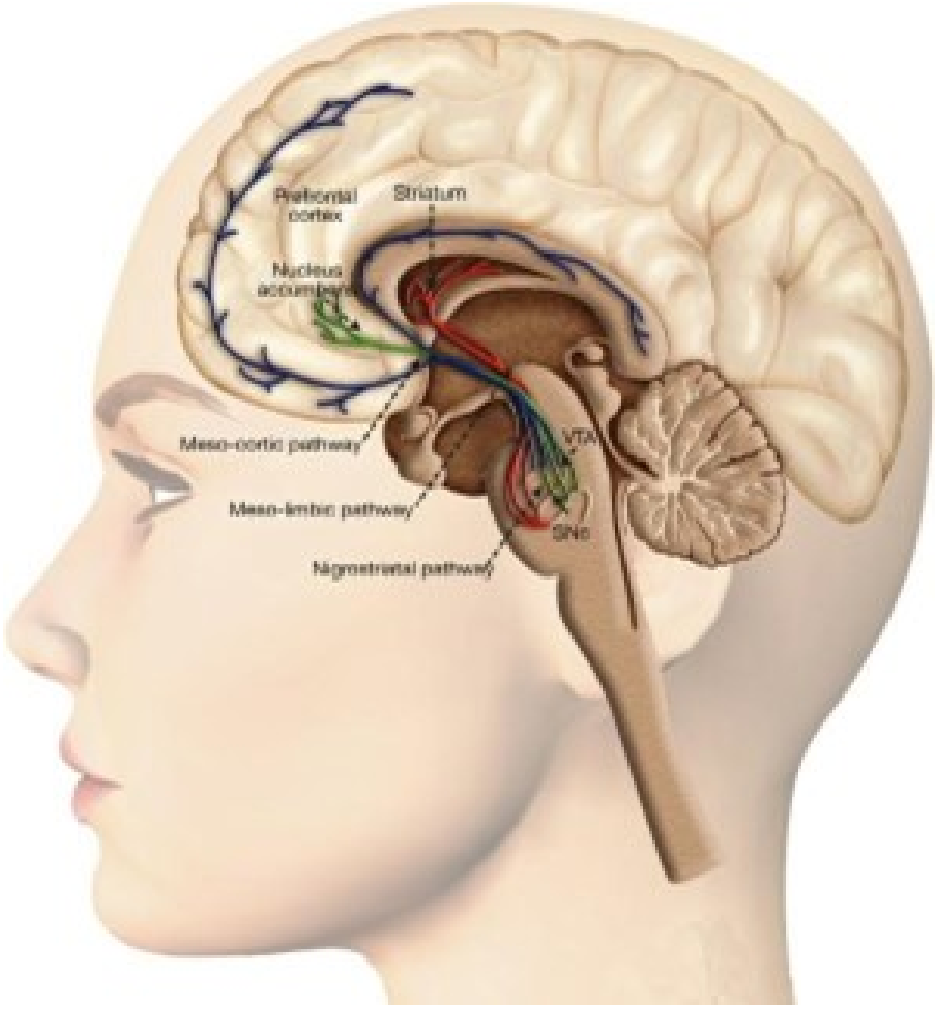

Figure 3.6 Localization of the dopaminergic system within the human brain.

the term parkinsonism, which includes bradykinesia, resting tremor, stiffness and postural instability [346]. However, in several cases there are a series of non-motor symptoms, some of which often precede the diagnosis and in some cases constitute a fundamental element for the development of the latter, whose severity increases with the prolongation of the disease and which contribute to increasing the level of disability and reducing the patient's quality of life. Unfortunately, non-motor symptoms are often misinterpreted or not recognized as related to the disease resulting in a lack of adequate treatment [347–349].

Motor Symptoms **Bradykinesia**: it is the typical motor sign and the most easily recognizable of Parkinson's disease. Bradykinesia consists of a slowness in the patient's movements, a result of dopaminergic decrease within the motor cortex. This slowness is reflected on the patient difficulty of starting activities and performing tasks that are sequential or require very

fine motor control (such as the use of tools) [348]. This symptom can be evaluated by asking the patient to do fast and wide repetitive movements (open and close a hand, tap the indent and thumb, or beat a foot on the ground) and observing the occurrence of speed or amplitude loss [347].

Resting tremor: it is an involuntary and oscillatory movement, whose frequency is between 4 and 6 Hz, which is usually evident in distal parts of the extremities of the body, such as hands and feet, but can also be present in the lips, chin or jaw. This tremor is called "resting" as it tends to fade when the patient starts movements and actions and then recovers after a few seconds. There are different types of tremor present in the disease, such as flexion-extension of the fingers or adduction-abduction, however the most characteristic is the "pill-rolling", a kind of rubbing of the thumb and index finger of the hand. Tremor is present in 75% of patients during the course of the disease, however this sign may decrease in advanced stages [347, 348].

Stiffness: this symptom consists of an increase in muscle tone and resistance to passive movements; it can involve the neck, shoulders, hips and wrists and causes the patient to feel tense. Stiffness is one of the main symptoms of the disease, found in most patients, and is often associated with pain in the affected areas [347].

Postural and gait instability: it is a common sign especially in the advanced stages of the disease and is the main cause of falls, along with walk freezing. The instability is mainly due to the loss of postural reflexes; this sign leads to an impairment of balance, with consequent difficulty in walking and daily activities, and leads the patient to assume a bowed posture [349]. The walk of the patient suffering from Parkinson's disease becomes slow and creeping, the swinging movements of the arms are lost, and changing direction becomes slow and difficult. In some cases, finally, the normal walk can be interrupted by events such as festination, in which the patient undergoes an acceleration of the walk by performing a rapid succession of small steps, or by the freezing of the gait (FOG), during which the patient undergoes a motor blockage, especially in the presence of obstacles or directional changes. In order to assess postural and gait instability the doctor observes the patient's walking in narrow corridors and passages; in addition, a particular evaluation method called pull test is used, which consists in a strong and decisive push at the level of the patient's shoulders in order to evaluate the postural response [346].

The patient may eventually experience other motor symptoms: problems with handwriting, such as micrography (reduction of written characters) or difficulty in accurately grasping small objects.

3.1.3.3 Pyshiokinetic Therapeutic treatments

While stiffness, tremor and akinesia are often treatable through the use of medications, other symptoms such as speech disorders or complex disorders of walking and balance are much less susceptible to medical treatment. Dopamine-resistant deficits are also becoming increasingly prominent in advanced stages of the disease and significantly alter mobility, participation and quality of life [350]. In the motor circuit of the basal ganglia, the afferents from the motor regions of the cortex end on the striatum, which also receives dopaminergic innervation from the compact part of the sub stantia nigra: the inhibitory projections of the striatum end later on the external and internal segments of the globus pallidus and the inhibitory outputs of the internal segment of the globus pallidus it has been hypothesized that they have two distinct functions: the focused selection of the desired movement and the inhibition of competitive movements [351]. In Parkinson's patients, these functions are not activated following an abnormal transport from the basal ganglia to the thalamus, thus preventing the facilitation of the desired movement [352]. Following short strength training, significant gains in maximal strength production occur and it is hypothesized that it is neuronal adaptations responsible for this improvement [353]. Studies carried out on Parkinson's patients have found that physical therapy interventions can also improve not only muscle strength but also flexibility and balance [354], while the most immediate effects include an improvement in motor performance and cognitive and functional skills [355]. Exercise has also been shown to lead to a reduction in the mortality rate in individuals with Parkinson's disease and although modestly, to have a protective effect for the risk of developing the disease. Aerobic training in particular reduces motor symptoms and improves physical fitness [356]. Regular aerobic exercise has in fact beneficial effects on the frontal region as it mediates executive functions, increases brain volume, induces the production of neurotrophic factors that benefit glutamatergic neurons which in turn improve learning and neural function. It also has angiogenic effects, promotes neuroplasticity and improves cognitive function especially in executive processes [357]. An interesting study was carried out by Tanaka in 2009: the study lasted 6 months and which included 20 elderly people with Parkinson's disease, patients were distributed in 2 groups. The first group participated in a multimodal aerobic exercise program while the second carried out the usual daily routines without participating in any regular exercise program. The study demonstrated a significant interaction ($p<0.05$) between physical training and the executive function of participants in multimodal training sessions [358]. The results of this study therefore indicated that a generalized exercise program lasting 6 months may benefit the executive functions of older people with Parkinson's disease. These benefits also play an important role in the degree of

independence, autonomy and quality of life of this population and one of the physical activity interventions recommended by the existing literature is the use of the snare drum, which can also act as a source of external education, setting the type of walking and strengthening the neuronal circuits that contribute to the mode of walking. However, complications due to the importance of safety have been detected when snare carpet training is prescribed at the home of the sick. Deficits in postural control in patients with Parkinson's disease can instead be positively influenced by bio-feedback training based on dynamic balance [359]. The study group of fractures of osteoporotic origin also found that low levels of densitometry in the hip and spine are associated with Parkinson's disease, regardless of physical activity and neuromuscular function. The authors of this study argue, the reduction of the risk of fratture in people with Parkinson's, through physical training with the aim of reducing bone loss and promoting the favorable increase of bone substance [360]. With regard to the evidence-based recommendations on the use of physiotherapy in Parkinson's disease, with main areas of treatment such as walking, balancing, transfers (e.g. turning over the bed or getting up from a chair), the act of grasping objects, there were no differences between patients who received traditional physiotherapy or Parkinson's specific physiotherapy, because there are still a small number of operators specialized in the disease and if specialized they have still carried out only a few weeks of training and need further experience in the field of the disease [361]. Patients with Parkinson's disease should still resume or continue exercise as long as possible. Occupational and speech therapy, used to preserve speech and swallowing, are instead prescribed and practiced not only to improve motor functions and activities of daily life, but also to avoid the onset and aggravation of symptoms that place patients at risk of early death such as dysphagia [362]. Psycho-dynamic psychological therapies or cognitive-behavioral ones are also often recommended to Parkinson's patients and their care-givers, with the aim of providing them with costructive support in dealing with the diagnosis and course of the disease [363].

3.1.3.4 Gait Analysis

The gait analysis represents the study of locomotion, in particular the walking of the man; it is fundamental in the management of all those pathologies that afflict the locomotor system. Walking includes a whole series of voluntary movements that are the result of underlying processes involving the brain, spine, peripheral nerves, muscles, bones and joints. At the base of the study of walking there is the conjunction of three different disciplines: anatomy, physiology and biomechanics [364].

The study of walking is preliminarily a non-invasive technique that allows, by studying a series of parameters related to gait, to evaluate different functional or non-functional limits. It is applicable to different pathologies that develop in different areas of medicine with particular attention to neurological, orthopedic, orthopedictraumatological pathologies or attributable to different traumas such as spinal injuries that then become the exclusive competence of the physiatrist specialist. For example, applied to this concept, the role of the physiatrist specialist is precisely to improve the patient's gait and ability to move. The physiatrist deals with disability and how to deal with it. Walking allows to evaluate the severity of a pathology, evaluate the follow-up and / or the effectiveness of the drug therapy administered, evaluate the physical rehabilitation of the patient and also allows to create a pharmacological and physical rehabilitation plan personalized on the patient and modifiable depending on the response of the patient during the acquisition procedure. Depending on the purpose for which the gait analysis is intended, some specific parameters are selected. In particular, these can be grouped into four macro-categories:

- Kinematics: everything related to positions in space, velocity accelerations
- Dynamic: everything about forces and moments
- Electromyographic: everything related to the muscular response to stimuli
- Spatio-temporal: everything related to the step, its duration and frequency.

Process and equipment A typical gait analysis laboratory has several cameras (RGB or infrared) placed around a walkway or treadmill, which are connected to a computer. The patient has markers located at various parts of the body (eg. Iliac spines of the pelvis, malleolus of the ankle and condyles of the knee) or groups of markers applied to the middle of the limbs. The patient walks along the walkway or treadmill and the computer calculates the trajectory of each marker in three dimensions. A model is applied to calculate the movement of the underlying bones. This provides a complete breakdown of the movement of each joint. The common method is to use the Helen Hayes Hospital's set of markers, in which a total of 15 markers are attached to the lower body. The 15 markers movements are analyzed analytically and provide an angular movement of each joint. In order to calculate the kinetics of gait patterns, most laboratories have floor-mounted load transducers, also known as force platforms, that measure forces and moments of reaction, including intensity, direction, and position. The spatial distribution of forces can be measured with pedobarographic equipment. Adding this to the known dynamics of each segment of the body, one obtains the solution

of equations based on the Newton-Euler equations of motion that allow the calculation of the net forces and the net moments of force around each joint at any stage of the gait cycle. The computational method for this is known as inverse dynamics. This use of kinetics, however, does not allow to obtain information for individual muscles but for muscle groups, such as extensors or flexors of the limb. In order to detect the activity and contribution of individual muscles to movement it is necessary to study the electrical activity of the muscles. Many labs also use surface electrodes attached to the skin to detect the electrical activity or electromyogram (EMG) of muscles. In this way it is possible to study the response times of the muscles and, to a certain extent, the extent of their activation, thus evaluating their contribution to walking. Deviations from normal kinematic, kinetic or EMG patterns are used to diagnose specific pathologies, predict the results of treatments or determine the effectiveness of physiotherapy programs.

Phases of the gait cycle The support phase includes four subphases related to the events of response loading, intermediate position, terminal position, pre-oscillation. The oscillation phase includes three subphases related to the of initial oscillation, average oscillation, terminal oscillation. The initial contact takes place while the left foot is still on the ground and there is a period of double support; the oscillation phase involves a period of single right support that ends with the initial contact of the left foot, there is then another period of double support. This is followed by a single support of the left foot that corresponds to the oscillation of the foot right. The cycle ends with the next initiatory contact.

The first two phases involve a very important process of weight transfer and management which in turn includes three large studies related to the analysis of walking that allow to identify different disorders and dysfunctions that are shock absorption, initial stability of the limb and preservation of progression.

The gait cycle can be broken in seven steps:

- In the initial contact phase the foot has a contact with the floor that involves only the heel, the hip is flexed, the knee extended and the ankle in a neutral position. The other limb is located in the terminal position.

- In step two, a transfer of weight to the forelimb takes place. The flexed position of the knee and ankle allow shock absorption and avoid the impact between the foot and the floor. The opposite limb is in the pre-oscillation phase. Together phase one and two represent the period of "double stance".

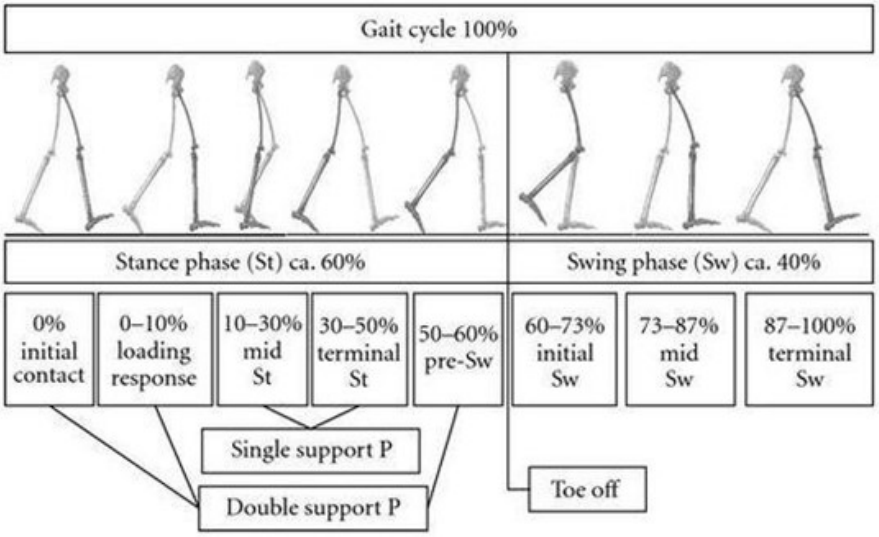

Figure 3.7 Represantation of the gait cycle.

- In phase three there is the extension of the knee and hip while the ankle undergoes a bending back, which allows the advancement on the stationary foot. The secondary foot, on the other hand, is reaching the medium oscillation phase. This phase ends with the alignment of the weight above the forefoot.
- In the fourth phase the heel rises and advances while the other limb is in terminal oscillation. This phase ends when the other foot rests on the floor. Phases three and four constitute what is called "single limb support" which provides, in fact, that one of the two limbs fully supports the weight both on the sagittal plane, and coronal during the progression.
- In phase five the second limb is in contact with the ground. The reference limb undergoes plantar flexion, knee flexion and hip extension. It is a phase of release and transfer of weight that allows the secondary limb to be free to start the oscillation phase.
- In phase six one foot lifts and advances thanks to a flexion of the hip and knee, the other limb and in mid stance.
- In phase seven there is a further bending of the hip that allows an advance of the weight line; the other limb is in the late mid stance phase . This phase ends when the oscillating limb moves forward in a vertical weight alignment on the tibia • In the

eighth and final phase the primary limb has completed the advancement while the other limb is in the terminal position [365].

3.1.3.5 Rehabilitation with cueing technique

The human brain has the ability to integrate, filter and prioritize a range of information and sensations from the outside world and, combining them with previous experiences, is able to create a unique perception. This is a process that takes place continuously and automatically in order to generate adaptive responses about your body and your surroundings. Sensory stimuli also have a great relevance in the perception of oneself and the surrounding world and guide and modify the action that is about to be performed. The integration of visual stimuli, tactile information, and proprioceptive information play a critical role in how we perceive our body, how we manage movement, and how we interact with the outside world [366]. Initially, the researchers focused on the effects of auditory-motor stimuli aimed at improving sports performance, improving personalized training and improving and speeding up the rehabilitation of sports injuries. Thanks to the support of the discipline of neuroimaging it has been shown that there is an activation of the premotor ventral cortex both during movement and when listening to the noise produced by the walk itself. This has led more and more specialists to experiment with auditory stimuli for the treatment or rehabilitation of the most disparate pathologies with particular attention to neurological pathologies. In addition to the sounds coming from the walk itself, other surrounding minor sounds, of which you are not always aware, can also affect the movement. As widely discussed, the parkinsonian patient care approach is an approach that to have maximum effectiveness must be multidisciplinary and as personalized as possible and studied on the needs of the individual patient [367]. Hence the need to support different types of rehabilitation including:

- Endurance Training;
- Mobilization of limbs;
- Stretching;
- Treadmill training;
- Emotional activation;
- Motivational activation;
- Cues.

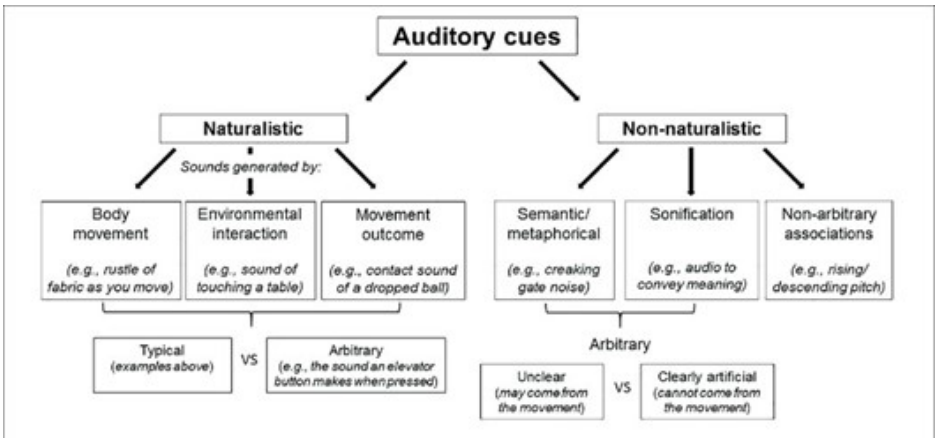

Figure 3.8 Classification of auditory cues.

Sensory cues technique The rehabilitation of the Parkinsonian patient, according to Morris, includes three macrophases:

- Phase 1: in which the patient is taught a series of movement incentive techniques (cognitive strategies);
- Phase 2: in which the management of musculoskeletal sequelae takes place;
- Phase 3: in which the patient is encouraged to carry out motor activities, such as to prevent secondary disorders.

The first phase includes the use of the cues technique. Using auditory cues means giving the patient audio stimuli [355]. These can be of different types; they can come from the body itself, be produced by the same walk or include slight natural sounds or they can be artificially provoked sounds. Hence the distinction in naturalistic and non-naturalistic as shown in the figure below.

The technique of auditory cues allows to activate alternative motor pathways such as visuo-motor or reticulo-spinal. It can be used in different modes depending on how many sound stimuli are reproduced and how often [352]. This allows to stimulate the patient at different times of the walking phase and in different ways; in particular:

1. one of cue: consists of using individual auditory stimuli. This mode allows to stimulate the patient in the phase of incentive to the movement. For example, it can be useful in the initial stages of lifting from a chair or at the stage when the patient wants to start the walk.

2. rhytmic recurrent cue: repeated series of auditory stimuli sent at a certain frequency to stimulate the patient to maintain a rhythm in the act of walking. It has been shown that the frequency of the suon (e.g. the sound of a metronome) has a fundamental relevance [368]. The ideal frequency is slightly higher than the step frequency of the individual patient. On the contrary, using excessive frequencies generates the opposite effect.

The use of these techniques individually or in a combined manner has a number of advantages, including greater responsiveness to the start and a rhythmicization of the step. Greater benefits are then obtained by using a combination of cues with intentional tools, for example by introducing verbal instructions (as a metaphor for the voice of the physiotherapist who follows the patient). The opposite effect occurs when the patient is prompted to perform multiple tasks at the same time [369]. The parameters that are most affected are:

- step cadence;
- step velocity;
- steps length;
- number of total steps.

In particular, there is a reduction in the number of steps in the literature in favor of an improvement in terms of the width of the length of the step. The use of recurrent cues produces a constant cadence of the step [370]. As highlighted by the neurologist and emerged during registration, there are still variables that cannot be controlled within the study; among these certainly must be counted the variable emotionality and psychological factors. In addition, many patients also have a cognitive deficit that does not allow the administration of the cues.

The first insight of autoencoder architecture on electromyographic signals is based on the application of an undercomplete autoencoder to extract spatial muscle synergies. The presented bio-inspired autoencoder topology (Section 3.2) has been trained to extract muscles synergies from EMG signals of the main upper-limb muscles, acquired during isometric reaching tasks. The extracted synergy activations have been also used to estimate the moments applied to the shoulder and elbow articulations. The experimental results were compared with the standard NNMF algorithm used in muscle synergy extraction. A second application (Section 3.3), starting from the results of the first one, make use of a customised autoencoder-based neural model able to extract the muscle synergy patterns simultaneously considering the performance in the task space (i.e., estimation of moments/forces exerted

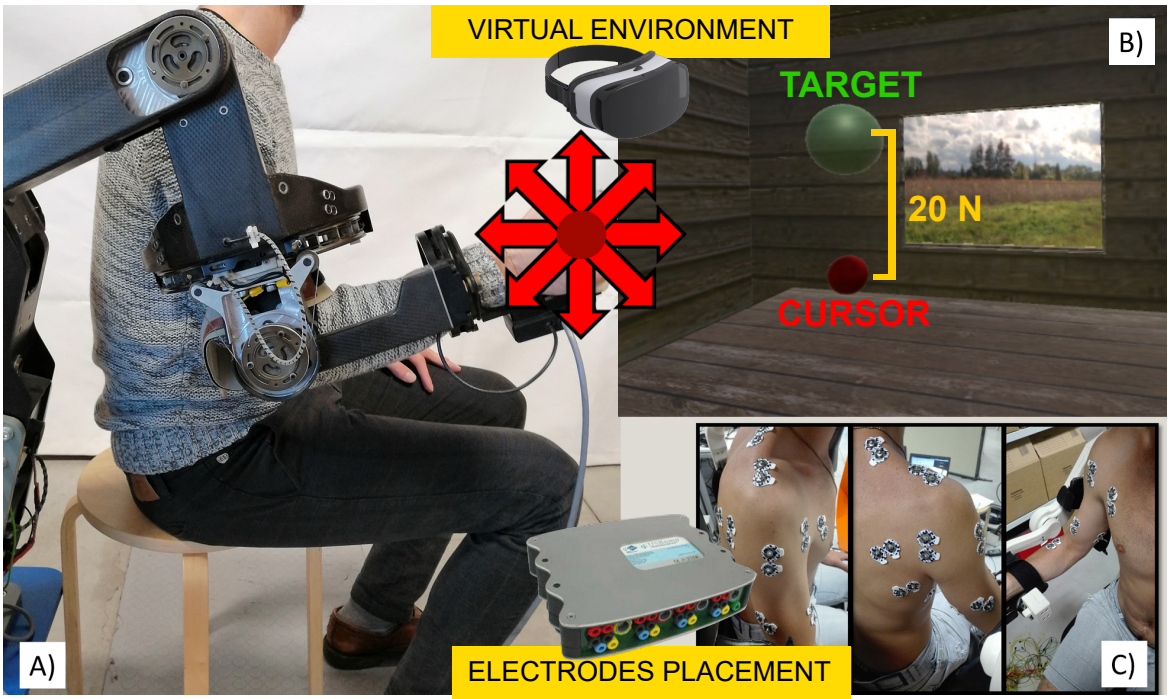

Figure 3.9 The experimental set-up. The subject that is wearing the upper limb L-Exos exoskeleton (A). The virtual environment showing the cursor and the target sphere (B). The surface EMG electrode placement (C).

by the human upper limb). Specifically, the model builds its synergy code considering both the EMG signals reconstruction performance and the estimation quality of the upper limb moments computed as a linear combination of the synergy activation signals, thus allowing a task-oriented synergy extraction. The creation of a more complex model is due to the assumption that a direct integration of task-space constraints in the algorithm used to extract the synergies, could produce a better task-space variable estimation, thus leading to a new class of optimized myo-controllers and, perhaps, providing a deeper understanding of the hypothetical modularity of the central nervous system and its relationship with the motor learning.

Part of this chapter has been published in international conferences and journals [371–374].

For the research purpose analysed in this section, two dataset have been considered.The first study involved six healthy subjects, while the second extends the first with a larger number of participant (nine right-handed healthy subjects, age 27.7 ± 4.9 years, weight 74.1 ± 9.1 kg). The experiments were conducted in accordance with the WMA Declaration of Helsinki and all subjects provided written consent to participate.

The setup was designed for measuring the subject upper-limb muscle EMG signals and forces exerted at the hand level during a set of isometric contractions (Figure 3.9). An electromechanical upper-limb exoskeleton, designed for upper-limb rehabilitation, namely L-Exos, was used for acquiring the interaction force between the subject's hand and the exoskeleton's cylindrical handle featuring a triaxial force sensor. The L-Exos has been designed as a wearable haptic interface, capable of providing a controllable force at the center of user's right hand palm, oriented along any direction of the space [375]. The L-Exos has four actuated DOFs for supporting elbow and shoulder movements: shoulder adduction/abduction; shoulder flexion/extension; shoulder internal/external rotation; elbow flexion/extension, and one passive DOF used for measuring the wrist pronosupination angle. All the motors of the exoskeleton have been located on the fixed frame. For each actuated DOF, the torque is delivered from the motor to the corresponding joint by means of steel cables and a reduction gear integrated at the joint axis. All actuated joints are driven with a proportional-derivative control strategy with gravity compensation. The force sensor readings have been then used to estimate the articulation moments.

Concerning the EMG acquisition system, two bio-signals amplifiers (g.USBamp, gTec, Austria) were included in the setup to record the activity of 13 muscle heads: biceps short head, biceps long head, brachioradial, triceps long head, triceps lateral head, deltoid anterior head, deltoid posterior head, trapezius, pectoralis major, teres major, infraspinatus, latissimus dorsi and rhomboid. Disposable Ag/AgCl surface electrodes were placed by following the SENIAM[1] recommendations, after a skin cleaning process, and the ground electrode attached to the right elbow. All the surface EMG signals were acquired at $1200Hz$ sampling frequency and filtered by the amplifier with a $5-500Hz$ band-pass filter and a $50Hz$ notch filter.

In order to make a more intuitive and easy experimental session, the subject was immersed in a virtual environment (VE) by wearing a head mounted display (Oculus Rift HMD, Oculus) to receive visual feedback. The force sensor measurements, VE signals and EMG data were synchronized on a Master PC (Figure 3.10), featuring Microsoft Windows 10 (64 bit), Intel i7 1.6 GHz, 8 Gb RAM and Matlab (Release 2018b). The Master PC has been also used to generate commands for driving the exoskeleton and the VE, according to the acquisition routine.

Data Acquisition Protocol Before starting the acquisition routine, subjects were invited to sit on a chair and wear the exoskeleton using the flip-off arm bands. By using stacked hard plastic layers under the chair, the height of the seat was adjusted in order to align the

[1] http://www.seniam.org/

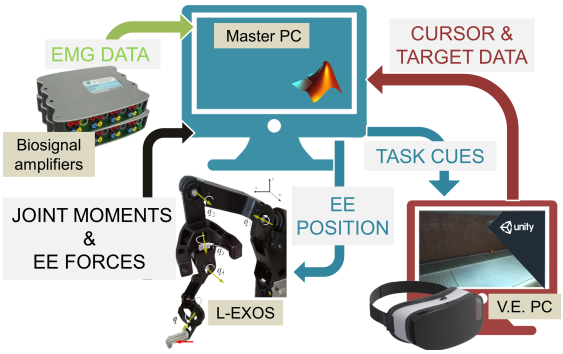

Figure 3.10 Main architecture of the acquisition system.

centres of rotation of the subject's and exoskeleton shoulder joint. At the beginning of the experiment the exoskeleton joint angles were automatically fixed to a pre-defined angles set: shoulder abduction/abduction angle equal to 0 degrees, shoulder internal rotation angle equal to 0 degrees, shoulder elevation angle equal to 10 degrees and elbow angle equal to 90 degrees. After the surface EMG electrodes were placed on the targeted muscles, elastic bands were used to keep electrodes and wires firmly attached to the body in such a way that the exoskeleton handle was easily reachable. Then, subjects were asked to perform 16 isometric virtual reaching tasks along 8 directions (two trials per direction) on the sagittal plane, equally spaced at 45 degrees and randomly sorted. Isometric contractions were achieved through the exoskeleton end effector position control, keeping the subjects upper-limb pose fixed. In the virtual environment, the subjects hand position corresponds to a red sphere (cursor) and the task target is represented as a green sphere. The distance between the two spheres is covered applying the target force of 20 $kg \cdot m/s^2$ on the sensor and the radius difference allowed a maximum positioning error equal to 3 $kg \cdot m/s^2$ ($1\ N = 1\ kg \cdot m/s^2$). Each virtual reaching task consists of: positioning the cursor inside the target, holding it in place for 2 s and then relaxing to move the cursor back to the rest position. The cursor position is driven by a spring model $P_c = K * F_{EE}$ where P_c is the 3D cursor position, F_{EE} is the applied isometric force vector and K is the elastic constant of the virtual spring.

3.2 An Undercomplete Autoencoder for Muscle Synergies Extraction

Among the several kinds of AE families cited in Section **??**, an undercomplete autoencoder has been chosen and firstly used to extract the spatial muscle synergies of the human upper limb while executing an isometric reaching task in a bi-dimensional space. In a second step,

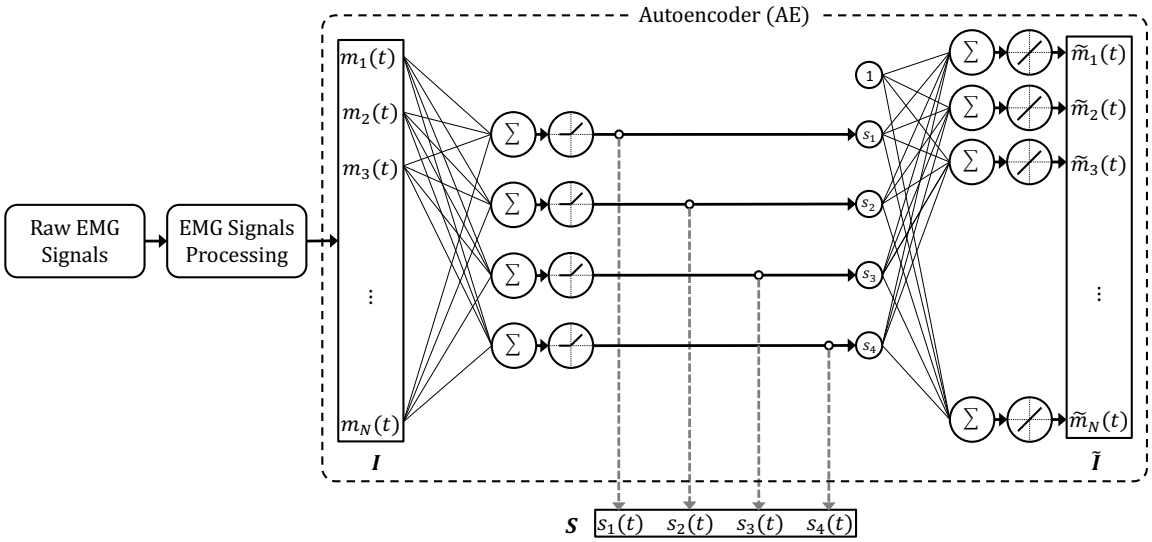

Figure 3.11 Architecture of the undercomplete autoencoder for synergies extraction.

the extracted muscles synergy signals have been used to predict the movement intention by estimating the shoulder and elbow articulation moments with a linear combination.

Given the input vector $I(t) = [m_1(t), m_2(t), \ldots, m_N(t)]$, where $m_i(t)$ represents the pre-processed activation of the i-th muscle and N is the number of considered muscles, the autoencoder has the objective to extract the activations of the muscle synergies s_i. The pre-processing phase considers the following steps for each raw EMG signal: high-pass filtering (20 Hz second-order Butterworth); rectification and low-pass filtering (5 Hz second-order Butterworth); normalization over the maximum value computed during the calibration procedure.

3.2.1 Materials and Methods

Model Design and Configuration The structure of the designed autoencoder is shown in Figure 3.11. The considered topology has one hidden layer with four positive linear neurons that produce the synergy activations named $s_1(t)$, $s_2(t)$, $s_3(t)$ and $s_4(t)$. Such configuration replicates the physiological model of the spatial muscles synergies reported by Berger *et al.* [376]. The problem of selecting the best number of the hidden neurons was not faced with the topology definition, i.e. the number of extracted muscles synergies, but a fixed number (4) of hidden neurons has been chosen since some studies have reported that the isometric activation of the human upper limb muscles can be accurately described by four muscle synergies [376, 377]. Considering the definition of autoencoders, the output layer has the same dimension as the input layer. As suggested by Goodfellow *et al.* , a simple

linear decoder with biases is sufficient to avoid the copying task without extracting useful information, caused by too much learning capacity [378].

The model has been implemented with the Neural Network toolbox of Matlab (Release 2018b) and trained using a gradient descent with momentum and adaptive learning rate algorithm and considering 1000 training epochs. Given a single train set, the training was repeated 20 times with different initial weights. Among the 20 models, the best one has been chosen as the model featuring the minimum correlation index among the four synergy activations. Such index has been computed as the sum of the elements of the absolute upper triangular matrix extracted by the correlation matrix of $s_1(t)$, $s_2(t)$, $s_3(t)$ and $s_4(t)$. Considering a train set composed by about 4000 time point, the training process of each autoencoder lasts about 1.5 seconds. All the trainings have been run on a PC featuring two Intel XEON E5 2630 v3 CPUs and 64 GB of RAM.

Joint Moment Estimation Based on Muscle Synergies: Comparison with the State-of the Art For this study, the bi-dimensional motion intention estimator that takes the AE-extracted muscles synergies as input has been compared with other methods already proposed in literature and based on the same model described by the Equation **??**. Each model is able to estimates the shoulder and elbow moments. In detail:

- **Model** Hm: $T = H \cdot m$, where m is the muscle activation signal vector processed as the input data of the AE (Figure 3.11) [376];
- **Model** $HWW^{+}m$: $T = H \cdot W \cdot W^{+} \cdot m$, where H is exactly the same EMG-to-moment matrix extracted for the Model Hm [376] and W is the synergy matrix extracted with the NNMF by using the Matlab function $nnmf(\dots)$;
- **Model** $\hat{H}c$: $T = \hat{H} \cdot c$, where c is extracted with the NNMF for the model calibration and computed as reported in Equation **??** for the model evaluation [377];
- **Model** AE: $T = H_{AE} \cdot S$, where S is the synergy activation vector extracted by the autoencoder.

It is worth noting that the matrix H has dimension equal to $2 \times N$ (two is the number of moment components: shoulder and elbow joint moments), whereas the matrices $\hat{H}$ and H_{AE} have size 2×4 (four is the number of considered muscle synergies).

Model Calibration and Performance Metrics Each subject-specific model has been independently trained with 256 (2^8) different train sets, where 2 is the number of reaching

trials executed for each of the target sphere positioned in the 8 directions. Hence, a single train set contains the EMG and shoulder/elbow moment data acquired in one trial along all directions. Fixed a single train set, then all models have been evaluated on the complementary test set, that contains the data acquired during the contractions that have not been considered for the calibration.

The multivariate R^2 index has been computed for each test set in order to evaluate the synergy extraction performance of both the NNMF and AE. The multivariate R^2 index represents the fraction of total variation accounted by the synergy reconstruction and then is a global indicator of the goodness of reconstruction. The R^2 has been computed as follows [379]:

$$R^2 = 1 - \frac{SSE}{SST} = 1 - \frac{\sum_s \sum_{k=1}^{k_s} \|m_s(t_k) - m_s^r(t_k)\|^2}{\sum_s \sum_{k=1}^{k_s} \|m_s(t_k) - \bar{m}\|^2} \tag{3.9}$$

where SSE is the sum of the squared errors, and SST is the sum of the squared residual from the mean activation vector $\bar{m}$, i.e. the total variation multiplied by the total number of samples $K = \sum_s k_s$.

The shoulder and elbow articulation moment reconstruction by the models presented above has been evaluated computing the root mean square error (E_{RMS}) between the measured and estimated torques.

Statistics In order to compare the proposed methods, the average values of the R^2 and E_{RMS} among the 256 test sets for each subject have been computed. The two synergy extraction methods, i.e., AE-based and NNMF, have been compared with the Wilcoxon test. The four moment estimator models, i.e. Hm, HWW^+m, $\hat{H}c$ and AE-based model, have been compared running the Friedman test and the Dunn's pairwise post-hoc tests with Bonferroni correction. The significance level has been set to 0.05. Non-parametric tests were adopted since the assumptions underlying parametric tests resulted to be violated for all sets of data. All the analyses have been performed using the SPSS[2] software (Version 21).

3.2.2 Results

In order to evaluate the ability of the proposed autoencoder to extract representative muscles synergies, the NNMF method and the autoencoder were compared in terms of the multi-

[2]https://www.ibm.com/analytics/spss-statistics-software

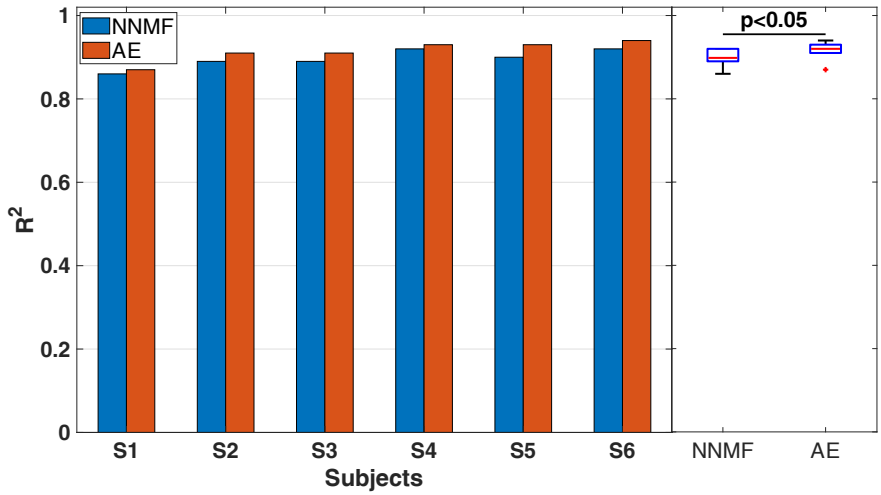

Figure 3.12 Quality index of the muscle activation reconstruction.

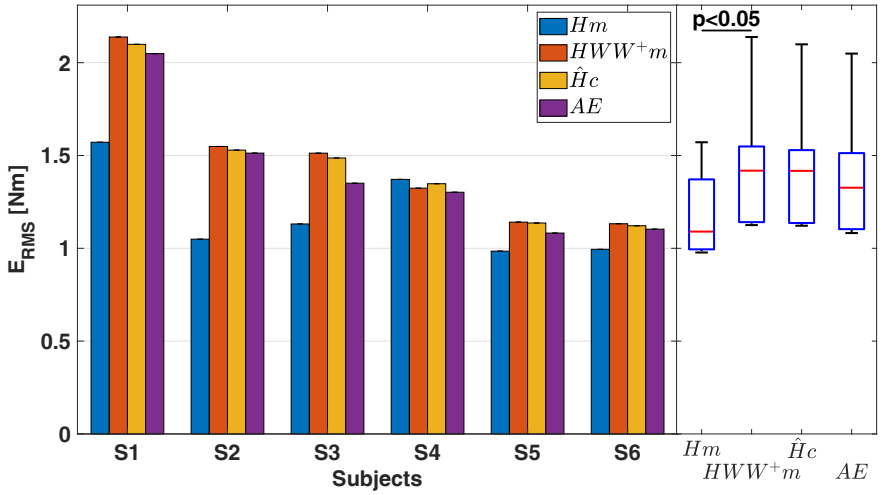

Figure 3.13 Shoulder moment estimation error.

variate R^2 index computed between the processed measured muscle activations m_i and the reconstructed $\tilde{m}_i$ computed as $\tilde{m}_i = W \cdot W^+ \cdot m_i$.

Figure 3.12 reports the average R^2 among the several test sets for each subject. It resulted that the R^2 of the muscle activation reconstruction based on the AE is significantly higher than the NNMF R^2 ($z = -2.201$, $p = 0.028$).

To validate the estimation ability of the method based on the muscle synergies extracted with the proposed autoencoder, the four models were compared in terms of E_{RMS} between the moments predicted by the model and reference (or measured) joint moments.

Figure 3.13 and Figure 3.14 report, for each subject, the averaged E_{RMS} among the several test sets. Concerning the shoulder joint moment estimation, the E_{RMS} of the four methods are

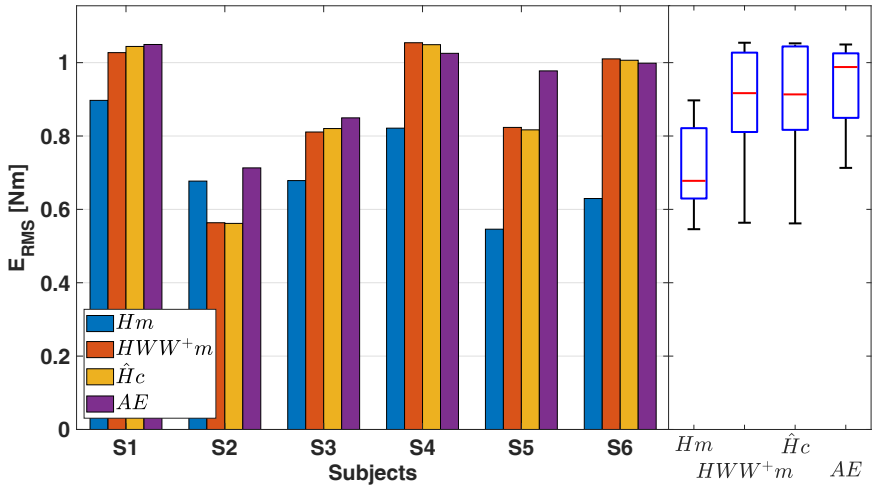

Figure 3.14 Elbow moment estimation error.

Table 3.1 E_{RMS} performance Bonferroni corrected post-hoc comparisons for the shoulder joint.

Pairwise comparison	T Statistics	p-value
Hm - $HWW^{+}m$	-2.167	**0.022**
Hm - $\hat{H}c$	-1.500	0.265
Hm - AE	-0.333	1.000
$HWW^{+}m$ - $\hat{H}c$	0.667	1.000
$HWW^{+}m$ - AE	1.833	0.083
$\hat{H}c$ - AE	1.167	0.705

significantly different ($\chi^2(3) = 11$, $p = 0.012$). Dunn tests with the Bonferroni correction were used to follow up this finding. It appeared that there is only a significant difference between the Model Hm and the model $HWW^{+}m$ ($T = -2.167$, $p = 0.022$). Regarding the elbow joint moment estimation, no significant difference between the E_{RMS} of the four methods has been found ($\chi^2(3) = 7.8$, $p = 0.050$).

3.2.3 Discussion and Conclusions

As reported in 3.12, comparing the averaged R^2 values computed on the test sets, it resulted that the autoencoder performs better than the NNMF (Wilcoxon test, z=-2.201, p=0.028). This means that the AE generates synergy activations that better reconstruct the original muscle activation signals. It also worth noting that the AE and the NNMF have not been tested on the reconstruction of the same EMG signals used to calibrate the synergy model,

but on different muscle activations acquired in the same condition, i.e. the same upper limb pose.

In conclusion, summarising the results,the statistical analysis revealed that the only found significant difference in estimating the shoulder moment is between the models Hm and $HWW^{+}m$ (Dunn test with the Bonferroni correction, $T = -2.167$, $p = 0.022$). The clear messages that arises from the statistical analysis, Figure 3.13 and Figure 3.14 are that: the Hm model is better than the $HWW^{+}m$, $\hat{H}c$ and AE models, even if such difference is not significant in the case of elbow moment estimation; the three methods $HWW^{+}m$, $\hat{H}c$ and AE performs similarly. This result is reasonable since the Model Hm is not synergy based, i.e. it does not introduce any loss of EMG signal information, and it uses a bigger H matrix allowing a better learning. However this results are limited by the fact that the estimator has been calibrated and tested in the same upper limb pose. A synergy-based method should achieve better performances when a complex calibrated model is tested in different conditions [377].

3.3 Autoencoder for Task-Oriented Muscle Synergy Extraction

Even though a certain number of procedures for muscles synergy extraction has been proposed in the literature [380, 381], the main drawback of the existing approaches, such as the one presented before, concerns the fact that muscle synergies are estimated by analysing recorded muscle activities without having any information about neither the underlying task nor the final application. This means that the synergy extraction procedure considers the total variance reconstruction rate of the EMG signals as the only performance index to be optimized. Cristiano *et al.* [380] reported: *"We suggest that synergy extraction methods should explicitly take into account task execution variables, thus moving from a perspective purely based on input-space to one grounded on task-space as well ... In conclusion, the evidence reviewed here provides support for the existence of muscle synergies. However, many issues are still unresolved. A deeper investigation of the relationship between synergies and task variables might help to address some of the open questions"*. Few works have investigated the concept of functional synergies that are an initial attempt to link muscle synergies with task variables [305, 306, 380, 382]. However, as deeply discussed by Barradas *et al.* [383] and Cristiano *et al.* [380], functional synergies present some issues and limitations. After an extensive argumentation, Cristiano and his colleagues state that a novel

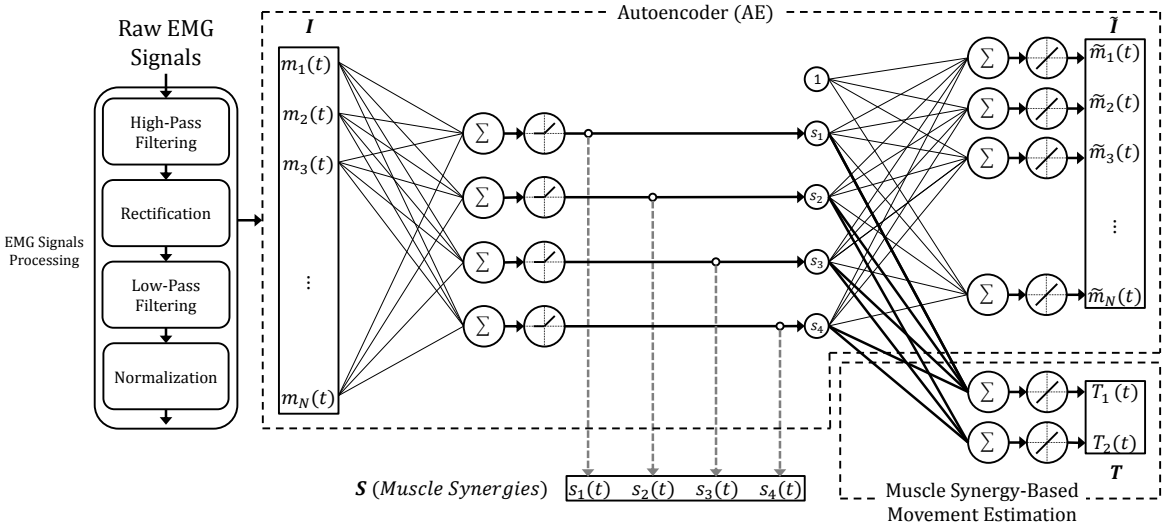

Figure 3.15 The proposed extended autoencoder model.

required technique for muscle synergy extraction *"... should optimize the reconstruction error of the EMG signals, and constrain a good fit of the task-variables"*.

3.3.1 Materials and Methods

Model Design and Configuration Starting from the architecture proposed in Section 3.2, a novel architecture that is able to learn the optimised muscles synergies patterns that lead to the optimized muscle synergy-based movement intention detection has been designed. The structure of the presented model (Figure 3.15) is composed of two main blocks: an undercomplete autoencoder for muscle synergies extraction and a feed-forward layer for movement estimation based on muscle synergy activations.

Referring to the Figure 3.15, part of the modified autoencoder, works to learn and extract the muscles synergies patterns; in fact, given the input feature vector $I(t) = [m_1(t)m_2(t)\dots m_N(t)]$, where $m_i(t)$ indicates the pre-processed activation of the i-th muscle and N is the number of considered muscles, the AE preserves the objective to extract muscle synergy activations s_i. The topology has one hidden layer with four positive linear neurons that encode the muscle activations into synergy activations named $s_1(t)$, $s_2(t)$, $s_3(t)$ and $s_4(t)$. As before, the number of hidden neurons is set to four, and the overall configuration has been chosen with aim to replicate the physiological model of the spatial muscles synergies reported and deeply discussed in the work of Berger *et al.* [376]. The same three step pre-processing routine is also executed on each raw electromyographic signal: high-pass filtering (20 Hz second-order Butterworth); rectification and low-pass filtering (5 Hz second-order Butter-

worth); per-channel normalization over the maximum value computed during the calibration procedure.

Differently from the previous Section 3.2, the synergy-based movement intention detection has been achieved by adding a feed-forward block on top of the encoding hidden layer of the AE. By adding such block, the proposed neural model is able to compute the best muscle-synergy patterns that leads to the best trade-off between muscle activation reconstruction and movement intention estimation, that is, hand forces or articulation moment predictions. From the study of literature, this is the first attempt to build a model that is able to extract muscles synergies considering the performance into the task space, i.e. movement. Regarding the activation function, the layer considers a linear function and no bias has been added. Such configuration allows for the computation of the forces/moments as a linear combination of the synergy activations. In detail, the output vector $T(t) = [T_1(t), T_2(t)]$ represents the estimated moments. It is important mentioning that the moment components $T_1(t)$ and $T_2(t)$ have been normalized to range within the interval $[-0.5, 0.5]$.

Network Training The network has been implemented using the Neural Network toolbox of Matlab (Release 2018b), and trained using a gradient descent with momentum and adaptive learning rate algorithm for 1000 epochs. Given a single training set, the training of the neural model has been repeated 10 times considering different initial weights [384], then the model featuring the best performance has been considered for the next analysis. Considering a training set composed of about 1000 time points, the training process of the model lasts about 4.5 s. All the training sequences have been run on a PC featuring two Intel XEON E5 2630 v3 CPUs and 64 GB of RAM.

Joint moment estimation based on muscle synergies: comparison with the state of the art. As the previous application, the performance of the bi-dimensional motion intention estimator has been compared with the same standard methods. In detail:

- **Model** Hm: $T = H \cdot m$, where m is the muscle activation signal vector processed as the input data of the AE (see Figure 3.15) [376];
- **Model** $HWW^{+}m$: $T = H \cdot W \cdot W^{+} \cdot m$, where H is exactly the same EMG-to-moment matrix extracted for the model Hm [376] and W is the synergy matrix extracted with the NNMF by using the Matlab function $nnmf(\dots)$ (Release 2018b);
- **Model** $\hat{H}c$: $T = \hat{H} \cdot c$, where c is extracted with the NNMF for the model calibration and computed as reported in Equation (**??**) for the model evaluation [377];

- **AE-based model**: $T = H_{model} \cdot S$, where S is the synergy activation vector extracted by the autoencoder and H_{model} are the weights of the model block devoted to the synergy-based movement intention detection.

As before, the matrix H has dimension equal to $2 \times N$ (two is the number of moment components: shoulder and elbow joint moments), whereas the matrices $\hat{H}$ and H_{model} have size 2×4 (four is the number of considered muscle synergies). All methods have been tested using the same set of muscle activation recordings.

3.3.2 Results

In order to compare the proposed methods, the same model calibration, performance metrics and statistic methodologies used before were replicated. The proposed neural model has been evaluated both in terms of joint moment estimation and sEMG signal reconstruction. Figure 3.16 (top-left and bottom-left) and Figure 3.16 (top-right) report the mean value of the E_{RMS} and the mean R^2 values among all test sets for each subject, respectively. Table 3.2 reports the E_{RMS} and multivariate R^2 values averaged among all subjects for each compared methodology.

The Friedman test revealed that there is a significant difference among the four investigated techniques in terms of E_{RMS} relative to both shoulder moment prediction ($\chi^2 = 18.733$, $p < 0.001$) and elbow moment prediction ($\chi^2 = 15.000$, $p = 0.002$). Dunn test with Bonferroni correction was then used to perform the post-hoc tests (see Table 3.3). The results of the post-hoc analysis showed that the shoulder moment E_{RMS} error observed with AE-based model is significantly lower than both the errors obtained by the $HWW^{+}m$ model ($Z = 2.556$, $p < 0.001$) and $\hat{H}c$ model ($Z = 1.778$, $p = 0.021$). No significant differences were found between the AE-based model and Hm model ($Z = 1.222$, $p = 0.268$). Similar results were found analyzing the moment elbow E_{RMS} errors. In detail, the elbow moment E_{RMS} error observed with AE-based model is significantly lower than both the errors obtained by the $HWW^{+}m$ model ($Z = 2.111$, $p = 0.003$) and $\hat{H}c$ model ($Z = 1.778$, $p = 0.021$). No significant differences were found between the AE-based model and Hm model ($Z = 0.778$, $p = 1.000$).

The Friedman test also revealed that there is a significant difference among the four investigated techniques in terms of multivariate R^2 index between the measured and predicted joint moments, $\chi^2 = 21.400$, $p < 0.001$. The post-hoc analysis has reported that there is a significant difference between three pairs of models (see Table 3.3): the R^2 index of the AE-based model is higher than both the R^2 index of the $HWW^{+}m$ model ($Z = -2.667$,

$p < 0.001$) and $\hat{H}c$ model ($Z = -1.889$, $p = 0.011$), respectively; the Hm model outperforms the $HWW^{+}m$ model ($Z = 1.667$, $p = 0.037$); then no significant difference was found between the AE-based model and the Hm model ($Z = -1.000$, $p = 0.602$).

The difference between the autoencoder and the NNMF algorithm were also assessed in terms of sEMG signals reconstruction quality by comparing the multivariate R^2 index between the acquired and reconstructed EMG signals (see Figure 3.16 (bottom-right) and Table 3.4). The Wilcoxon test results showed that the NNMF achieved a significant higher R^2 index value than the autoencoder ($Z = -2.666$, $p = 0.008$).

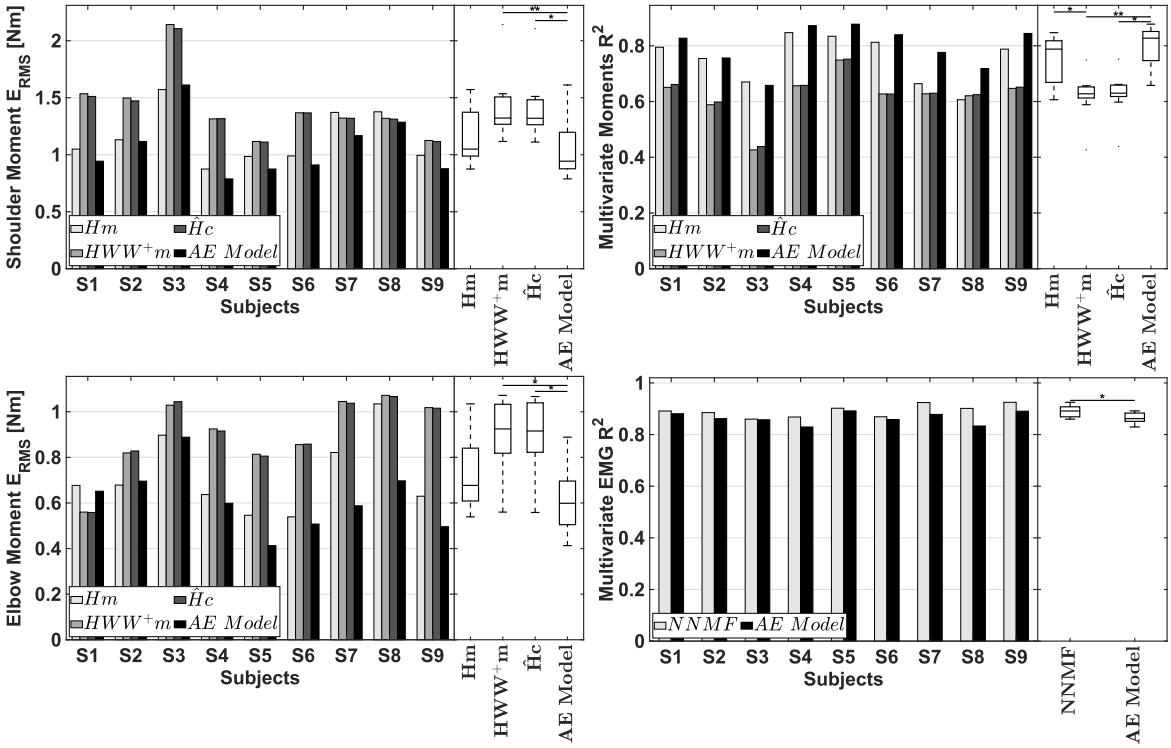

Figure 3.16 Results averaged among the test sets for each subject and each compared technique/model. Shoulder moment E_{RMS} errors (top-left). Elbow moment E_{RMS} errors (bottom-left). Moment Multivariate R^2 index values (top-right). sEMG Multivariate R^2 index values (bottom-right).

3.3.3 Discussion and Conclusions

To summurise, the statistical analysis on the data acquired from nine healthy subjects and the Figure 3.16 revealed that: the proposed method outperforms the two synergy-based approaches $HWW^{+}m$ and $\hat{H}c$ and such difference is statistically significant; no statistical difference has been found between the proposed method and the Hm model that considers

Table 3.2 Means and standard deviations of the shoulder/elbow moment RMS errors and multivariate R^2 index values among all subjects.

Model	**Shoulder Moment RMS Error [Nm] (M ± SD)**	**Elbow Moment RMS Error [Nm] (M ± SD)**	**Shoulder and Elbow Moment Multivariate R^2 (M ± SD)**
Hm	1.15 ± 0.24	0.72 ± 0.17	0.75 ± 0.09
$HWW^{+}m$	1.42 ± 0.31	0.90 ± 0.16	0.62 ± 0.09
$\hat{H}c$	1.40 ± 0.30	0.90 ± 0.16	0.63 ± 0.08
AE model	1.06 ± 0.26	0.62 ± 0.14	0.80 ± 0.07

Table 3.3 Results of the post-hoc analysis about the joint moments (p-values lower than 0.05 are in bold text).

	Shoulder Moment RMS Error		**Elbow Moment RMS Error**		**Moment Multivariate R^2**	
Pairwise Comparison	**Z**	***p*-Value**	**Z**	***p*-Value**	**Z**	***p*-Value**
$Hm - HWW^{+}m$	-1.333	0.171	-1.333	0.171	1.667	**0.037**
$Hm - \hat{H}c$	-0.556	1.000	-1.000	0.602	0.889	0.865
$Hm - AE\,model$	1.222	0.268	0.778	1.000	-1.000	0.602
$HWW^{+}m - \hat{H}c$	0.778	1.000	0.333	1.000	-0.778	1.000
$HWW^{+}m - AE\,model$	2.556	**<0.001**	2.111	**0.003**	-2.667	**<0.001**
$\hat{H}c - AE\,model$	1.778	**0.021**	1.778	**0.021**	-1.889	**0.011**

Table 3.4 Means and standard deviations of the sEMG multivariate R^2 index values among all subjects. Results of the Wilcoxon Test about the comparison between the non-negative matrix factorization (NNMF) and autoencoder.

Model	**sEMG multivariate R^2**	
	M ± SD	**Wilcoxon Test**
NNMF	0.89 ± 0.02	$Z = -2.666, p = 0.008$
AE	0.86 ± 0.02	

a direct mapping between the EMG signals and the joint moments. Such findings seem promising since the proposed method is able to achieve the comparable performance of the Hm model even if introduces some loss in the EMG signal information due to the AE bottleneck.

About the quality of the muscle activity reconstruction, as reported in Figure 3.16, it turned out that the proposed AE-based model has shown slightly lower performance than the NNMF (Wilcoxon test, $z = -2.666$, $p = 0.008$). This means that the NNMF generates synergy activations that better reconstruct the original muscle activation signals. This finding is not a big surprise since, differently from the NNMF, the proposed neural model has simultaneously focused on the reconstruction of both the EMG signals and joint moment. It is also worth noting that the AE and the NNMF have not been tested on the reconstruction of the same EMG signals used to calibrate the synergy model, but on different muscle activations acquired in the same condition (i.e., the same upper limb pose).

This work does not address the study of the relationship between the model accuracy and the number of considered muscles [385]. All the main superficial upper limb muscles that contribute to the shoulder and elbow moment generation have been considered [376]. Clearly, a reduction in the number of considered muscles would lead to a loss of model accuracy, and such loss would be related to the functional contribution of the specific excluded set of muscles. A further study could investigate the role of the considered muscles in moment estimation when using the proposed approach. However, it is important to remark that the main goal was to propose a general methodology. The specific set-up (i.e. considered muscles, task-space variables and acquisition procedure) needs to be customized case by case.

In conclusion, the proposed work represents a first attempt to develop a muscle synergy-based myo-controller that is tailored to the specific subject by simultaneously considering the synergy extraction and the mapping between the synergy activations and the variables used in the task space, i.e. forces or moments. Concerning the specific experimental setup used in this study, the obtained results have clearly showed that the proposed model has lead to a better moment estimation when compared with other synergy-based models. However, at the same time, the quality of the EMG signals reconstruction was slightly degraded. This finding demonstrated that a trade-off between the capability of the extracted muscle synergies to better describe the EMG signals variability and the task performance in terms of force reconstruction might exist and can be exploited to develop more intuitive myo-controllers that are mainly evaluated in the task space [380, 383].

3.4 Gait Analysis and Rehabilitation in Parkinson's Disease

The WHO declares a serious increase in the incidences of degenerative cronic diseases. These chronic diseases are characterized by a slow and progressive decay of normal physiological

functions that entail in most cases a considerable lowering of the quality of life, due to the impossibility of carrying out daily activities. The second most widespread chronic-neurodegenerative disease is the "Parkinson's disease" or "Parkinson's disease" (PD) from the name of the one who first described its characteristics and peculiarities [386]. It is a pathology that affects both the central nervous system and the peripheral nervous system with early death of dopaminergic neurons and that in the long run involves very disabling motor and non-motor symptoms such as resting tremor, freezing of movement, camptocormia, dementia etc [343]. Erroneously described at the time of its first detection as a disease caused exclusively by environmental factors, and in particular the pollution produced by the industrial revolution, it is instead a pathology associated with different causes and risk factors that include: genetic factors, age, family history, exposure to chemicals etc.

Recent studies related to the causes of Parkinson have led neurologists to support the use of levodopa-based drug therapy with a therapeutic/rehabilitation path [387]. Medical science has made great progress on mitigate the symptoms for parkinsonian patients by applying new rehabilitation techniques [388, 389]. Many tools for early diagnosis and correct analysis of Parkinson's disease symptoms have been developed [388, 390].

This study is based on this concept and it aims to define a new rehabilitation model focusing on those disabling motor symptoms that do not have a significant response to drug therapy. In particular, walking capability is considered in all its aspects: cadence, speed, depreciation, length, number of steps, frequency. For this purpose, the efficacy of cueing technique PD subjects gait was evaluated with a software built ad-hoc. The cue is a sensory stimulus has the aim to trigger the movement in the subject or support a given gait pace. Recent works have proved that Parkinson's Disease (PD) patients can be largely benefit by performing rehabilitation exercises based on audio cueing and music therapy [391–394]. Specially, gait can benefit from repetitive sessions of exercises using auditory cues. For this reason this study focuses on auditory cue.

3.4.1 Materials and Methods

Participants Five subjects affected by Parkinson's disease were selected for the experiment by a neurophysiology team with the collaboration Parkinson Italia association. The subjects had different Parkinson's Disease severity, that in some cases compromised also the autonomy of the movement. The details of the subjects are summarized in Table 3.5.

The following inclusion criteria were considered:

- Diagnosis of Parkinson's disease for at least 4 years;

Table 3.5 Details of the subjects selected for the experiment

ID	Sex	Age	PD Diagnosis (years)	Motor Autonomy
A.B.	F	60	4	Autonomous
O.B.	F	66	5	Autonomous
A.A.	M	70	7	Autonomous
D.B.	M	78	9	Not autonomous
M.Z.	M	76	5	Not autonomus

- Absence of comorbidities relevant for walking purposes;
- Under therapy with levodopa.

It was important that the subjects stopped levodopa therapy the day before the experiment to make it the most reliable as possible. All the participants were informed about the experiment and gave their consent.

Experiment Setup and Protocol The experiment took place in one of the neuro-rehabilitation gyms of the Medica Sud s.r.l. clinic with stable lighting condition and adequate spaces to allow comfortable walking and resting of the subjects (about 10-12 meters), A straight path has been defined with a starting point placed at a distance of 4.6 m and with an effective length of walkable space of 3.6 m.In order to ease the walking of the sujects and avoid measurement errors, a guide for the path was drawn with a tape on the floor. The Azure Kinect was placed at 0.5 m from the ending point of the path, with height of 94 cm above the ground and was calibrated the floor.

In order to track the movement of the subject walking following the defined path, a C++ application based on the Azure Kinect was designed and developed. The software used the Azure Body Tracking module to detect and track the 3D position and orientation of the human body main joints (up to 32 joints as shown in).

Since the purpose of the study was to evaluate the influence of auditory stimuli in walking of subjects with Parkinson's Disease from mild to severe, the software implemented the following walking acquisition modes:

- Simple Acquisition: no external stimuli were submitted (reference acquisition);
- Acquisition with Metronome: a variable frequency metronome sound was used to stimulate the pace of the walk.

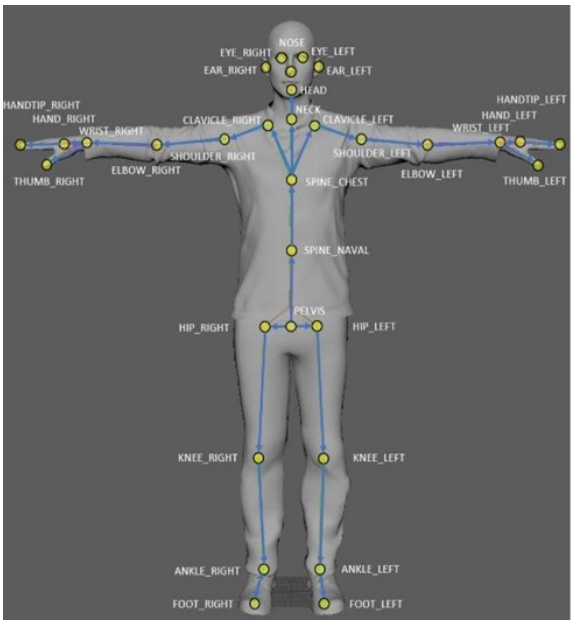

Figure 3.17 Joints detected with Azure Kinect Body Tracking module.

The software integrates also a post processing module developed ad-hoc to analyze the path, calculate the spatio-temporal parameters and extract gait cycle features.

The experimental protocol consisted of the following phases:

1. Acquisition of 2 walks following the defined path performed without the use of the metronome;
2. Acquisition of 2 walks following the defined path performed with the use of the metronome set at the frequency of the average cadence recorded in the previous two walks;
3. Acquisition of 2 walks following the defined path performed with the use of the metronome set at a frequency 15% higher than the average cadence recorded in the previous two walks.

For each acquisition, the following features were extracted:

- CadenceL - Cadence of the Step in the left foot
- CadenceR - Cadence of the Step in the right foot
- CycleTimeL - Left Step cycle time
- CycleTimeR - Right Step cycle time

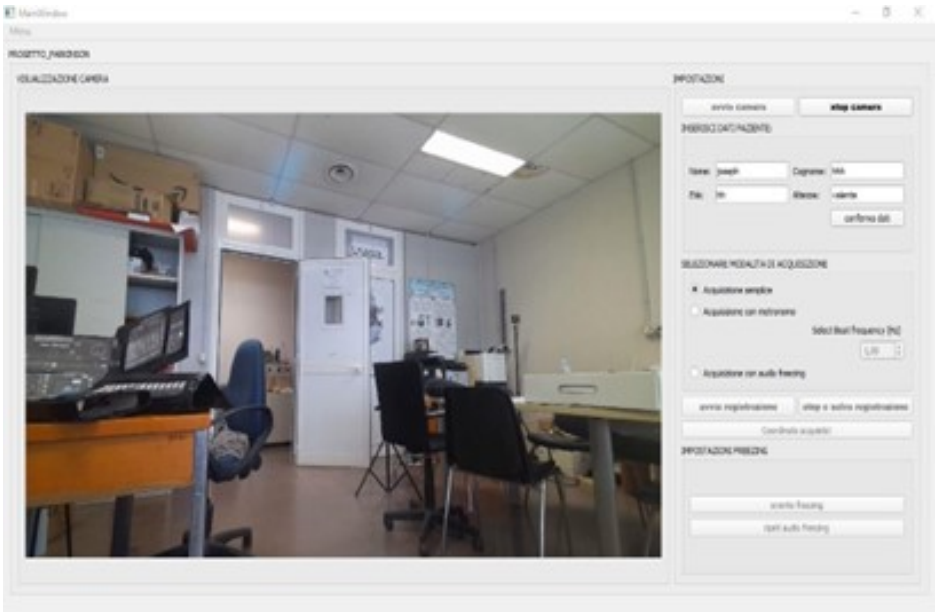

Figure 3.18 GUI of the application developed for the study.

- DoubleSupport - Time when both feet are on the ground
- StanceL - Duration as a percentage of the left Stance phase
- StanceR - Duration as a percentage of the right Stance phase
- StanceTimeL - Time when the left foot is in the Stance phase
- StanceTimeR - Time when the left foot is in the Stance phase
- StepLengthL - Left Step length
- StepLengthR - Left Step length
- StepWidthL - Left Step width
- StepWidthR - Right Step width
- StrideLengthL - Left Stride length
- StrideLengthR - Right Stride length
- StrideVelocityL - Speed in the Stride phase of the left foot
- StrideVelocityR - Speed in the Stride phase of the left foot

- SwingL - Duration as a percentage of the left Swing phase
- SwingR - Duration as a percentage of the right Swing phase
- SwingTimeL - Time of the Swing phase of the left foot
- SwingTimeR - Time of the Swing phase of the right foot
- SwingVelocityL - Speed in the Swing phase of the left foot
- SwingVelocityR - Speed in the Swing phase of the right foot

3.4.2 Results

For each of the six acquisitions, the features related to all the gait cycles (Left,Right) identified in a walk were extracted. Then they were grouped according to the acquisition mode: "Without Metronome","With Metronome". In order to conduct a visual inspection of the data, box-plots were created for each patient and for each feature for enhancing possible differences in the features between the two conditions. A statistical analysis was conducted with IBM SPSS Statistics software. In particular, the Wilcoxon nonparametric test for paired samples was used to compare the variables related to conditions without and with metronome, since the assumptions for the use of the parametric t-test for paired samples were violated.

3.6 shows the p-values of all comparisons conducted for each feature and for each patient. The significance level of the test was set at $\alpha = .05$. All p-value values lower than the set significance level have been bolded and highlighted. At first look, it is possible to see that there were significant differences only for two subjects. Indeed, some features of the subjects D.B. and M.Z. are characterized by a significant difference between the without and with metronome conditions. On the other hand, features extracted by A.A., A.B. and O.B. walks do not present any difference between the two conditions.

In details, the statistical analysis conducted on the features extracted from the walks of the subject M.Z. showed the following significant differences:

- the cadence (Steps per minute) of the right and left gait cycles related to the walks with metronome is significantly greater than the cadence related to the walks without the metronome (Figure 3.19);
- the duration of right and left cycles related to the walks with metronome is significantly shorter than the duration of gait cycles related to the walks without the metronome Figure 3.20);

Table 3.6 p-values results of Wilcoxon nonparametric test for paired samples applied on features for With and Without Metronome conditions.

Features	**Subjects**				
	A.A.	**A.B.**	**D.B.**	**M.Z.**	**O.B.**
Cadence Left	0.1775	0.9048	0.4984	**0.0010**	0.2371
Cycle Time Left	0.1364	0.9048	0.2987	**0.0010**	0.2438
Double Support Left	0.5649	0.9048	0.5043	0.5422	0.5135
Stance Left	1.0000	0.4127	0.1006	0.1702	0.4129
Stance Time Left	0.2727	0.6032	0.1838	**0.0060**	0.0859
Step Length Left	0.3095	0.7302	**0.0010**	0.4053	0.2824
Step Width Left	0.1797	0.4127	**0.0010**	0.4043	0.7546
Stride Length Left	0.0649	0.9048	**0.0010**	0.1150	0.4230
Stride Velocity Left	0.2069	0.9048	**0.0100**	0.2722	0.0813
Swing Left	1.0000	0.4127	0.1896	0.1953	0.4129
Swing Time Left	0.2273	0.3651	0.3520	0.1285	0.8851
Swing Velocity Left	0.4468	0.4127	**0.0040**	0.4316	0.5728
Cadence Right	0.1978	0.6993	0.5125	**0.0020**	0.1224
Cycle Time Right	0.0891	0.6993	0.4200	**0.0020**	0.1224
Double Support Right	0.8506	0.3341	0.4920	0.4960	0.6282
Stance Right	0.4069	0.1709	0.0848	0.3508	0.3834
Stance Time Right	0.0563	0.8143	0.3524	**0.0040**	0.1294
Step Length Right	0.4848	0.6216	**0.0400**	0.2810	0.8357
Step Width Right	0.4848	0.5369	**0.0010**	0.2312	0.2949
Stride Length Right	0.4848	0.9433	**0.0010**	0.0805	0.7308
Stride Velocity Right	0.3939	0.9433	**0.0020**	0.5198	0.9452
Swing Right	0.4264	0.1709	0.0939	0.3896	0.3834
Swing Time Right	0.7446	0.2953	0.0969	0.0536	0.1294
Swing Velocity Right	0.4848	0.2844	**0.0010**	0.2789	0.6282

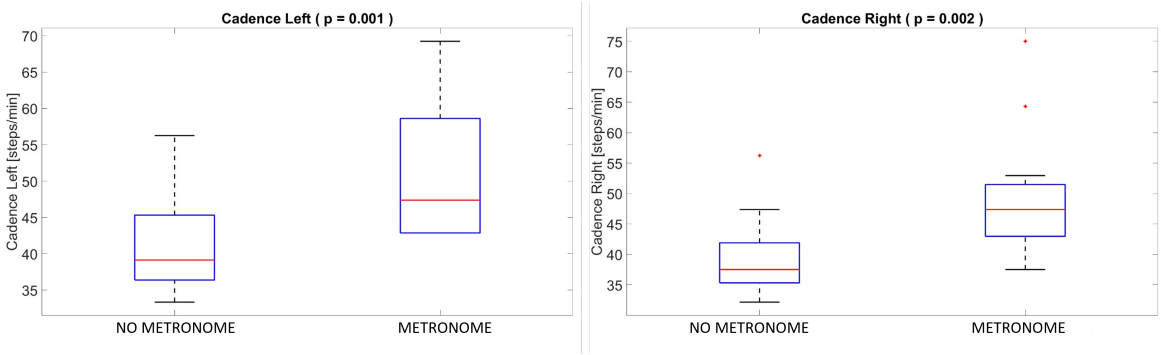

Figure 3.19 Box-plots and p-values of cadence for left and right gait cycles in no metronome and metronome conditions for subject M.Z..

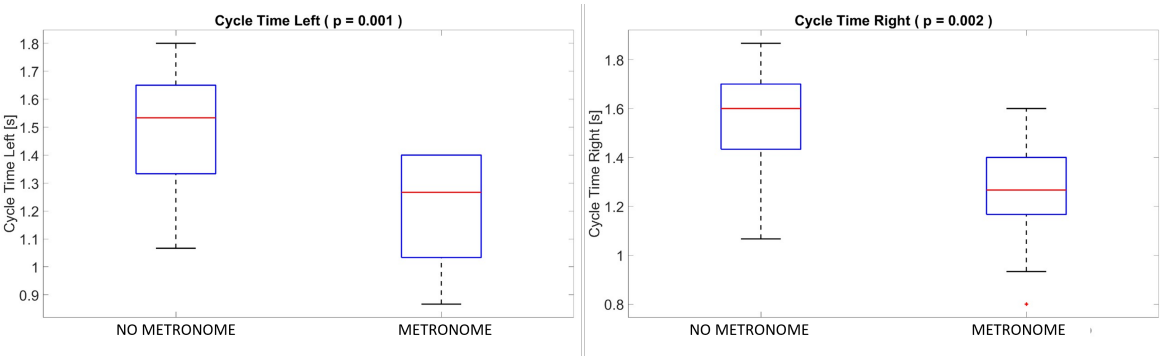

Figure 3.20 Box-plots and p-values of left and right cycles time in no metronome and metronome conditions for subject M.Z..

- the duration of the stance phase in right and left gait cycles related to the walks with metronome is significantly shorter than the duration of the gait cycles related to the walks without the metronome(Figure 3.21).

No other significant differences were observed for the subjects. It follows that the other features didn't reveal any significant change with the introduction of the metronome.

Furthermore, the statistical analysis conducted on the features extracted from the walks of the subject M.Z. showed the following significant differences:

- the step length for the right and left gait cycles related to the walks with metronome is significantly greater than the length related to the walks without the metronome (Figure 3.22);
- the step width for the right and left gait cycles related to the walks with metronome is significantly greater than the step width related to the walks without the metronome(Figure 3.23);

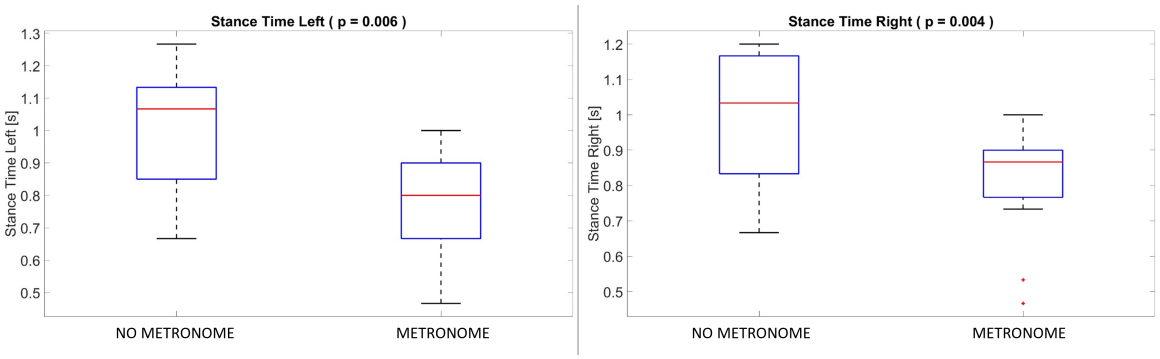

Figure 3.21 Box-plots and p-values of stance time for left and right gait cycles in no metronome and metronome conditions for subject M.Z..

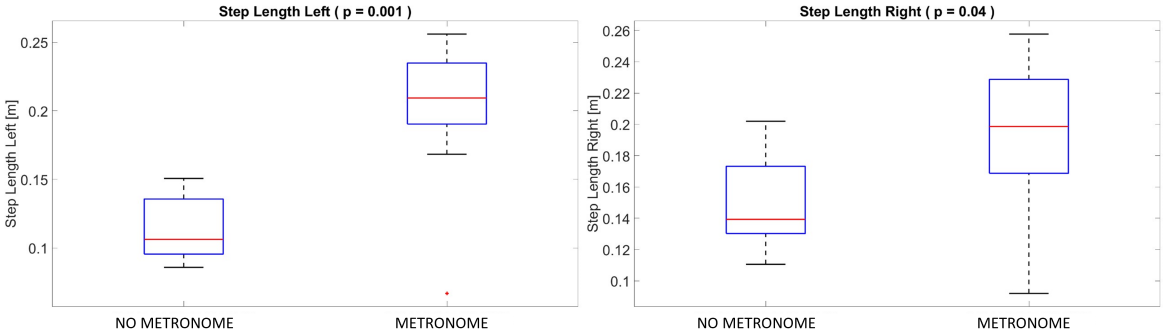

Figure 3.22 Box-plots and p-values of step length for left and right gait cycles in no metronome and metronome conditions for subject D.B..

- the stride phase length for the right and left gait cycles related to the walks with metronome is significantly greater than the stride length related to the walks without the metronome(Figure 3.24);
- the stride velocity in the right and left gait cycles related to the walks with metronome is significantly higher than the stride velocity related to the walks without the metronome (Figure 3.25);
- the swing phase velocity in the right and left gait cycles acquired during metronome walks is significantly higher than the swing phase velocity related to the walks without the metronome(Figure 3.26).

No other significant differences were observed for the subjects. It follows that the other features didn't reveal any significant change with the introduction of the metronome.

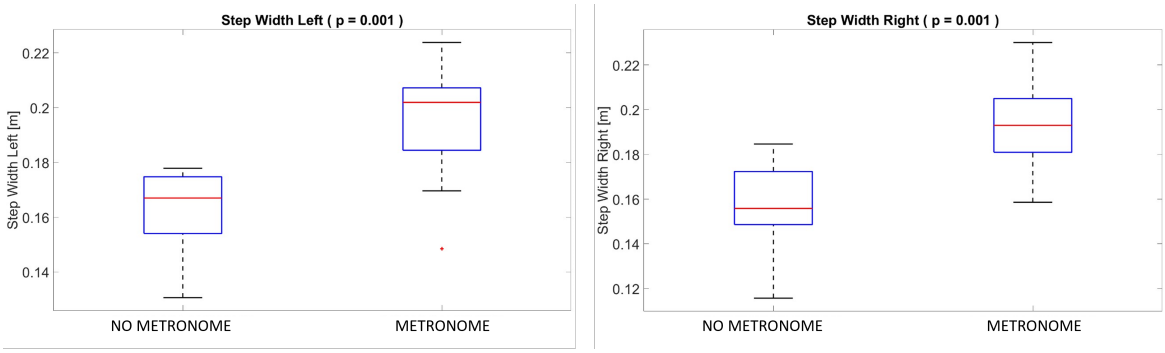

Figure 3.23 Box-plots and p-values of step width for left and right gait cycles in no metronome and metronome conditions for subject D.B..

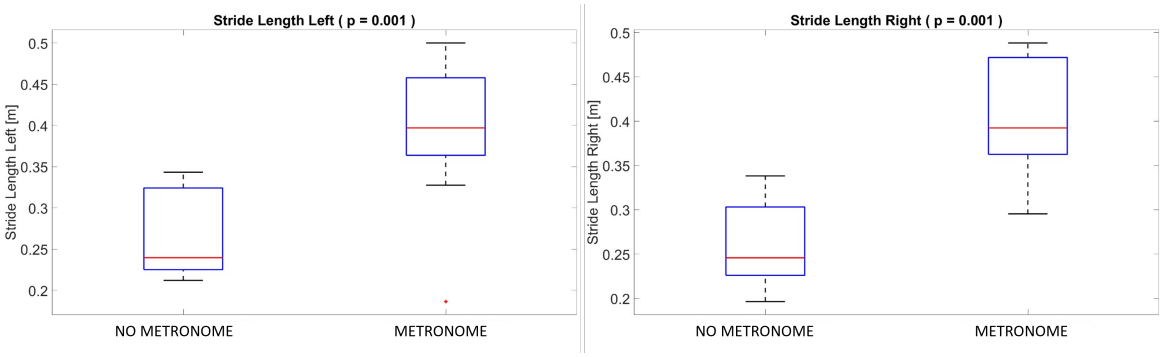

Figure 3.24 Box-plots and p-values of stride length for left and right gait cycles in no metronome and metronome conditions for subject D.B..

3.4.3 Discussion and Conclusions

As reported in the previous paragraph, from the analysis of all the features extracted from the walks of each subject in metronome and no metronome conditions, emerged that no features were significantly different between the two conditions for three of the subjects but some of the features of two subjects (M.Z. and D.B.) showed statistically significant differences between the two conditions. In details, for the subject M.Z., the use of the metronome with a frequency higher than the cadence recorded during the walking tests without metronome led to observe of an increase in the cadence for both left and right gait cycles. The increase in cadence is clearly a consequence of the significant reduction of the left and right step cycles duration. Analyzing in more detail the characteristics of the gait cycles acquired in "metronome" mode, it emerged that a significant reduction in the stance phase was recorded and this explains the reduction of the duration of the step cycle. An improvement in the walking of that subject was then observed in terms of the cadence of the step that increased. For subject D.B., the use of the metronome with a frequency higher

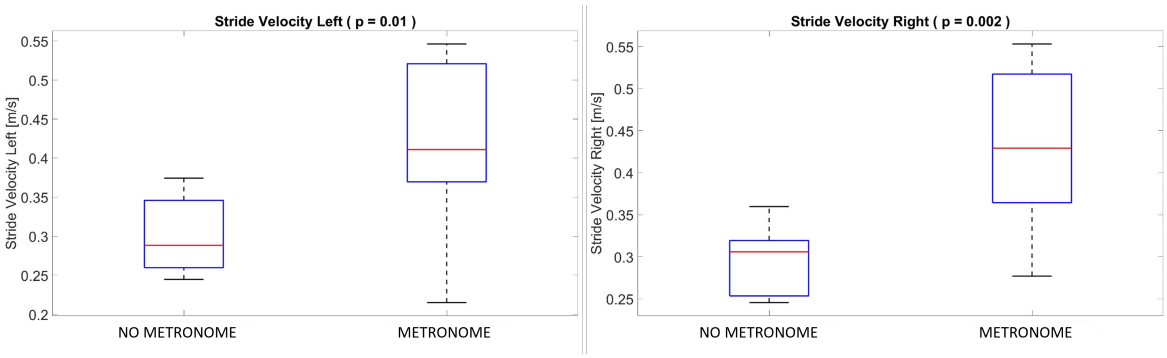

Figure 3.25 Box-plots and p-values of stride velocity for left and right gait cycles in no metronome and metronome conditions for subject D.B..

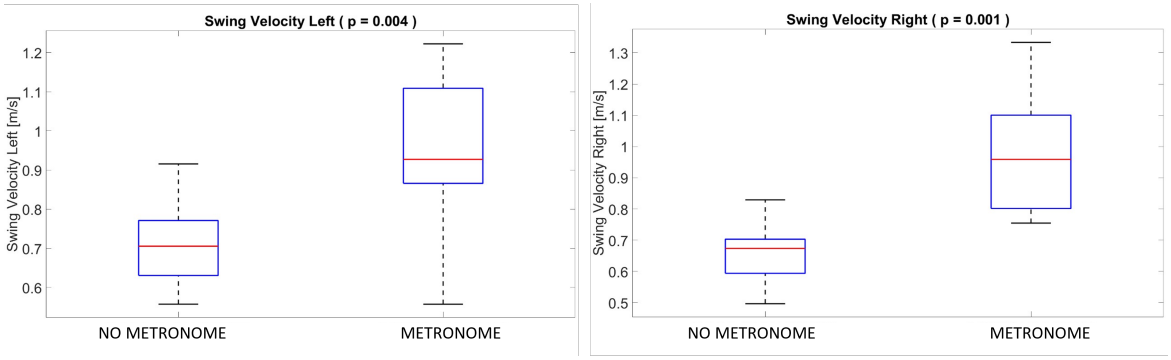

Figure 3.26 Box-plots and p-values of swing phase velocity for left and right gait cycles in no metronome and metronome conditions for subject D.B..

than the cadence recorded during the walking tests without metronome led to observe an increase in the length of the half-steps and steps for both left and right gait cycles. Unlike what emerged in the data of patient M.Z., the walking acquisitions of patient D.B. did not show statically significant differences in cadence. Indeed, the cadence is statistically unchanged because, in the condition with metronome, in addition to the increase in length of the half-steps and steps, a significant increase in the velocity of the step and therefore in the velocity of the swing phases of the step cycle was observed. An improvement in the subject's walking was therefore observed in terms of stride length and swing phases velocity. A further improvement in the quality of walking has been evaluated in terms of the width of the step which is significantly greater with the introduction of the metronome. A greater step width translates into better stability and balance.

From these results, it's clear not all the subjects had an effective response to the auditory cueing and even the ones that respond to it showed different changes in term of gait features. The cause can be related to the experiment design and execution itself: some subjects could

require more sessions or longer sessions to feel comfortable and benefit from the auditory cues or some can require other kind of cues. It's a matter of fact, Parkinson's Disease is characterized by a great variability subjects by subjects even if in the same stage of pathology; this can influence the effectiveness of cueing technique.

In this study, five Parkinsonian patients who were asked to walk along a straight path without and with a metronome-type auditory cue. This cue is characterized by a higher frequency of the cadence of the walk acquired without auditory cue. A softare based on Azure Kinect Body Tracking was designed and developed for the purose. The subjects 3D data of body joints of a subject were acquired and gait cycles features were calculated. A statistical analysis of the acquired data showed the influence of auditory cue on the main features of walking of two subjects on five. Specifically, in one subject an increase in cadence was revealed, in the another subject an increase in both the length of the step and the width of the step was observed.

Considering the low cost and accuracy of Azure Kinect, it is a great alternative to expensive gait analysis platforms and it can be the base technology of a low cost system for rehabilitation and evaluation of parkinsonian patients. It could be adopted in a clinical context or even used to serve home sessions overcoming the stress of reaching dedicated facilities that is a big challenge for PD patients because of low motor autonomy and pandemic risks too. At the end, the designed software could support also diagnostic and rehabilitation protocols for other neurodegenerative diseases with implications on walking, such as: senile dementia, Alzheimer's disease, Huntington's chorea, amyotrophic lateral sclerosis or other rarer diseases such as spongiform encephalopathies.

Chapter 4

Conclusion

In Industry 4.0 the attention to human factors has been particularly sparse, despite the evident centrality of Human Factor in the developmental priorities (i.e. managing complex systems, safety and security, work organization and design, and training and professional development).

The studies collected in this thesis aimed to propose a set of innovative work-flows for real systems based on enabling technologies of Industry 4.0 and Healthcare 4.0 that put the humans at the center. The outcomes could be summarized with four important contributions:

- The body tracking is usually performed with really expensive and delicate systems that can't be introduced in a factory, also hand tools tracking can't be done without invasive and bulky systems. This result with the proposal of low-cost devices and Computer Vision/Deep Learning techniques for tracking the human body actions and tool handled by the operator in the industry context are a strong point that contribute to close the gap between research around Human Factor and real applications in Industry 4.0.

- During my visiting period at Toyota Motor Europe, I transferred the results of research concerning Industry 4.0 enabling technologies and Human factors into application responding the concrete need of maintenance training transformation in automotive industry. It's a matter of fact that digitization of training experience with AR/MR technologies is the future of learning in every field because it's an investment for efficiency and cost reduction.

- Starting from muscle synergies evidence, new methods of extraction have been investigated, employing machine learning techniques in different scenarios, as well

as interesting cues about the interpretation of their changing. This new extraction algorithms can be used to improve myo-control performance during task-oriented therapies.

- The success of cueing technique on people suffering of Parkinson's Disease opens new important paths towards a next-generation rehabilitation and Industry 4.0 enabling technologies are great tools to shape it building low-cost, easy and home deliverable solutions

Future works will focus on provide significant advancement on all the topics already investigated in this thesis. Industry 4.0 research and application results will converge into the design and development of a framework able to acquire kinematic, electromyographic and video signals of a subject carrying out manual maintenance activities in an industrial context and with deep learning techniques for action recognition and classification recognizing the actions performed by the subject and evaluate their correctness and at the same time the ergonomic risk. Concerning Healthcare 4.0, new studies will be conducted around movement disorders rehabilitation on both branches, muscle synergies and cueing technique in order to explore new approaches and consolidating the results with the aim of improving the human tailored clinical practice.

References

[1] W Patrick Neumann, Sven Winkelhaus, Eric H Grosse, and Christoph H Glock. Industry 4.0 and the human factor–a systems framework and analysis methodology for successful development. *International journal of production economics*, 233:107992, 2021.

[2] European Commission, Directorate-General for Research, Innovation, M Breque, L De Nul, and A Petridis. *Industry 5.0 : towards a sustainable, human-centric and resilient European industry*. Publications Office, 2021. doi: doi/10.2777/308407.

[3] Jingshan Li and Pascale Carayon. Health care 4.0: A vision for smart and connected health care. *IISE transactions on healthcare systems engineering*, 11(3):171–180, 2021.

[4] Mario Hermann, Tobias Pentek, Boris Otto, et al. Design principles for industrie 4.0 scenarios: a literature review. *Technische Universität Dortmund, Dortmund*, 45, 2015.

[5] Erik Hofmann and Marco Rüsch. Industry 4.0 and the current status as well as future prospects on logistics. *Computers in industry*, 89:23–34, 2017.

[6] Henning Kagermann, Wolfgang Wahlster, and Johannes Helbig. Securing the future of german manufacturing industry: Recommendations for implementing the strategic initiative industrie 4.0. *Final report of the Industrie*, 4(0), 2013.

[7] Jay Lee, Behrad Bagheri, and Hung-An Kao. A cyber-physical systems architecture for industry 4.0-based manufacturing systems. *Manufacturing letters*, 3:18–23, 2015.

[8] Dominik Lucke, Carmen Constantinescu, and Engelbert Westkämper. Smart factory-a step towards the next generation of manufacturing. In *Manufacturing systems and technologies for the new frontier*, pages 115–118. Springer, 2008.

[9] Keliang Zhou, Taigang Liu, and Lifeng Zhou. Industry 4.0: Towards future industrial opportunities and challenges. In *2015 12th International conference on fuzzy systems and knowledge discovery (FSKD)*, pages 2147–2152. IEEE, 2015.

[10] Dominic Gorecky, Mathias Schmitt, Matthias Loskyll, and Detlef Zühlke. Human-machine-interaction in the industry 4.0 era. In *2014 12th IEEE international conference on industrial informatics (INDIN)*, pages 289–294. Ieee, 2014.

[11] Egon Mueller, Xiao-Li Chen, and Ralph Riedel. Challenges and requirements for the application of industry 4.0: a special insight with the usage of cyber-physical system. *Chinese Journal of Mechanical Engineering*, 30(5):1050–1057, 2017.

[12] Brett P Conner, Guha P Manogharan, Ashley N Martof, Lauren M Rodomsky, Caitlyn M Rodomsky, Dakesha C Jordan, and James W Limperos. Making sense of 3-d printing: Creating a map of additive manufacturing products and services. *Additive Manufacturing*, 1:64–76, 2014.

[13] William E Frazier. Metal additive manufacturing: a review. *Journal of Materials Engineering and performance*, 23(6):1917–1928, 2014.

[14] Kaufui V Wong and Aldo Hernandez. A review of additive manufacturing. *International scholarly research notices*, 2012, 2012.

[15] Roger N Lumley. Aluminium investment casting and rapid prototyping for aerospace applications. In *Fundamentals of Aluminium Metallurgy*, pages 123–158. Elsevier, 2018.

[16] P Lopes, Paulo Flores, and Eurico Seabra. Rapid prototyping technology in medical applications: A critical review. *Computational Modelling of Objects Represented in Images*, pages 255–260, 2018.

[17] Fabrizio Regina, Fulvio Lavecchia, and Luigi Maria Galantucci. Preliminary study for a full colour low cost open source 3d printer, based on the combination of fused deposition modelling (fdm) or fused filament fabrication (fff) and inkjet printing. *International Journal on Interactive Design and Manufacturing (IJIDeM)*, 12(3):979–993, 2018.

[18] Wei Sun, Jae Hyun Nam, Andrew Leete Darling, and Saif Khalil. Method and apparatus for computer-aided tissue engineering for modeling, design and freeform fabrication of tissue scaffolds, constructs, and devices, January 28 2014. US Patent 8,639,484.

[19] Nicholas P Cowley, Ruchir Saraswat, and Richard J Goldman. Biofeedback sensors in a body area network, August 14 2018. US Patent 10,045,735.

[20] Ehsan Kargaran, Danilo Manstretta, and Rinaldo Castello. Design considerations for a sub-mw wireless medical body-area network receiver front end. *Micromachines*, 9(1): 31, 2018.

[21] G Elhayatmy, Nilanjan Dey, and Amira S Ashour. Internet of things based wireless body area network in healthcare. In *Internet of things and big data analytics toward next-generation intelligence*, pages 3–20. Springer, 2018.

[22] Dong Wang, Monisha Ghosh, and Delroy Smith. Medical body area network (mban) with key-based control of spectrum usage, March 21 2017. US Patent 9,603,024.

[23] MG Li, XY Tian, and XB Chen. Review of dispensing-based rapid prototyping techniques in tissue scaffold fabrication. *MODELING OF THE DISPENSING-BASED*, page 5, 2010.

[24] Thomas Töppel, Holger Lausch, Michael Brand, Eric Hensel, Michael Arnold, and Christian Rotsch. Structural integration of sensors/actuators by laser beam melting for tailored smart components. *JOM*, 70(3):321–327, 2018.

[25] Antonio Emmanuele Uva, Michele Fiorentino, Michele Gattullo, Marco Colaprico, Maria F de Ruvo, Francescomaria Marino, Gianpaolo F Trotta, Vito M Manghisi, Antonio Boccaccio, Vitoantonio Bevilacqua, et al. Design of a projective ar workbench for manual working stations. In *International Conference on Augmented Reality, Virtual Reality and Computer Graphics*, pages 358–367. Springer, 2016.

[26] Vitoantonio Bevilacqua, Antonio Brunetti, Giuseppe Trigiante, Gianpaolo Francesco Trotta, Michele Fiorentino, Vito Manghisi, and Antonio Emmanuele Uva. Design and development of a forearm rehabilitation system based on an augmented reality serious game. In *Italian Workshop on Artificial Life and Evolutionary Computation*, pages 127–136. Springer, 2015.

[27] Francesco Porpiglia, Cristian Fiori, Enrico Checcucci, Daniele Amparore, and Riccardo Bertolo. Augmented reality robot-assisted radical prostatectomy: preliminary experience. *Urology*, 115:184, 2018.

[28] F Porpiglia, R Bertolo, E Checcucci, D Amparore, and C Fiori. Robot-assisted radical prostatectomy with 3d-based augmented reality. *European Urology Supplements*, 17(7): e2383, 2018.

[29] F Porpiglia, R Bertolo, E Checcucci, D Amparore, and C Fiori. 3d augmented reality robot-assisted radical prostatectomy. *European Urology Supplements*, 17(2):e1929, 2018.

[30] Oscar Blanco-Novoa, Tiago M Fernandez-Carames, Paula Fraga-Lamas, and Miguel A Vilar-Montesinos. A practical evaluation of commercial industrial augmented reality systems in an industry 4.0 shipyard. *Ieee Access*, 6:8201–8218, 2018.

[31] Iñigo Fernández del Amo, John Ahmet Erkoyuncu, Rajkumar Roy, and Stephen Wilding. Augmented reality in maintenance: An information-centred design framework. *Procedia Manufacturing*, 19:148–155, 2018.

[32] Riccardo Palmarini, John Ahmet Erkoyuncu, Rajkumar Roy, and Hosein Torabmostaedi. A systematic review of augmented reality applications in maintenance. *Robotics and Computer-Integrated Manufacturing*, 49:215–228, 2018.

[33] Stephen Smilevski, Gokul Sidarth Thirunavukkarasu, Mehdi Seyedmahmoudian, Scott McMillan, and Ben Horan. Mixed reality tool for training on pressure immobilization treatment of snake bite envenomation. In *Proceedings of the 23rd International ACM Conference on 3D Web Technology*, pages 1–7, 2018.

[34] Tiago França Melo Lima, João Paulo Ferreira Beltrame, Carlos Ramos Niquini, Breno Gonçalves Barbosa, and Clodoveu Augusto Davis. Design of a mixed-reality

serious game to tackle a public health problem. In *International Conference on Entertainment Computing*, pages 305–309. Springer, 2018.

[35] Joshua Warren Sappenfield, William Brit Smith, Lou Ann Cooper, David Lizdas, Drew Gonsalves, Nikolaus Gravenstein, Samsun Lampotang, and Albert R Robinson III. Visualization improves supraclavicular access to the subclavian vein in a mixed reality simulator. *Anesthesia and analgesia*, 127(1):83, 2018.

[36] Federico Gheza and Paolo Raimondi. Image fusion and mixed reality in abdominal surgery. *Annals of Surgery*, 2019.

[37] Robb Lindgren and Mina Johnson-Glenberg. Emboldened by embodiment: Six precepts for research on embodied learning and mixed reality. *Educational researcher*, 42(8): 445–452, 2013.

[38] Marientina Gotsis, Amanda Tasse, Maximilian Swider, Vangelis Lympouridis, Irina C Poulos, Alasdair G Thin, David Turpin, Diane Tucker, and Maryalice Jordan-Marsh. Mixed reality game prototypes for upper body exercise and rehabilitation. In *2012 IEEE Virtual Reality Workshops (VRW)*, pages 181–182. IEEE, 2012.

[39] Marta Kersten-Oertel, Pierre Jannin, and D Louis Collins. The state of the art of visualization in mixed reality image guided surgery. *Computerized Medical Imaging and Graphics*, 37(2):98–112, 2013.

[40] Jonathan Andrew Schlueter. *Remote maintenance assistance using real-time augmented reality authoring*. PhD thesis, Iowa State University, 2018.

[41] Geoffrey T Miller, Tyler Harris, Y Sammy Choi, Stephen M DeLellis, Kenneth Nelson, and J Harvey Magee. Augmented reality and telestrated surgical support for point of injury combat casualty care: A feasibility study. In *International Conference on Augmented Cognition*, pages 395–405. Springer, 2018.

[42] Max J Greenfield, Joshua Luck, Michael L Billingsley, Richard Heyes, Oliver J Smith, Afshin Mosahebi, Abu Khoussa, Ghassan Abu-Sittah, and Nadine Hachach-Haram. Demonstration of the effectiveness of augmented reality telesurgery in complex hand reconstruction in gaza. *Plastic and Reconstructive Surgery Global Open*, 6(3), 2018.

[43] Antonio E Uva, Michele Gattullo, Vito M Manghisi, Daniele Spagnulo, Giuseppe L Cascella, and Michele Fiorentino. Evaluating the effectiveness of spatial augmented reality in smart manufacturing: a solution for manual working stations. *The International Journal of Advanced Manufacturing Technology*, 94(1):509–521, 2018.

[44] Qiang Tang, Yan Chen, Gerald Schaefer, and Alastair G Gale. Development of an augmented reality approach to mammographic training: overcoming some real world challenges. In *Medical Imaging 2018: Image-Guided Procedures, Robotic Interventions, and Modeling*, volume 10576, page 105762M. International Society for Optics and Photonics, 2018.

[45] Abdulrahman Al-Ahmari, Wadea Ameen, Mustufa Haider Abidi, and Syed Hammad Mian. Evaluation of 3d printing approach for manual assembly training. *International Journal of Industrial Ergonomics*, 66:57–62, 2018.

[46] Paula Fraga-Lamas, Tiago M Fernández-Caramés, Oscar Blanco-Novoa, and Miguel A Vilar-Montesinos. A review on industrial augmented reality systems for the industry 4.0 shipyard. *Ieee Access*, 6:13358–13375, 2018.

[47] Oliver Bimber and Ramesh Raskar. *Spatial augmented reality: merging real and virtual worlds*. CRC press, 2005.

[48] Michele Di Donato, Michele Fiorentino, Antonio E Uva, Michele Gattullo, and Giuseppe Monno. Text legibility for projected augmented reality on industrial workbenches. *Computers in Industry*, 70:70–78, 2015.

[49] Konjengbam Jackichand Singh and LP Saikia. A survey on augmented reality technologies and applications. *International Research Journal of Engineering and Technology*, 5 (6):791–794, 2018.

[50] Jiri Kovar, Katerina Mouralova, Filip Ksica, Jiri Kroupa, Ondrej Andrs, and Zdenek Hadas. Virtual reality in context of industry 4.0 proposed projects at brno university of technology. In *2016 17th international conference on mechatronics-mechatronika (ME)*, pages 1–7. IEEE, 2016.

[51] Glyn Lawson, Davide Salanitri, and Brian Waterfield. Future directions for the development of virtual reality within an automotive manufacturer. *Applied ergonomics*, 53: 323–330, 2016.

[52] Peter Zimmermann. Virtual reality aided design. a survey of the use of vr in automotive industry. In *Product Engineering*, pages 277–296. Springer, 2008.

[53] KLAUS-PETER BEIER. Virtual reality in automotive design and manufacturing. *LEADING CHANGE*, 1994.

[54] Antonino Gomes De Sa and Gabriel Zachmann. Virtual reality as a tool for verification of assembly and maintenance processes. *Computers & Graphics*, 23(3):389–403, 1999.

[55] Daniel Paes, Eduardo Arantes, and Javier Irizarry. Immersive environment for improving the understanding of architectural 3d models: Comparing user spatial perception between immersive and traditional virtual reality systems. *Automation in Construction*, 84:292–303, 2017.

[56] Fadzidah Abdullah, Mohd Hisyamuddin Bin Kassim, and Aliyah Nur Zafirah Sanusi. Go virtual: exploring augmented reality application in representation of steel architectural construction for the enhancement of architecture education. *Advanced Science Letters*, 23(2):804–808, 2017.

[57] Dusan Maga, Juraj Dudak, Sona Pavlikova, Jiri Hajek, and Boris Simak. Support of technical education at primary and secondary level. In *Proceedings of 15th International Conference MECHATRONIKA*, pages 1–4. IEEE, 2012.

[58] Yusuf Altintas, Christian Brecher, Manfred Weck, and S Witt. Virtual machine tool. *CIRP annals*, 54(2):115–138, 2005.

[59] Sanjay Jain, Ngai Fong Choong, Khin Maung Aye, and Ming Luo. Virtual factory: an integrated approach to manufacturing systems modeling. *International Journal of Operations & Production Management*, 2001.

[60] Alfredo Sanz, Ignaciof González, Agustin Javier Castejón, and Jose Leopoldo Casado. Using virtual reality in the teaching of manufacturing processes with material removal in cnc machine-tools. In *Materials Science Forum*, volume 692, pages 112–119. Trans Tech Publ, 2011.

[61] Antonie J Van den Bogert, Thomas Geijtenbeek, Oshri Even-Zohar, Frans Steenbrink, and Elizabeth C Hardin. A real-time system for biomechanical analysis of human movement and muscle function. *Medical & biological engineering & computing*, 51(10): 1069–1077, 2013.

[62] Z Sheikh, R Jackson, P Tharmanathan, and A Keding. Virtual reality simulation in minimally invasive surgery training: A systematic review and meta-analysis. In *BRITISH JOURNAL OF SURGERY*, volume 105, pages 31–31. WILEY 111 RIVER ST, HOBOKEN 07030-5774, NJ USA, 2018.

[63] Laura Stone McGuire and Ali Alaraj. Competency assessment in virtual reality-based simulation in neurosurgical training. In *Comprehensive Healthcare Simulation: Neurosurgery*, pages 153–157. Springer, 2018.

[64] Gerald B Schulz, Tobias Grimm, Alexander Buchner, Friedrich Jokisch, Jozefina Casuscelli, Alexander Kretschmer, Jan-Niclas Mumm, Brigitte Ziegelmüller, Christian G Stief, and Alexander Karl. Validation of a high-end virtual reality simulator for training transurethral resection of bladder tumors. *Journal of Surgical Education*, 76(2):568–577, 2019.

[65] Yeshwanth Pulijala, Minhua Ma, Matthew Pears, David Peebles, and Ashraf Ayoub. Effectiveness of immersive virtual reality in surgical training—a randomized control trial. *Journal of Oral and Maxillofacial Surgery*, 76(5):1065–1072, 2018.

[66] Hana Yokoi, Jian Chen, Mihir M Desai, and Andrew J Hung. Impact of virtual reality simulator in training of robotic surgery. In *Robotics in Genitourinary Surgery*, pages 183–202. Springer, 2018.

[67] Stefan Rahm, Karl Wieser, David E Bauer, Felix WA Waibel, Dominik C Meyer, Christian Gerber, and Sandro F Fucentese. Efficacy of standardized training on a virtual reality simulator to advance knee and shoulder arthroscopic motor skills. *BMC musculoskeletal disorders*, 19(1):1–7, 2018.

[68] Vitoantonio Bevilacqua, Antonio Brunetti, Davide de Biase, Giacomo Tattoli, Rosario Santoro, Gianpaolo Francesco Trotta, Fabio Cassano, Michele Pantaleo, Giuseppe Mastronardi, Fabio Ivona, et al. A p300 clustering of mild cognitive impairment patients stimulated in an immersive virtual reality scenario. In *International Conference on Intelligent Computing*, pages 226–236. Springer, 2015.

[69] Cristina Botella, Rosa M Baños, Helena Villa, Conxa Perpiñá, and Azucena García-Palacios. Virtual reality in the treatment of claustrophobic fear: A controlled, multiple-baseline design. *Behavior therapy*, 31(3):583–595, 2000.

[70] Carlos M Coelho, Allison M Waters, Trevor J Hine, and Guy Wallis. The use of virtual reality in acrophobia research and treatment. *Journal of Anxiety disorders*, 23(5): 563–574, 2009.

[71] Mar Rus-Calafell, José Gutiérrez-Maldonado, Cristina Botella, and Rosa M Baños. Virtual reality exposure and imaginal exposure in the treatment of fear of flying: a pilot study. *Behavior modification*, 37(4):568–590, 2013.

[72] Erica K Yuen, James D Herbert, Evan M Forman, Elizabeth M Goetter, Ronald Comer, and Jean-Claude Bradley. Treatment of social anxiety disorder using online virtual environments in second life. *Behavior therapy*, 44(1):51–61, 2013.

[73] Youssef Shiban, Paul Pauli, and Andreas Mühlberger. Effect of multiple context exposure on renewal in spider phobia. *Behaviour research and therapy*, 51(2):68–74, 2013.

[74] Fadi Shrouf, Joaquin Ordieres, and Giovanni Miragliotta. Smart factories in industry 4.0: A review of the concept and of energy management approached in production based on the internet of things paradigm. In *2014 IEEE international conference on industrial engineering and engineering management*, pages 697–701. IEEE, 2014.

[75] Vittorio Miori and Dario Russo. Domotic evolution towards the iot. In *2014 28th International Conference on Advanced Information Networking and Applications Workshops*, pages 809–814. IEEE, 2014.

[76] Subhas Chandra Mukhopadhyay and Nagender K Suryadevara. Internet of things: Challenges and opportunities. In *Internet of Things*, pages 1–17. Springer, 2014.

[77] Shi-Wan Lin, Bradford Miller, Jacques Durand, Rajive Joshi, Paul Didier, Amine Chigani, Reinier Torenbeek, David Duggal, Robert Martin, Graham Bleakley, et al. Industrial internet reference architecture. *Industrial Internet Consortium (IIC), Tech. Rep*, 2015.

[78] Kenneth C Crater and Craig E Goldman. Distributed interface architecture for programmable industrial control systems, September 8 1998. US Patent 5,805,442.

[79] Robert J Kretschmann. Mobile human/machine interface for use with industrial control systems for controlling the operation of process executed on spatially separate machines, December 26 2000. US Patent 6,167,464.

[80] Jonathan R Engdahl. Walk-through human/machine interface for industrial control, August 28 2001. US Patent 6,282,455.

[81] Lane Thames and Dirk Schaefer. Software-defined cloud manufacturing for industry 4.0. *Procedia cirp*, 52:12–17, 2016.

[82] Dazhong Wu, David W Rosen, Lihui Wang, and Dirk Schaefer. Cloud-based design and manufacturing: A new paradigm in digital manufacturing and design innovation. *Computer-Aided Design*, 59:1–14, 2015.

[83] Marcos A Pisching, Fabrício Junqueira, Paulo E Miyagi, et al. Service composition in the cloud-based manufacturing focused on the industry 4.0. In *Doctoral Conference on Computing, Electrical and Industrial Systems*, pages 65–72. Springer, 2015.

[84] Gang Li and Mingchuan Wei. Everything-as-a-service platform for on-demand virtual enterprises. *Information Systems Frontiers*, 16(3):435–452, 2014.

[85] Yucong Duan. Value modeling and calculation for everything as a service (xaas) based on reuse. In *2012 13th ACIS International Conference on Software Engineering, Artificial Intelligence, Networking and Parallel/Distributed Computing*, pages 162–167. IEEE, 2012.

[86] Yucong Duan, Guohua Fu, Nianjun Zhou, Xiaobing Sun, Nanjangud C Narendra, and Bo Hu. Everything as a service (xaas) on the cloud: origins, current and future trends. In *2015 IEEE 8th International Conference on Cloud Computing*, pages 621–628. IEEE, 2015.

[87] Dazhong Wu, J Lane Thames, David W Rosen, and Dirk Schaefer. Enhancing the product realization process with cloud-based design and manufacturing systems. *Journal of Computing and Information Science in Engineering*, 13(4), 2013.

[88] Mohsen Attaran and Sharmin Attaran. The rise of embedded analytics: empowering manufacturing and service industry with big data. *International Journal of Business Intelligence Research (IJBIR)*, 9(1):16–37, 2018.

[89] Sachin S Kamble, Angappa Gunasekaran, and Shradha A Gawankar. Sustainable industry 4.0 framework: A systematic literature review identifying the current trends and future perspectives. *Process safety and environmental protection*, 117:408–425, 2018.

[90] Dominik Kozjek, Borut Rihtaršič, Peter Butala, et al. Big data analytics for operations management in engineer-to-order manufacturing. *Procedia CIRP*, 72:209–214, 2018.

[91] Q Peter He and Jin Wang. Statistical process monitoring as a big data analytics tool for smart manufacturing. *Journal of Process Control*, 67:35–43, 2018.

[92] Kannan Govindan, TC Edwin Cheng, Nishikant Mishra, and Nagesh Shukla. Big data analytics and application for logistics and supply chain management, 2018.

[93] Wullianallur Raghupathi and Viju Raghupathi. Big data analytics in healthcare: promise and potential. *Health information science and systems*, 2(1):1–10, 2014.

[94] C Burghard et al. Big data and analytics key to accountable care success. *IDC health insights*, 1:1–9, 2012.

[95] Ibrahim Abaker Targio Hashem, Ibrar Yaqoob, Nor Badrul Anuar, Salimah Mokhtar, Abdullah Gani, and Samee Ullah Khan. The rise of "big data" on cloud computing: Review and open research issues. *Information systems*, 47:98–115, 2015.

[96] Anushree Priyadarshini et al. A map reduce based support vector machine for big data classification. *International Journal of Database Theory and Application*, 8(5):77–98, 2015.

[97] Marcus G Pandy. Computer modeling and simulation of human movement. *Annual review of biomedical engineering*, 3(1):245–273, 2001.

[98] M Zaeh and D Siedl. A new method for simulation of machining performance by integrating finite element and multi-body simulation for machine tools. *CIRP annals*, 56 (1):383–386, 2007.

[99] P Schrock, F Farelo, R Alqasemi, and R Dubey. Design, simulation and testing of a new modular wheelchair mounted robotic arm to perform activities of daily living. In *2009 IEEE International Conference on Rehabilitation Robotics*, pages 518–523. IEEE, 2009.

[100] Gilberto Echeverria, Séverin Lemaignan, Arnaud Degroote, Simon Lacroix, Michael Karg, Pierrick Koch, Charles Lesire, and Serge Stinckwich. Simulating complex robotic scenarios with morse. In *International Conference on Simulation, Modeling, and Programming for Autonomous Robots*, pages 197–208. Springer, 2012.

[101] Lingguang Song and Neil N Eldin. Adaptive real-time tracking and simulation of heavy construction operations for look-ahead scheduling. *Automation in Construction*, 27:32–39, 2012.

[102] George F Studor, Robert W Womack, Michael F Hilferty, William B Isbell, Jason A Taylor, and Bruce R Bacon. Real time simulation using position sensing, November 28 2000. US Patent 6,152,856.

[103] Giorgio Mustafaraj, Dashamir Marini, Andrea Costa, and Marcus Keane. Model calibration for building energy efficiency simulation. *Applied Energy*, 130:72–85, 2014.

[104] Christoph Herrmann and Sebastian Thiede. Process chain simulation to foster energy efficiency in manufacturing. *CIRP journal of manufacturing science and technology*, 1 (4):221–229, 2009.

[105] Libin Han, Keyi Xing, Xiao Chen, and Fuli Xiong. A petri net-based particle swarm optimization approach for scheduling deadlock-prone flexible manufacturing systems. *Journal of Intelligent Manufacturing*, 29(5):1083–1096, 2018.

[106] Victor RL Shen, Cheng-Ying Yang, Rong-Kuan Shen, and Yu-Chia Chen. Application of petri nets to deadlock avoidance in ipad-like manufacturing systems. *Journal of Intelligent Manufacturing*, 29(6):1363–1378, 2018.

[107] Bjoern Heckel, Antonio E Uva, Bernd Hamann, and Kenneth I Joy. Surface reconstruction using adaptive clustering methods. In *Geometric Modelling*, pages 199–218. Springer, 2001.

[108] Michele Fiorentino, Rafael Radkowski, Christian Stritzke, Antonio E Uva, and Giuseppe Monno. Design review of cad assemblies using bimanual natural interface. *International Journal on Interactive Design and Manufacturing (IJIDeM)*, 7(4):249–260, 2013.

[109] Michele Fiorentino, Antonio E Uva, Michele Gattullo, Saverio Debernardis, and Giuseppe Monno. Augmented reality on large screen for interactive maintenance instructions. *Computers in Industry*, 65(2):270–278, 2014.

[110] Antonio Boccaccio, Antonio Emmanuele Uva, Michele Fiorentino, Luciano Lamberti, and Giuseppe Monno. A mechanobiology-based algorithm to optimize the microstructure geometry of bone tissue scaffolds. *International journal of biological sciences*, 12(1):1, 2016.

[111] F Semeraro, M Bergamasco, A Frisoli, M Holtzer, and EL Cerchiari. Virtual reality prototype in healthcare simulation training. *Resuscitation*, 77:S60–S61, 2008.

[112] David M Gaba. The future vision of simulation in health care. *BMJ Quality & Safety*, 13(suppl 1):i2–i10, 2004.

[113] Berglind Smaradottir, Santiago Martinez, Elin Thygesen, Elisabeth Holen-Rabbersvik, Torunn Kitty Vatnøy, and Rune Werner Fensli. Innovative simulation of health care services in the usability laboratory: experiences from the model for telecare alarm services-project. In *Proceedings from The 15th Scandinavian Conference on Health Informatics 2017 Kristiansand, Norway, August 29–30, 2017*, 2017.

[114] Jennifer Jewer, Adam Dubrowski, Kristopher Hoover, Andrew Smith, and Michael Parsons. Development of a mobile tele-simulation unit prototype for training of rural and remote emergency health care providers. 2018.

[115] Yuhua Jiang, Keyun Liu, and Youxiang Li. Initial clinical trial of robot of endovascular treatment with force feedback and cooperating of catheter and guidewire. *Applied Bionics and Biomechanics*, 2018, 2018.

[116] Dominik Delisle, Markus Schreiber, Christian Krombholz, and Jan Stüve. Production of fiber composite structures by means of cooperating robots. *Lightweight Design worldwide*, 11(2):42–47, 2018.

[117] Timo Salmi, Jari M Ahola, Tapio Heikkilä, Pekka Kilpeläinen, and Timo Malm. Human-robot collaboration and sensor-based robots in industrial applications and construction. In *Robotic building*, pages 25–52. Springer, 2018.

[118] Tomoya Yamamoto, Daisuke Kawase, Toshifumi Enomoto, and Masakazu Utsunomiya. Robot safety system, January 2 2018. US Patent 9,855,664.

[119] Shiyong Wang, Jiafu Wan, Daqiang Zhang, Di Li, and Chunhua Zhang. Towards smart factory for industry 4.0: a self-organized multi-agent system with big data based feedback and coordination. *Computer networks*, 101:158–168, 2016.

[120] Wenshan Wang, Xiaoxiao Zhu, Liyu Wang, Qiang Qiu, and Qixin Cao. Ubiquitous robotic technology for smart manufacturing system. *Computational Intelligence and Neuroscience*, 2016, 2016.

[121] Sh Wang, J Wan, D Li, and Ch Zhang. Implementing smart factory of industrie. 2016.

[122] Constantin-Bala Zamfirescu, Bogdan-Constantin Pirvu, Jochen Schlick, and Detlef Zuehlke. Preliminary insides for an anthropocentric cyber-physical reference architecture of the smart factory. *Studies in Informatics and Control*, 22(3):269–278, 2013.

[123] D Gorecky, R Campos, and G Meixner. Seamless augmented reality support on the shopfloor based on cyber-physical-systems. In *Proceedings of the 14th International Conference on Human-computer Interaction with Mobile Devices and Services*, 2012.

[124] Erkki Jantunen, Giovanni Di Orio, Csaba Hegedűs, Pal Varga, Istvan Moldovan, Felix Larrinaga, Martin Becker, Michele Albano, and Pedro Maló. Maintenance 4.0 world of integrated information. In *Enterprise Interoperability VIII*, pages 67–78. Springer, 2019.

[125] Giacomo Quaranta, Emmanuelle Abisset-Chavanne, Francisco Chinesta, and Jean-Louis Duval. A cyber physical system approach for composite part: From smart manufacturing to predictive maintenance. In *AIP conference proceedings*, volume 1960, page 020025. AIP Publishing LLC, 2018.

[126] Felix Larrinaga, Javier Fernandez, Ekhi Zugasti, Iñaki Garitano, Urko Zurutuza, Mikel Anasagasti, and Mikel Mondragon. Implementation of a reference architecture for cyber physical systems to support condition based maintenance. In *2018 5th International Conference on Control, Decision and Information Technologies (CoDIT)*, pages 773–778. IEEE, 2018.

[127] Jonny Herwan, Seisuke Kano, Ryabov Oleg, Hiroyuki Sawada, and Nagayoshi Kasashima. Cyber-physical system architecture for machining production line. In *2018 IEEE Industrial Cyber-Physical Systems (ICPS)*, pages 387–391. IEEE, 2018.

[128] Alberto Villalonga, Gerardo Beruvides, Fernando Castaño, and Rodolfo Haber. Industrial cyber-physical system for condition-based monitoring in manufacturing processes. In *2018 IEEE Industrial Cyber-Physical Systems (ICPS)*, pages 637–642. IEEE, 2018.

[129] Kunpeng Zhu and Yu Zhang. A cyber-physical production system framework of smart cnc machining monitoring system. *IEEE/ASME Transactions on Mechatronics*, 23(6): 2579–2586, 2018.

[130] Mingfu Tuo, Cheng Zhou, Zhonghai Yin, Xin Zhao, and Lei Wang. Modelling behaviour of cyber-physical system and verifying its safety based on algebra of event. *International Journal of Intelligent Information and Database Systems*, 11(2-3):169–185, 2018.

[131] Luís Diogo Couto, Stylianos Basagiannis, El Hassan Ridouane, Alie El-Din Mady, Miran Hasanagic, and Peter Gorm Larsen. Injecting formal verification in fmi-based co-simulations of cyber-physical systems. In *International Conference on Software Engineering and Formal Methods*, pages 284–299. Springer, 2017.

[132] Nuno Canadas, José Machado, Filomena Soares, Carlos Barros, and Leonilde Varela. Simulation of cyber physical systems behaviour using timed plant models. *Mechatronics*, 54:175–185, 2018.

[133] Mathias Schmitt, Gerrit Meixner, Dominic Gorecky, Marc Seissler, and Matthias Loskyll. Mobile interaction technologies in the factory of the future. *IFAC Proceedings volumes*, 46(15):536–542, 2013.

[134] Steven J Vaughan Nichols. New interfaces at the touch of a fingertip. *Computer*, 40 (8):12–15, 2007.

[135] Dean Weber. Conversational voice interface of connected devices, including toys, cars, avionics, mobile, iot and home appliances, June 7 2018. US Patent App. 15/789,248.

[136] Daniel Wigdor and Dennis Wixon. *Brave NUI world: designing natural user interfaces for touch and gesture*. Elsevier, 2011.

[137] Nicholas Caporusso, Meng Ding, Matthew Clarke, Gordon Carlson, Vitoantonio Bevilacqua, and Gianpaolo Francesco Trotta. Analysis of the relationship between content and interaction in the usability design of 360 o videos. In *International Conference on Applied Human Factors and Ergonomics*, pages 593–602. Springer, 2018.

[138] Francisco J García-Peñalvo and Lourdes Moreno. Special issue on exploring new natural user experiences, 2019.

[139] Rachel Plotnick. Force, flatness and touch without feeling: Thinking historically about haptics and buttons. *New Media & Society*, 19(10):1632–1652, 2017.

[140] Nimesha Ranasinghe, Pravar Jain, Shienny Karwita, David Tolley, and Ellen Yi-Luen Do. Ambiotherm: enhancing sense of presence in virtual reality by simulating real-world environmental conditions. In *Proceedings of the 2017 CHI Conference on Human Factors in Computing Systems*, pages 1731–1742, 2017.

[141] Graham Alasdair Wilson. *Using pressure input and thermal feedback to broaden haptic interaction with mobile devices*. PhD thesis, University of Glasgow, 2013.

[142] Graham Wilson, Martin Halvey, Stephen A Brewster, and Stephen A Hughes. Some like it hot: thermal feedback for mobile devices. In *Proceedings of the SIGCHI Conference on Human Factors in Computing Systems*, pages 2555–2564, 2011.

[143] C Sarafoleanu, C Mella, M Georgescu, and C Perederco. The importance of the olfactory sense in the human behavior and evolution. *Journal of Medicine and life*, 2(2): 196, 2009.

[144] Stephen Brewster, David McGookin, and Christopher Miller. Olfoto: designing a smell-based interaction. In *Proceedings of the SIGCHI conference on Human Factors in computing systems*, pages 653–662, 2006.

[145] Haruka Matsukura, Tatsuhiro Yoneda, and Hiroshi Ishida. Smelling screen: development and evaluation of an olfactory display system for presenting a virtual odor source. *IEEE transactions on visualization and computer graphics*, 19(4):606–615, 2013.

[146] Judith Amores and Pattie Maes. Essence: Olfactory interfaces for unconscious influence of mood and cognitive performance. In *Proceedings of the 2017 CHI conference on human factors in computing systems*, pages 28–34, 2017.

[147] Marianna Obrist, Alexandre N Tuch, and Kasper Hornbaek. Opportunities for odor: experiences with smell and implications for technology. In *Proceedings of the SIGCHI Conference on Human Factors in Computing Systems*, pages 2843–2852, 2014.

[148] Dan Maynes-Aminzade. Edible bits: Seamless interfaces between people, data and food. In *Conference on Human Factors in Computing Systems (CHI'05)-Extended Abstracts*, pages 2207–2210. Citeseer, 2005.

[149] RANASINGHE ARACHCHILAGE NIMESHA RANASINGHE. Digitally stimulating the sensation of taste through electrical and thermal stimulation. 2012.

[150] Takuji Narumi, Shinya Nishizaka, Takashi Kajinami, Tomohiro Tanikawa, and Michitaka Hirose. Augmented reality flavors: gustatory display based on edible marker and cross-modal interaction. In *Proceedings of the SIGCHI conference on human factors in computing systems*, pages 93–102, 2011.

[151] Limin Paul Fu, James Landay, Michael Nebeling, Yingqing Xu, and Chen Zhao. Redefining natural user interface. In *Extended Abstracts of the 2018 CHI Conference on Human Factors in Computing Systems*, pages 1–3, 2018.

[152] Kashif Kifayat, Paul Fergus, Simon Cooper, and Madjid Merabti. Body area networks for movement analysis in physiotherapy treatments. In *2010 IEEE 24th International Conference on Advanced Information Networking and Applications Workshops*, pages 866–872. IEEE, 2010.

[153] Adso Fern'ndez-Baena, Antonio Susin, and Xavier Lligadas. Biomechanical validation of upper-body and lower-body joint movements of kinect motion capture data for rehabilitation treatments. In *2012 fourth international conference on intelligent networking and collaborative systems*, pages 656–661. IEEE, 2012.

[154] Franco Tecchia, Giovanni Avveduto, Raffaello Brondi, Marcello Carrozzino, Massimo Bergamasco, and Leila Alem. I'm in vr! using your own hands in a fully immersive mr system. In *Proceedings of the 20th ACM Symposium on Virtual Reality Software and Technology*, pages 73–76, 2014.

[155] Ahmed Elhayek, Edilson de Aguiar, Arjun Jain, Jonathan Thompson, Leonid Pishchulin, Mykhaylo Andriluka, Christoph Bregler, Bernt Schiele, and Christian Theobalt. Marconi—convnet-based marker-less motion capture in outdoor and indoor scenes. *IEEE transactions on pattern analysis and machine intelligence*, 39(3):501–514, 2016.

[156] João F Nunes, Pedro M Moreira, and João Manuel RS Tavares. Human motion analysis and simulation tools: a survey. In *Handbook of Research on Computational Simulation and Modeling in Engineering*, pages 359–388. IGI Global, 2016.

[157] Alberto Leardini, Zimi Sawacha, Gabriele Paolini, Stefania Ingrosso, Roberto Nativo, and Maria Grazia Benedetti. A new anatomically based protocol for gait analysis in children. *Gait & posture*, 26(4):560–571, 2007.

[158] Roy B Davis III, Sylvia Ounpuu, Dennis Tyburski, and James R Gage. A gait analysis data collection and reduction technique. *Human movement science*, 10(5):575–587, 1991.

[159] Lynn McAtamney and E Nigel Corlett. Rula: a survey method for the investigation of work-related upper limb disorders. *Applied ergonomics*, 24(2):91–99, 1993.

[160] Michelle Robertson, Benjamin C Amick III, Kelly DeRango, Ted Rooney, Lianna Bazzani, Ron Harrist, and Anne Moore. The effects of an office ergonomics training and chair intervention on worker knowledge, behavior and musculoskeletal risk. *Applied ergonomics*, 40(1):124–135, 2009.

[161] Sara Dockrell, Eleanor O'Grady, Kathleen Bennett, Clare Mullarkey, Rachel Mc Connell, Rachel Ruddy, Seamus Twomey, and Colleen Flannery. An investigation of the reliability of rapid upper limb assessment (rula) as a method of assessment of children's computing posture. *Applied ergonomics*, 43(3):632–636, 2012.

[162] Stephen Bao, Ninica Howard, Peregrin Spielholz, Barbara Silverstein, and Nayak Polissar. Interrater reliability of posture observations. *Human factors*, 51(3):292–309, 2009.

[163] Brian D Lowe. Accuracy and validity of observational estimates of shoulder and elbow posture. *Applied ergonomics*, 35(2):159–171, 2004.

[164] Bruno Bonnechere, Bart Jansen, Patrick Salvia, Hakim Bouzahouene, Lubos Omelina, Fedor Moiseev, Victor Sholukha, Jan Cornelis, Marcel Rooze, and S Van Sint Jan. Validity and reliability of the kinect within functional assessment activities: comparison with standard stereophotogrammetry. *Gait & posture*, 39(1):593–598, 2014.

[165] Ross A Clark, Yong-Hao Pua, Karine Fortin, Callan Ritchie, Kate E Webster, Linda Denehy, and Adam L Bryant. Validity of the microsoft kinect for assessment of postural control. *Gait & posture*, 36(3):372–377, 2012.

[166] Tilak Dutta. Evaluation of the kinect™ sensor for 3-d kinematic measurement in the workplace. *Applied ergonomics*, 43(4):645–649, 2012.

[167] Jose Antonio Diego-Mas and Jorge Alcaide-Marzal. Using kinect™ sensor in observational methods for assessing postures at work. *Applied ergonomics*, 45(4):976–985, 2014.

[168] Alfredo Patrizi, Ettore Pennestrì, and Pier Paolo Valentini. Comparison between low-cost marker-less and high-end marker-based motion capture systems for the computer-aided assessment of working ergonomics. *Ergonomics*, 59(1):155–162, 2016.

[169] Simone Zennaro, Matteo Munaro, Simone Milani, Pietro Zanuttigh, Andrea Bernardi, Stefano Ghidoni, and Emanuele Menegatti. Performance evaluation of the 1st and 2nd generation kinect for multimedia applications. In *2015 IEEE International Conference on Multimedia and Expo (ICME)*, pages 1–6. IEEE, 2015.

[170] Qifei Wang, Gregorij Kurillo, Ferda Ofli, and Ruzena Bajcsy. Evaluation of pose tracking accuracy in the first and second generations of microsoft kinect. In *2015 international conference on healthcare informatics*, pages 380–389. IEEE, 2015.

[171] Xu Xu and Raymond W McGorry. The validity of the first and second generation microsoft kinect™ for identifying joint center locations during static postures. *Applied ergonomics*, 49:47–54, 2015.

[172] Inma García-Pereira, Pablo Casanova-Salas, Jesús Gimeno, Pedro Morillo, and Dirk Reiners. Cross-device augmented reality annotations method for asynchronous collaboration in unprepared environments. *Information*, 12(12):519, 2021.

[173] Antonio Brunetti, Domenico Buongiorno, Gianpaolo Francesco Trotta, and Vitoantonio Bevilacqua. Computer vision and deep learning techniques for pedestrian detection and tracking: A survey. *Neurocomputing*, 300:17–33, 2018.

[174] Vito Modesto Manghisi, Antonio Emmanuele Uva, Michele Fiorentino, Vitoantonio Bevilacqua, Gianpaolo Francesco Trotta, and Giuseppe Monno. Real time rula assessment using kinect v2 sensor. *Applied ergonomics*, 65:481–491, 2017.

[175] Ercan Oztemel and Samet Gursev. Literature review of industry 4.0 and related technologies. *Journal of Intelligent Manufacturing*, 31(1):127–182, 2020.

[176] Li Da Xu, Eric L Xu, and Ling Li. Industry 4.0: state of the art and future trends. *International Journal of Production Research*, 56(8):2941–2962, 2018.

[177] Washington X Quevedo, Jorge S Sánchez, Oscar Arteaga, Marcelo Álvarez, Víctor D Zambrano, Carlos R Sánchez, and Víctor H Andaluz. Virtual reality system for training in automotive mechanics. In *International Conference on Augmented Reality, Virtual Reality and Computer Graphics*, pages 185–198. Springer, 2017.

[178] Raj Kumar, Harish Kumar Banga, Raman Kumar, Sehijpal Singh, Sunpreet Singh, Maria-Luminiţa Scutaru, and Cătălin Iulian Pruncu. Ergonomic evaluation of workstation design using taguchi experimental approach: a case of an automotive industry. *International Journal on Interactive Design and Manufacturing (IJIDeM)*, 15(4):481–498, 2021.

[179] Yan Cao, Feng Jia, and Gunasekaran Manogaran. Efficient traceability systems of steel products using blockchain-based industrial internet of things. *IEEE Transactions on Industrial Informatics*, 16(9):6004–6012, 2019.

[180] Panagiotis Kostakis and Antonios Kargas. Big-data management: A driver for digital transformation? *Information*, 12(10):411, 2021.

[181] Sabine Webel, Ulrich Bockholt, and Jens Keil. Design criteria for ar-based training of maintenance and assembly tasks. In *International Conference on Virtual and Mixed Reality*, pages 123–132. Springer, 2011.

[182] Kangdon Lee. Augmented reality in education and training. *TechTrends*, 56(2):13–21, 2012.

[183] Patrik Zajec, Jože M Rožanec, Elena Trajkova, Inna Novalija, Klemen Kenda, Blaž Fortuna, and Dunja Mladenić. Help me learn! architecture and strategies to combine recommendations and active learning in manufacturing. *Information*, 12(11):473, 2021.

[184] Vive | vive tracker. URL https://www.vive.com/us/vive-tracker/.

[185] Till Bockemühl, Nikolaus F Troje, and Volker Dürr. Inter-joint coupling and joint angle synergies of human catching movements. *Human Movement Science*, 29(1):73–93, 2010.

[186] Katherine RS Holzbaur, Wendy M Murray, and Scott L Delp. A model of the upper extremity for simulating musculoskeletal surgery and analyzing neuromuscular control. *Annals of biomedical engineering*, 33(6):829–840, 2005.

[187] Scott L Delp, Frank C Anderson, Allison S Arnold, Peter Loan, Ayman Habib, Chand T John, Eran Guendelman, and Darryl G Thelen. Opensim: open-source software to create and analyze dynamic simulations of movement. *IEEE transactions on biomedical engineering*, 54(11):1940–1950, 2007.

[188] Andrea d'Avella, Alessandro Portone, Laure Fernandez, and Francesco Lacquaniti. Control of fast-reaching movements by muscle synergy combinations. *Journal of Neuroscience*, 26(30):7791–7810, 2006.

[189] Martin K Burns, Vrajeshri Patel, Ionut Florescu, Kishore V Pochiraju, and Ramana Vinjamuri. Low-dimensional synergistic representation of bilateral reaching movements. *Frontiers in bioengineering and biotechnology*, 5:2, 2017.

[190] RI Cooper. Multivariate statistical methods: a primer, 1987.

[191] Vitoantonio Bevilacqua, Dario D'Ambruoso, Giovanni Mandolino, and Marco Suma. A new tool to support diagnosis of neurological disorders by means of facial expressions. In *2011 IEEE International Symposium on Medical Measurements and Applications*, pages 544–549. IEEE, 2011.

[192] Ilaria Bortone, Gianpaolo Francesco Trotta, Antonio Brunetti, Giacomo Donato Cascarano, Claudio Loconsole, Nadia Agnello, Alberto Argentiero, Giuseppe Nicolardi, Antonio Frisoli, and Vitoantonio Bevilacqua. A novel approach in combination of 3d gait analysis data for aiding clinical decision-making in patients with parkinson's disease. In *International Conference on Intelligent Computing*, pages 504–514. Springer, 2017.

[193] Antonio I Triggiani, Vitoantonio Bevilacqua, Antonio Brunetti, Roberta Lizio, Giacomo Tattoli, Fabio Cassano, Andrea Soricelli, Raffaele Ferri, Flavio Nobili, Loreto Gesualdo, et al. Classification of healthy subjects and alzheimer's disease patients with dementia from cortical sources of resting state eeg rhythms: a study using artificial neural networks. *Frontiers in neuroscience*, 10:604, 2017.

[194] Domenico Buongiorno, Ilaria Bortone, Giacomo Donato Cascarano, Gianpaolo Francesco Trotta, Antonio Brunetti, and Vitoantonio Bevilacqua. A low-cost vision system based on the analysis of motor features for recognition and severity rating of parkinson's disease. *BMC Medical Informatics and Decision Making*, 19(9):1–13, 2019.

[195] Dirk Holz, Alexandru E Ichim, Federico Tombari, Radu B Rusu, and Sven Behnke. Registration with the point cloud library: A modular framework for aligning in 3-d. *IEEE Robotics & Automation Magazine*, 22(4):110–124, 2015.

[196] Guoguang Du, Kai Wang, Shiguo Lian, and Kaiyong Zhao. Vision-based robotic grasping from object localization, object pose estimation to grasp estimation for parallel grippers: a review. *Artificial Intelligence Review*, 54(3):1677–1734, 2021.

[197] Nicola Altini, Giuseppe De Giosa, Nicola Fragasso, Claudia Coscia, Elena Sibilano, Berardino Prencipe, Sardar Mehboob Hussain, Antonio Brunetti, Domenico Buongiorno, Andrea Guerriero, et al. Segmentation and identification of vertebrae in ct scans using cnn, k-means clustering and k-nn. In *Informatics*, volume 8, page 40. Multidisciplinary Digital Publishing Institute, 2021.

[198] Menglong Zhu, Konstantinos G Derpanis, Yinfei Yang, Samarth Brahmbhatt, Mabel Zhang, Cody Phillips, Matthieu Lecce, and Kostas Daniilidis. Single image 3d object detection and pose estimation for grasping. In *2014 IEEE International Conference on Robotics and Automation (ICRA)*, pages 3936–3943. IEEE, 2014.

[199] Max Schwarz, Hannes Schulz, and Sven Behnke. Rgb-d object recognition and pose estimation based on pre-trained convolutional neural network features. In *2015 IEEE international conference on robotics and automation (ICRA)*, pages 1329–1335. IEEE, 2015.

[200] Arul Selvam Periyasamy, Max Schwarz, and Sven Behnke. Robust 6d object pose estimation in cluttered scenes using semantic segmentation and pose regression networks. In *2018 IEEE/RSJ International Conference on Intelligent Robots and Systems (IROS)*, pages 6660–6666. IEEE, 2018.

[201] Alex Kendall, Matthew Grimes, and Roberto Cipolla. Posenet: A convolutional network for real-time 6-dof camera relocalization. In *Proceedings of the IEEE international conference on computer vision*, pages 2938–2946, 2015.

[202] Harish Kumar Banga, Pankaj Goel, Raman Kumar, Vikas Kumar, Parveen Kalra, Sehijpal Singh, Sunpreet Singh, Chander Prakash, and Catalin Pruncu. Vibration exposure and transmissibility on dentist's anatomy: A study of micro motors and air-turbines. *International Journal of Environmental Research and Public Health*, 18(8):4084, 2021.

[203] Francisco J Romero-Ramirez, Rafael Muñoz-Salinas, and Rafael Medina-Carnicer. Speeded up detection of squared fiducial markers. *Image and vision Computing*, 76: 38–47, 2018.

[204] Sergio Garrido-Jurado, Rafael Munoz-Salinas, Francisco José Madrid-Cuevas, and Rafael Medina-Carnicer. Generation of fiducial marker dictionaries using mixed integer linear programming. *Pattern Recognition*, 51:481–491, 2016.

[205] Alexey Bochkovskiy, Chien-Yao Wang, and Hong-Yuan Mark Liao. Yolov4: Optimal speed and accuracy of object detection. *arXiv preprint arXiv:2004.10934*, 2020.

[206] Chien-Yao Wang, Alexey Bochkovskiy, and Hong-Yuan Mark Liao. Scaled-yolov4: Scaling cross stage partial network. In *Proceedings of the IEEE/CVF Conference on Computer Vision and Pattern Recognition*, pages 13029–13038, 2021.

[207] Laura Romeo, Roberto Marani, Matteo Malosio, Anna G Perri, and Tiziana D'Orazio. Performance analysis of body tracking with the microsoft azure kinect. In *2021 29th*

Mediterranean Conference on Control and Automation (MED), pages 572–577. IEEE, 2021.

[208] Michal Tölgyessy, Martin Dekan, L'uboš Chovanec, and Peter Hubinskỳ. Evaluation of the azure kinect and its comparison to kinect v1 and kinect v2. *Sensors*, 21(2):413, 2021.

[209] Z. Cao, G. Hidalgo Martinez, T. Simon, S. Wei, and Y. A. Sheikh. Openpose: Realtime multi-person 2d pose estimation using part affinity fields. *IEEE Transactions on Pattern Analysis and Machine Intelligence*, 2019.

[210] Tomas Simon, Hanbyul Joo, Iain Matthews, and Yaser Sheikh. Hand keypoint detection in single images using multiview bootstrapping. In *CVPR*, 2017.

[211] Zhe Cao, Tomas Simon, Shih-En Wei, and Yaser Sheikh. Realtime multi-person 2d pose estimation using part affinity fields. In *CVPR*, 2017.

[212] Shih-En Wei, Varun Ramakrishna, Takeo Kanade, and Yaser Sheikh. Convolutional pose machines. In *CVPR*, 2016.

[213] Nicola Altini, Giacomo Donato Cascarano, Antonio Brunetti, Irio De Feudis, Domenico Buongiorno, Michele Rossini, Francesco Pesce, Loreto Gesualdo, and Vitoantonio Bevilacqua. A deep learning instance segmentation approach for global glomerulosclerosis assessment in donor kidney biopsies. *Electronics*, 9(11), 2020. ISSN 2079-9292. doi: 10.3390/electronics9111768. URL https://www.mdpi.com/2079-9292/9/11/1768.

[214] Mohamed Sadiq Ikbal, Vishal Ramadoss, and Matteo Zoppi. Dynamic pose tracking performance evaluation of htc vive virtual reality system. *IEEE Access*, 9:3798–3815, 2020.

[215] Diederick C Niehorster, Li Li, and Markus Lappe. The accuracy and precision of position and orientation tracking in the htc vive virtual reality system for scientific research. *i-Perception*, 8(3):2041669517708205, 2017.

[216] Miguel Borges, Andrew Symington, Brian Coltin, Trey Smith, and Rodrigo Ventura. Htc vive: Analysis and accuracy improvement. In *2018 IEEE/RSJ International Conference on Intelligent Robots and Systems (IROS)*, pages 2610–2615. IEEE, 2018.

[217] Jonathan Lwowski, Abhijit Majumdat, Patrick Benavidez, John J Prevost, and Mo Jamshidi. Htc vive tracker: Accuracy for indoor localization. *IEEE Systems, Man, and Cybernetics Magazine*, 6(4):15–22, 2020.

[218] Irio De Feudis, Domenico Buongiorno, Giacomo Donato Cascarano, Antonio Brunetti, Donato Micele, and Vitoantonio Bevilacqua. A nonlinear autoencoder for kinematic synergy extraction from movement data acquired with htc vive trackers. In *Progresses in Artificial Intelligence and Neural Systems*, pages 231–241. Springer, 2021.

[219] Alexander Smirnov. Hand tracking for mobile virtual reality. 2021.

[220] Guilherme Luz Tortorella, Flavio Sanson Fogliatto, Alejandro Mac Cawley Vergara, Roberto Vassolo, and Rapinder Sawhney. Healthcare 4.0: trends, challenges and research directions. *Production Planning & Control*, 31(15):1245–1260, 2020.

[221] Mark Wehde. Healthcare 4.0. *IEEE Engineering Management Review*, 47(3):24–28, 2019.

[222] Geng Yang, Zhibo Pang, M Jamal Deen, Mianxiong Dong, Yuan-Ting Zhang, Nigel Lovell, and Amir M Rahmani. Homecare robotic systems for healthcare 4.0: visions and enabling technologies. *IEEE journal of biomedical and health informatics*, 24(9): 2535–2549, 2020.

[223] Fátima De NAP Shelton and Michael J Reding. Effect of lesion location on upper limb motor recovery after stroke. *Stroke*, 32(1):107–112, 2001.

[224] Hirofumi Nakayama, Henrik Stig Jørgensen, Hans Otto Raaschou, and Tom Skyhøj Olsen. Recovery of upper extremity function in stroke patients: the copenhagen stroke study. *Archives of physical medicine and rehabilitation*, 75(4):394–398, 1994.

[225] Hanna C Persson, Marina Parziali, Anna Danielsson, and Katharina S Sunnerhagen. Outcome and upper extremity function within 72 hours after first occasion of stroke in an unselected population at a stroke unit. a part of the salgot study. *BMC neurology*, 12 (1):1–6, 2012.

[226] Reva C Lawrence, Charles G Helmick, Frank C Arnett, Richard A Deyo, David T Felson, Edward H Giannini, Stephen P Heyse, Rosemarie Hirsch, Marc C Hochberg, Gene G Hunder, et al. Estimates of the prevalence of arthritis and selected musculoskeletal disorders in the united states. *Arthritis & Rheumatism: Official Journal of the American College of Rheumatology*, 41(5):778–799, 1998.

[227] Pamela W Duncan, Larry B Goldstein, David Matchar, George W Divine, and John Feussner. Measurement of motor recovery after stroke. outcome assessment and sample size requirements. *Stroke*, 23(8):1084–1089, 1992.

[228] Pamela W Duncan, Larry B Goldstein, Ronnie D Horner, Pamela B Landsman, Gregory P Samsa, and David B Matchar. Similar motor recovery of upper and lower extremities after stroke. *Stroke*, 25(6):1181–1188, 1994.

[229] L Simpson, K Hayward, M McPeake, and J Eng. An updated distribution of upper limb weakness post stroke: are fewer people experiencing arm weakness today? In *International Journal of Stroke*, volume 13, pages 41–41. SAGE PUBLICATIONS LTD 1 OLIVERS YARD, 55 CITY ROAD, LONDON EC1Y 1SP, ENGLAND, 2018.

[230] Kathryn S Hayward, Sharon F Kramer, Vincent Thijs, Julie Ratcliffe, Nick S Ward, Leonid Churilov, Laura Jolliffe, Dale Corbett, Geoffrey Cloud, Tina Kaffenberger, et al.

A systematic review protocol of timing, efficacy and cost effectiveness of upper limb therapy for motor recovery post-stroke. *Systematic reviews*, 8(1):1–8, 2019.

[231] Qing Miao, Mingming Zhang, Jinghui Cao, and Sheng Q Xie. Reviewing high-level control techniques on robot-assisted upper-limb rehabilitation. *Advanced Robotics*, 32 (24):1253–1268, 2018.

[232] Sandy K Tatla, Navid Shirzad, Keith R Lohse, Naznin Virji-Babul, Alison M Hoens, Liisa Holsti, Linda C Li, Kimberly J Miller, Melanie Y Lam, and HF Machiel Van der Loos. Therapists' perceptions of social media and video game technologies in upper limb rehabilitation. *JMIR serious games*, 3(1):e3401, 2015.

[233] Dick Stegeman and Hermie Hermens. Standards for surface electromyography: The european project surface emg for non-invasive assessment of muscles (seniam). *Enschede: Roessingh Research and Development*, 10:8–12, 2007.

[234] Daniel M Corcos, Gerald L Gottlieb, Mark L Latash, Gil L Almeida, and Gyan C Agarwal. Electromechanical delay: An experimental artifact. *Journal of Electromyography and Kinesiology*, 2(2):59–68, 1992.

[235] Felix E Zajac. Muscle and tendon: properties, models, scaling, and application to biomechanics and motor control. *Critical reviews in biomedical engineering*, 17(4): 359–411, 1989.

[236] HS Milner-Brown, Richard B Stein, and R Yemm. Changes in firing rate of human motor units during linearly changing voluntary contractions. *The Journal of physiology*, 230(2):371, 1973.

[237] Craig W Heckathorne and Dudley S Childress. Relationships of the surface electromyogram to the force, length, velocity, and contraction rate of the cineplastic human biceps. *American Journal of Physical Medicine*, 60(1):1–19, 1981.

[238] JJ Woods and B Bigland-Ritchie. Linear and non-linear surface emg/force relationships in human muscles. an anatomical/functional argument for the existence of both. *American journal of physical medicine*, 62(6):287–299, 1983.

[239] David G Lloyd and Thor F Besier. An emg-driven musculoskeletal model to estimate muscle forces and knee joint moments in vivo. *Journal of biomechanics*, 36(6):765–776, 2003.

[240] DG Lloyd and TS Buchanan. A model of load sharing between muscles and soft tissues at the human knee during static tasks. 1996.

[241] Kurt Manal, Roger V Gonzalez, David G Lloyd, and Thomas S Buchanan. A real-time emg-driven virtual arm. *Computers in biology and medicine*, 32(1):25–36, 2002.

[242] Luzheng Bi, Cuntai Guan, et al. A review on emg-based motor intention prediction of continuous human upper limb motion for human-robot collaboration. *Biomedical Signal Processing and Control*, 51:113–127, 2019.

[243] Bence J Borbély and Péter Szolgay. Real-time inverse kinematics for the upper limb: a model-based algorithm using segment orientations. *Biomedical engineering online*, 16 (1):1–29, 2017.

[244] Yasuharu Koike and Mitsuo Kawato. Estimation of dynamic joint torques and trajectory formation from surface electromyography signals using a neural network model. *Biological cybernetics*, 73(4):291–300, 1995.

[245] Edward A Clancy, Lukai Liu, Pu Liu, and Daniel V Zandt Moyer. Identification of constant-posture emg–torque relationship about the elbow using nonlinear dynamic models. *IEEE Transactions on Biomedical Engineering*, 59(1):205–212, 2011.

[246] Pu Liu, Lukai Liu, and Edward A Clancy. Influence of joint angle on emg-torque model during constant-posture, torque-varying contractions. *IEEE Transactions on neural systems and rehabilitation engineering*, 23(6):1039–1046, 2015.

[247] Kishor Koirala, Meera Dasog, Pu Liu, and Edward A Clancy. Using the electromyogram to anticipate torques about the elbow. *IEEE Transactions on Neural Systems and Rehabilitation Engineering*, 23(3):396–402, 2014.

[248] Javad Hashemi, Evelyn Morin, Parvin Mousavi, Katherine Mountjoy, and Keyvan Hashtrudi-Zaad. Emg–force modeling using parallel cascade identification. *Journal of Electromyography and Kinesiology*, 22(3):469–477, 2012.

[249] Andrew F Huxley. Muscle structure and theories of contraction. *Prog. Biophys. Biophys. Chem*, 7:255–318, 1957.

[250] Andrew F Huxley and Ro M Simmons. Proposed mechanism of force generation in striated muscle. *Nature*, 233(5321):533–538, 1971.

[251] George I Zahalak. A comparison of the mechanical behavior of the cat soleus muscle with a distribution-moment model. 1986.

[252] Richard Heine, Kurt Manal, and Thomas S Buchanan. Using hill-type muscle models and emg data in a forward dynamic analysis of joint moment: Evaluation of critical parameters. *Journal of Mechanics in Medicine and Biology*, 3(02):169–186, 2003.

[253] Domenico Buongiorno, Francesco Barone, Massimiliano Solazzi, Vitoantonio Bevilacqua, and Antonio Frisoli. A linear optimization procedure for an emg-driven neuromusculoskeletal model parameters adjusting: validation through a myoelectric exoskeleton control. In *International Conference on Human Haptic Sensing and Touch Enabled Computer Applications*, pages 218–227. Springer, 2016.

[254] Domenico Buongiorno, Michele Barsotti, Edoardo Sotgiu, Claudio Loconsole, Massimiliano Solazzi, Vitoantonio Bevilacqua, and Antonio Frisoli. A neuromusculoskeletal model of the human upper limb for a myoelectric exoskeleton control using a reduced number of muscles. In *2015 IEEE World Haptics Conference (WHC)*, pages 273–279. IEEE, 2015.

[255] Altinus Lucilus Hof and JW Van den Berg. Emg to force processing i: an electrical analogue of the hill muscle model. *Journal of biomechanics*, 14(11):747–758, 1981.

[256] Jacob Rosen, Moshe Brand, Moshe B Fuchs, and Mircea Arcan. A myosignal-based powered exoskeleton system. *IEEE Transactions on systems, Man, and Cybernetics-part A: Systems and humans*, 31(3):210–222, 2001.

[257] MW Jiang, RC Wang, JZ Wang, and DW Jin. A method of recognizing finger motion using wavelet transform of surface emg signal. In *2005 IEEE Engineering in Medicine and Biology 27th Annual Conference*, pages 2672–2674. IEEE, 2006.

[258] J-U Chu, Inhyuk Moon, and M-S Mun. A real-time emg pattern recognition system based on linear-nonlinear feature projection for a multifunction myoelectric hand. *IEEE Transactions on biomedical engineering*, 53(11):2232–2239, 2006.

[259] P Geethanjali, KK Ray, and P Vivekananda Shanmuganathan. Actuation of prosthetic drive using emg signal. In *TENCON 2009-2009 IEEE Region 10 Conference*, pages 1–5. IEEE, 2009.

[260] Minas V Liarokapis, Panagiotis K Artemiadis, Pantelis T Katsiaris, Kostas J Kyriakopoulos, and Elias S Manolakos. Learning human reach-to-grasp strategies: Towards emg-based control of robotic arm-hand systems. In *2012 IEEE International Conference on Robotics and Automation*, pages 2287–2292. IEEE, 2012.

[261] Sachin Negi, Yatindra Kumar, and VM Mishra. Feature extraction and classification for emg signals using linear discriminant analysis. In *2016 2nd International Conference on Advances in Computing, Communication, & Automation (ICACCA)(Fall)*, pages 1–6. IEEE, 2016.

[262] Daohui Zhang, Xingang Zhao, Jianda Han, and Yiwen Zhao. A comparative study on pca and lda based emg pattern recognition for anthropomorphic robotic hand. In *2014 IEEE International Conference on Robotics and Automation (ICRA)*, pages 4850–4855. IEEE, 2014.

[263] Rhonira Latif, Saeid Sanei, and Kianoush Nazarpour. Classification of elbow electromyography signals based on directed transfer functions. In *2008 International Conference on BioMedical Engineering and Informatics*, volume 2, pages 371–374. IEEE, 2008.

[264] Xiao Hu, Ping Yu, Qun Yu, Waixi Liu, and Jian Qin. Classification of surface emg signal based on energy spectra change. In *2008 International Conference on BioMedical Engineering and Informatics*, volume 2, pages 375–379. IEEE, 2008.

[265] Ram Murat Singh, S Chatterji, and A Kumar. Trends and challenges in emg based control scheme of exoskeleton robots-a review. *Int. J. Sci. Eng. Res*, 3(8):933–940, 2012.

[266] Daniele Leonardis, Michele Barsotti, Claudio Loconsole, Massimiliano Solazzi, Marco Troncossi, Claudio Mazzotti, Vincenzo Parenti Castelli, Caterina Procopio, Giuseppe Lamola, Carmelo Chisari, et al. An emg-controlled robotic hand exoskeleton for bilateral rehabilitation. *IEEE transactions on haptics*, 8(2):140–151, 2015.

[267] Claudio Loconsole, Daniele Leonardis, Michele Barsotti, Massimiliano Solazzi, Antonio Frisoli, Massimo Bergamasco, Marco Troncossi, M Mozaffari Foumashi, Claudio Mazzotti, and V Parenti Castelli. An emg-based robotic hand exoskeleton for bilateral training of grasp. In *2013 World Haptics Conference (WHC)*, pages 537–542. IEEE, 2013.

[268] Claudio Loconsole, Stefano Dettori, Antonio Frisoli, Carlo Alberto Avizzano, and Massimo Bergamasco. An emg-based approach for on-line predicted torque control in robotic-assisted rehabilitation. In *2014 IEEE Haptics Symposium (HAPTICS)*, pages 181–186. IEEE, 2014.

[269] Rong Song and Kai-Yu Tong. Using recurrent artificial neural network model to estimate voluntary elbow torque in dynamic situations. *Medical and Biological Engineering and Computing*, 43(4):473–480, 2005.

[270] Kazuo Kiguchi, Takakazu Tanaka, and Toshio Fukuda. Neuro-fuzzy control of a robotic exoskeleton with emg signals. *IEEE Transactions on fuzzy systems*, 12(4): 481–490, 2004.

[271] Kazuo Kiguchi, Yasunobu Imada, and Manoj Liyanage. Emg-based neuro-fuzzy control of a 4dof upper-limb power-assist exoskeleton. In *2007 29th Annual International Conference of the IEEE Engineering in Medicine and Biology Society*, pages 3040–3043. IEEE, 2007.

[272] Kazuo Kiguchi and Qilong Quan. Muscle-model-oriented emg-based control of an upper-limb power-assist exoskeleton with a neuro-fuzzy modifier. In *2008 IEEE International Conference on Fuzzy Systems (IEEE World Congress on Computational Intelligence)*, pages 1179–1184. IEEE, 2008.

[273] Agamemnon Krasoulis, Sethu Vijayakumar, and Kianoush Nazarpour. Evaluation of regression methods for the continuous decoding of finger movement from surface emg and accelerometry. In *2015 7th International IEEE/EMBS Conference on Neural Engineering (NER)*, pages 631–634. IEEE, 2015.

[274] Panagiotis K Artemiadis and Kostas J Kyriakopoulos. A switching regime model for the emg-based control of a robot arm. *IEEE Transactions on Systems, Man, and Cybernetics, Part B (Cybernetics)*, 41(1):53–63, 2010.

[275] Panagiotis K Artemiadis and Kostas J Kyriakopoulos. An emg-based robot control scheme robust to time-varying emg signal features. *IEEE Transactions on Information Technology in Biomedicine*, 14(3):582–588, 2010.

[276] Michele Barsotti, Sigrid Dupan, Ivan Vujaklija, Strahinja Došen, Antonio Frisoli, and Dario Farina. Online finger control using high-density emg and minimal training data for robotic applications. *IEEE Robotics and Automation Letters*, 4(2):217–223, 2018.

[277] Michal A Mikulski. Electromyogram control algorithms for the upper limb single-dof powered exoskeleton. In *2011 4th International Conference on Human System Interactions, HSI 2011*, pages 117–122. IEEE, 2011.

[278] Mitchell JH Lum, Denny Trimble, Jacob Rosen, Kenneth Fodero, H Hawkeye King, Ganesh Sankaranarayanan, Jesse Dosher, Rainer Leuschke, Brandon Martin-Anderson, Mika N Sinanan, et al. Multidisciplinary approach for developing a new minimally invasive surgical robotic system. In *The First IEEE/RAS-EMBS International Conference on Biomedical Robotics and Biomechatronics, 2006. BioRob 2006.*, pages 841–846. IEEE, 2006.

[279] Md Rasedul Islam, Christopher Spiewak, Mohammad Habibur Rahman, and Raouf Fareh. A brief review on robotic exoskeletons for upper extremity rehabilitation to find the gap between research porotype and commercial type. *Adv Robot Autom*, 6(3):2, 2017.

[280] Peter S Lum, Charles G Burgar, Peggy C Shor, Matra Majmundar, and Machiel Van der Loos. Robot-assisted movement training compared with conventional therapy techniques for the rehabilitation of upper-limb motor function after stroke. *Archives of physical medicine and rehabilitation*, 83(7):952–959, 2002.

[281] Peter S Lum, Charles G Burgar, and Peggy C Shor. Evidence for improved muscle activation patterns after retraining of reaching movements with the mime robotic system in subjects with post-stroke hemiparesis. *IEEE Transactions on Neural Systems and Rehabilitation Engineering*, 12(2):186–194, 2004.

[282] Peter S Lum, Charles G Burgar, Machiel Van der Loos, Peggy C Shor, Matra Majmundar, and Ruth Yap. Mime robotic device for upper-limb neurorehabilitation in subacute stroke subjects: A follow-up study. *Journal of rehabilitation research and development*, 43(5):631, 2006.

[283] Rosen Sanchez, DERIC Reinkensmeyer, P Shah, J Liu, S Rao, R Smith, S Cramer, T Rahman, and J Bobrow. Monitoring functional arm movement for home-based therapy after stroke. In *The 26th Annual International Conference of the IEEE Engineering in Medicine and Biology Society*, volume 2, pages 4787–4790. IEEE, 2004.

[284] Irene Aprile, Marco Germanotta, Arianna Cruciani, Simona Loreti, Cristiano Pecchioli, Francesca Cecchi, Angelo Montesano, Silvia Galeri, Manuela Diverio, Catuscia Falsini,

et al. Upper limb robotic rehabilitation after stroke: a multicenter, randomized clinical trial. *Journal of Neurologic Physical Therapy*, 44(1):3–14, 2020.

[285] Charles G Burgar, Peter S Lum, Peggy C Shor, HF Machiel Van der Loos, et al. Development of robots for rehabilitation therapy: The palo alto va/stanford experience. *Journal of rehabilitation research and development*, 37(6):663–674, 2000.

[286] Rui Loureiro, Farshid Amirabdollahian, Michael Topping, Bart Driessen, and William Harwin. Upper limb robot mediated stroke therapy—gentle/s approach. *Autonomous Robots*, 15(1):35–51, 2003.

[287] Rocco Salvatore Calabrò, Margherita Russo, Antonino Naro, Demetrio Milardi, Tina Balletta, Antonino Leo, Serena Filoni, and Placido Bramanti. Who may benefit from armeo power treatment? a neurophysiological approach to predict neurorehabilitation outcomes. *PM&R*, 8(10):971–978, 2016.

[288] Antonio Frisoli, Caterina Procopio, Carmelo Chisari, Ilaria Creatini, Luca Bonfiglio, Massimo Bergamasco, Bruno Rossi, and Maria Chiara Carboncini. Positive effects of robotic exoskeleton training of upper limb reaching movements after stroke. *Journal of neuroengineering and rehabilitation*, 9(1):1–16, 2012.

[289] Susan Coote, Brendan Murphy, William Harwin, and Emma Stokes. The effect of the gentle/s robot-mediated therapy system on arm function after stroke. *Clinical rehabilitation*, 22(5):395–405, 2008.

[290] Hermano I Krebs, N Hogan, BT Volpe, ML Aisen, L Edelstein, and C Diels. Overview of clinical trials with mit-manus: a robot-aided neuro-rehabilitation facility. *Technology and Health Care*, 7(6):419–423, 1999.

[291] Hermano I Krebs, Mark Ferraro, Stephen P Buerger, Miranda J Newbery, Antonio Makiyama, Michael Sandmann, Daniel Lynch, Bruce T Volpe, and Neville Hogan. Rehabilitation robotics: pilot trial of a spatial extension for mit-manus. *Journal of neuroengineering and rehabilitation*, 1(1):1–15, 2004.

[292] Hermano Igo Krebs, Jerome Joseph Palazzolo, Laura Dipietro, Mark Ferraro, Jennifer Krol, Keren Rannekleiv, Bruce T Volpe, and Neville Hogan. Rehabilitation robotics: Performance-based progressive robot-assisted therapy. *Autonomous robots*, 15(1):7–20, 2003.

[293] Neville Hogan, Hermano Igo Krebs, Jain Charnnarong, Padmanabhan Srikrishna, and Andre Sharon. Mit-manus: a workstation for manual therapy and training. i. In *[1992] Proceedings IEEE International Workshop on Robot and Human Communication*, pages 161–165. IEEE, 1992.

[294] Tobias Nef, Marco Guidali, Verena Klamroth-Marganska, and Robert Riener. Armin-exoskeleton robot for stroke rehabilitation. In *World Congress on Medical Physics and Biomedical Engineering, September 7-12, 2009, Munich, Germany*, pages 127–130. Springer, 2009.

[295] Kyle D Fitle, Ali Utku Pehlivan, and Marcia K O'Malley. A robotic exoskeleton for rehabilitation and assessment of the upper limb following incomplete spinal cord injury. In *2015 IEEE International Conference on Robotics and Automation (ICRA)*, pages 4960–4966. IEEE, 2015.

[296] Grace J Kim, Michael Taub, Carly Creelman, Christine Cahalan, Michael W O'Dell, and Joel Stein. Feasibility of an electromyography-triggered hand robot for people after chronic stroke. *The American Journal of Occupational Therapy*, 73(4):7304345040p1–7304345040p9, 2019.

[297] Sivakumar Balasubramanian and Jiping He. Adaptive control of a wearable exoskeleton for upper-extremity neurorehabilitation. *Applied Bionics and Biomechanics*, 9(1): 99–115, 2012.

[298] XL Hu, KY Tong, XJ Wei, W Rong, EA Susanto, and SK Ho. The effects of post-stroke upper-limb training with an electromyography (emg)-driven hand robot. *Journal of Electromyography and Kinesiology*, 23(5):1065–1074, 2013.

[299] NSK Ho, KY Tong, XL Hu, KL Fung, XJ Wei, W Rong, and EA Susanto. An emg-driven exoskeleton hand robotic training device on chronic stroke subjects: task training system for stroke rehabilitation. In *2011 IEEE international conference on rehabilitation robotics*, pages 1–5. IEEE, 2011.

[300] Angelo Basteris, Sharon M Nijenhuis, Arno HA Stienen, Jaap H Buurke, Gerdienke B Prange, and Farshid Amirabdollahian. Training modalities in robot-mediated upper limb rehabilitation in stroke: a framework for classification based on a systematic review. *Journal of neuroengineering and rehabilitation*, 11(1):1–15, 2014.

[301] Albert C Lo, Peter D Guarino, Lorie G Richards, Jodie K Haselkorn, George F Wittenberg, Daniel G Federman, Robert J Ringer, Todd H Wagner, Hermano I Krebs, Bruce T Volpe, et al. Robot-assisted therapy for long-term upper-limb impairment after stroke. *New England Journal of Medicine*, 362(19):1772–1783, 2010.

[302] Leonard E Kahn, Peter S Lum, W Zev Rymer, and David J Reinkensmeyer. Robot-assisted movement training for the stroke-impaired arm: Does it matter what the robot does? *Journal of rehabilitation research and development*, 43(5):619–630, 2014.

[303] Hermano I Krebs, Bruce T Volpe, Mark Ferraro, S Fasoli, J Palazzolo, B Rohrer, L Edelstein, and N Hogan. Robot-aided neurorehabilitation: from evidence-based to science-based rehabilitation. *Topics in stroke rehabilitation*, 8(4):54–70, 2002.

[304] Andrea d'Avella, Philippe Saltiel, and Emilio Bizzi. Combinations of muscle synergies in the construction of a natural motor behavior. *Nature neuroscience*, 6(3):300–308, 2003.

[305] Gelsy Torres-Oviedo, Jane M Macpherson, and Lena H Ting. Muscle synergy organization is robust across a variety of postural perturbations. *Journal of neurophysiology*, 96(3):1530–1546, 2006.

[306] Lena H Ting and Jane M Macpherson. A limited set of muscle synergies for force control during a postural task. *Journal of neurophysiology*, 93(1):609–613, 2005.

[307] Simon A Overduin, Andrea d'Avella, Jinsook Roh, Jose M Carmena, and Emilio Bizzi. Representation of muscle synergies in the primate brain. *Journal of Neuroscience*, 35 (37):12615–12624, 2015.

[308] Philippe Saltiel, Kuno Wyler-Duda, Andrea D'Avella, Matthew C Tresch, and Emilio Bizzi. Muscle synergies encoded within the spinal cord: evidence from focal intraspinal nmda iontophoresis in the frog. *Journal of neurophysiology*, 85(2):605–619, 2001.

[309] Simon A Overduin, Andrea d'Avella, Jinsook Roh, and Emilio Bizzi. Modulation of muscle synergy recruitment in primate grasping. *Journal of Neuroscience*, 28(4): 880–892, 2008.

[310] Ron Jacobs and Jane M Macpherson. Two functional muscle groupings during postural equilibrium tasks in standing cats. *Journal of neurophysiology*, 76(4):2402–2411, 1996.

[311] Matthew C Tresch, Philippe Saltiel, and Emilio Bizzi. The construction of movement by the spinal cord. *Nature neuroscience*, 2(2):162–167, 1999.

[312] Alessandro Santuz, Antonis Ekizos, Lars Janshen, Vasilios Baltzopoulos, and Adamantios Arampatzis. On the methodological implications of extracting muscle synergies from human locomotion. *International journal of neural systems*, 27(05):1750007, 2017.

[313] Stacie A Chvatal and Lena H Ting. Common muscle synergies for balance and walking. *Frontiers in computational neuroscience*, 7:48, 2013.

[314] Filipe O Barroso, Diego Torricelli, Juan C Moreno, Julian Taylor, Julio Gomez-Soriano, Elisabeth Bravo-Esteban, Stefano Piazza, Cristina Santos, and José L Pons. Shared muscle synergies in human walking and cycling. *Journal of neurophysiology*, 112(8):1984–1998, 2014.

[315] Filipe Barroso, Diego Torricelli, Juan C Moreno, Julian Taylor, Julio Gómez-Soriano, Elizabeth B Esteban, Cristina Santos, and José L Pons. Similarity of muscle synergies in human walking and cycling: preliminary results. In *2013 35th Annual International Conference of the IEEE Engineering in Medicine and Biology Society (EMBC)*, pages 6933–6936. IEEE, 2013.

[316] James M Wakeling and Tamara Horn. Neuromechanics of muscle synergies during cycling. *Journal of neurophysiology*, 101(2):843–854, 2009.

[317] Vijaya Krishnamoorthy, Mark L Latash, John P Scholz, and Vladimir M Zatsiorsky. Muscle synergies during shifts of the center of pressure by standing persons. *Experimental brain research*, 152(3):281–292, 2003.

[318] Gelsy Torres-Oviedo and Lena H Ting. Muscle synergies characterizing human postural responses. *Journal of neurophysiology*, 98(4):2144–2156, 2007.

[319] Gelsy Torres-Oviedo and Lena H Ting. Subject-specific muscle synergies in human balance control are consistent across different biomechanical contexts. *Journal of neurophysiology*, 103(6):3084–3098, 2010.

[320] Silvia Muceli, Andreas Trøllund Boye, Andrea d'Avella, and Dario Farina. Identifying representative synergy matrices for describing muscular activation patterns during multidirectional reaching in the horizontal plane. *Journal of neurophysiology*, 103(3): 1532–1542, 2010.

[321] Andrea d'Avella and Francesco Lacquaniti. Control of reaching movements by muscle synergy combinations. *Frontiers in computational neuroscience*, 7:42, 2013.

[322] Jason J Kutch and Francisco J Valero-Cuevas. Challenges and new approaches to proving the existence of muscle synergies of neural origin. *PLoS computational biology*, 8(5):e1002434, 2012.

[323] Emanuel Todorov and Zoubin Ghahramani. Analysis of the synergies underlying complex hand manipulation. In *The 26th Annual International Conference of the IEEE Engineering in Medicine and Biology Society*, volume 2, pages 4637–4640. IEEE, 2004.

[324] Matthew C Tresch and Anthony Jarc. The case for and against muscle synergies. *Current opinion in neurobiology*, 19(6):601–607, 2009.

[325] Matthew P Rearick, Amparo Casares, and Marco Santello. Task-dependent modulation of multi-digit force coordination patterns. *Journal of neurophysiology*, 89(3):1317–1326, 2003.

[326] Laura Dipietro, Hermano I Krebs, Susan E Fasoli, Bruce T Volpe, Joel Stein, C Bever, and Neville Hogan. Changing motor synergies in chronic stroke. *Journal of neurophysiology*, 98(2):757–768, 2007.

[327] Vincent CK Cheung, Andrea Turolla, Michela Agostini, Stefano Silvoni, Caoimhe Bennis, Patrick Kasi, Sabrina Paganoni, Paolo Bonato, and Emilio Bizzi. Muscle synergy patterns as physiological markers of motor cortical damage. *Proceedings of the National Academy of Sciences*, 109(36):14652–14656, 2012.

[328] Francesca Lunardini, Claudia Casellato, Andrea d'Avella, Terence D Sanger, and Alessandra Pedrocchi. Robustness and reliability of synergy-based myocontrol of a multiple degree of freedom robotic arm. *IEEE Transactions on Neural Systems and Rehabilitation Engineering*, 24(9):940–950, 2015.

[329] Luis Pelaez Murciego, Michele Barsotti, and Antonio Frisoli. Synergy-based multifingers forces reconstruction and discrimination from forearm emg. In *International Conference on Human Haptic Sensing and Touch Enabled Computer Applications*, pages 204–213. Springer, 2018.

[330] Francesca Lunardini, Alberto Antonietti, Claudia Casellato, and Alessandra Pedrocchi. Synergy-based myocontrol of a multiple degree-of-freedom humanoid robot for functional tasks. In *2019 41st Annual International Conference of the IEEE Engineering in Medicine and Biology Society (EMBC)*, pages 5108–5112. IEEE, 2019.

[331] Katherine M Steele, Adam Rozumalski, and Michael H Schwartz. Muscle synergies and complexity of neuromuscular control during gait in cerebral palsy. *Developmental Medicine & Child Neurology*, 57(12):1176–1182, 2015.

[332] Si Li, Cheng Zhuang, Chuanxin M Niu, Yong Bao, Qing Xie, and Ning Lan. Evaluation of functional correlation of task-specific muscle synergies with motor performance in patients poststroke. *Frontiers in neurology*, 8:337, 2017.

[333] Filipe O Barroso, Diego Torricelli, Elisabeth Bravo-Esteban, Julian Taylor, Julio Gómez-Soriano, Cristina Santos, Juan C Moreno, and José L Pons. Muscle synergies in cycling after incomplete spinal cord injury: correlation with clinical measures of motor function and spasticity. *Frontiers in human neuroscience*, 9:706, 2016.

[334] Bastien Berret, François Bonnetblanc, Charalambos Papaxanthis, and Thierry Pozzo. Modular control of pointing beyond arm's length. *Journal of Neuroscience*, 29(1): 191–205, 2009.

[335] TR Kaminski. The coupling between upper and lower extremity synergies during whole body reaching. *Gait & Posture*, 26(2):256–262, 2007.

[336] Enrico Chiovetto and Martin A Giese. Kinematics of the coordination of pointing during locomotion. *PloS one*, 8(11):e79555, 2013.

[337] James S Thomas, Daniel M Corcos, and Ziaul Hasan. Kinematic and kinetic constraints on arm, trunk, and leg segments in target-reaching movements. *Journal of neurophysiology*, 2005.

[338] Yuri P Ivanenko, Germana Cappellini, Nadia Dominici, Richard E Poppele, and Francesco Lacquaniti. Coordination of locomotion with voluntary movements in humans. *Journal of Neuroscience*, 25(31):7238–7253, 2005.

[339] Andrea d'Avella and MMCM Tresch. Modularity in the motor system: decomposition of muscle patterns as combinations of time-varying synergies. *Advances in neural information processing systems*, 14, 2001.

[340] Mohammad Fazle Rabbi, Claudio Pizzolato, David G Lloyd, Chris P Carty, Daniel Devaprakash, and Laura E Diamond. Non-negative matrix factorisation is the most appropriate method for extraction of muscle synergies in walking and running. *Scientific reports*, 10(1):1–11, 2020.

[341] Navid Lambert-Shirzad and HF Machiel Van der Loos. On identifying kinematic and muscle synergies: a comparison of matrix factorization methods using experimental data from the healthy population. *Journal of neurophysiology*, 117(1):290–302, 2017.

[342] Mamta Tiwari. Ayurvedic pathophysiology of parkinson's disease (kampvata). *European Journal of Biomedical and Pharmaceutical Sciences*, 2:1108–18, 2015.

[343] Heiko Braak and Eva Braak. Pathoanatomy of parkinson's disease. *Journal of neurology*, 247(2):II3–II10, 2000.

[344] D Hirtz, David J Thurman, Katrina Gwinn-Hardy, M Mohamed, AR Chaudhuri, and R Zalutsky. How common are the "common" neurologic disorders? *Neurology*, 68(5): 326–337, 2007.

[345] Shaking Palsy. James parkinson's essay on the shaking palsy. *JR Coll Physicians Edinb*, 45:84–6, 2015.

[346] John D Gazewood, D Roxanne Richards, and Karl T Clebak. Parkinson disease: an update. *American family physician*, 87(4):267–273, 2013.

[347] Alfredo Berardelli, John C Rothwell, Philip D Thompson, and Mark Hallett. Pathophysiology of bradykinesia in parkinson's disease. *Brain*, 124(11):2131–2146, 2001.

[348] Francois JG Vingerhoets, Michael Schulzer, Donald B Calne, and Barry J Snow. Which clinical sign of parkinson's disease best reflects the nigrostriatal lesion? *Annals of Neurology: Official Journal of the American Neurological Association and the Child Neurology Society*, 41(1):58–64, 1997.

[349] Robert S Turner, Scott T Grafton, Anthony R McIntosh, Mahlon R DeLong, and John M Hoffman. The functional anatomy of parkinsonian bradykinesia. *Neuroimage*, 19(1):163–179, 2003.

[350] Linda Resnik, Susan Allen, Deborah Isenstadt, Melanie Wasserman, and Lisa Iezzoni. Perspectives on use of mobility aids in a diverse population of seniors: Implications for intervention. *Disability and health journal*, 2(2):77–85, 2009.

[351] Georg Ebersbach, Daniela Edler, Olaf Kaufhold, and Joerg Wissel. Whole body vibration versus conventional physiotherapy to improve balance and gait in parkinson's disease. *Archives of physical medicine and rehabilitation*, 89(3):399–403, 2008.

[352] Gerald C McIntosh, Susan H Brown, Ruth R Rice, and Michael H Thaut. Rhythmic auditory-motor facilitation of gait patterns in patients with parkinson's disease. *Journal of Neurology, Neurosurgery & Psychiatry*, 62(1):22–26, 1997.

[353] Lilian TB Gobbi, Maria DT Oliveira-Ferreira, M Joana D Caetano, Ellen Lirani-Silva, Fabio A Barbieri, Florindo Stella, and Sebastião Gobbi. Exercise programs improve mobility and balance in people with parkinson's disease. *Parkinsonism & related disorders*, 15:S49–S52, 2009.

[354] Maria H Nilsson, Gun-Marie Hariz, Susanne Iwarsson, and Peter Hagell. Walking ability is a major contributor to fear of falling in people with parkinson's disease: implications for rehabilitation. *Parkinson's disease*, 2012, 2012.

[355] Morris Suteerawattananon, GS Morris, BR Etnyre, J Jankovic, and EJ Protas. Effects of visual and auditory cues on gait in individuals with parkinson's disease. *Journal of the neurological sciences*, 219(1-2):63–69, 2004.

[356] Mariese A Hely, John GL Morris, Wayne GJ Reid, and Robert Trafficante. Sydney multicenter study of parkinson's disease: Non-l-dopa–responsive problems dominate at 15 years. *Movement disorders*, 20(2):190–199, 2005.

[357] Arthur Leslie Peck, Edward Seymour Forster, et al. Parts of animals; movement of animals; progression of animals/de partibus animalium. Technical report, Harvard University Press;, 1937.

[358] Richard Baker. The history of gait analysis before the advent of modern computers. *Gait & posture*, 26(3):331–342, 2007.

[359] Valerie Fleming, Debbie Tolson, and Elgin Schartau. Changing perceptions of womanhood: living with parkinson's disease. *International journal of nursing studies*, 41(5): 515–524, 2004.

[360] Beth E Fisher, Allan D Wu, George J Salem, Jooeun Song, Chien-Ho Janice Lin, Jeanine Yip, Steven Cen, James Gordon, Michael Jakowec, and Giselle Petzinger. The effect of exercise training in improving motor performance and corticomotor excitability in people with early parkinson's disease. *Archives of physical medicine and rehabilitation*, 89(7):1221–1229, 2008.

[361] Rosdinom Razali, Fazli Ahmad, Fairuz Nazri Abd Rahman, Marhani Midin, and Hatta Sidi. Burden of care among caregivers of patients with parkinson disease: a cross-sectional study. *Clinical Neurology and Neurosurgery*, 113(8):639–643, 2011.

[362] C LAWRENCE. Mechanics of the human walking apparatus-weber, w, weber, e, 1994.

[363] Diana Jones, Lynn Rochester, Angela Birleson, Victoria Hetherington, Alice Nieuwboer, A-M Willems, Erwin Van Wegen, and Gert Kwakkel. Everyday walking with parkinson's disease: understanding personal challenges and strategies. *Disability and rehabilitation*, 30(16):1213–1221, 2008.

[364] Michael W Whittle. *Gait analysis: an introduction*. Butterworth-Heinemann, 2014.

[365] Chiraz BenAbdelkader, Ross Cutler, and Larry Davis. Stride and cadence as a biometric in automatic person identification and verification. In *Proceedings of Fifth IEEE international conference on automatic face gesture recognition*, pages 372–377. IEEE, 2002.

[366] Gergely Darnai, Tibor Szolcsányi, Gábor Hegedüs, Péter Kincses, János Kállai, Márton Kovács, Eszter Simon, Zsófia Nagy, and József Janszky. Hearing visuo-tactile synchrony–sound-induced proprioceptive drift in the invisible hand illusion. *British Journal of Psychology*, 108(1):91–106, 2017.

[367] Tatiana Witjas, E Kaphan, JP Azulay, O Blin, M Ceccaldi, J Pouget, M Poncet, and A Ali Chérif. Nonmotor fluctuations in parkinson's disease: frequent and disabling. *Neurology*, 59(3):408–413, 2002.

[368] Lynn Rochester, Victoria Hetherington, Diana Jones, Alice Nieuwboer, Anne-Marie Willems, Gert Kwakkel, and Erwin Van Wegen. The effect of external rhythmic cues (auditory and visual) on walking during a functional task in homes of people with parkinson's disease. *Archives of physical medicine and rehabilitation*, 86(5):999–1006, 2005.

[369] Alice Nieuwboer, Gert Kwakkel, Lynn Rochester, Diana Jones, Erwin van Wegen, Anne Marie Willems, Fabienne Chavret, Victoria Hetherington, Katherine Baker, and Inge Lim. Cueing training in the home improves gait-related mobility in parkinson's disease: the rescue trial. *Journal of Neurology, Neurosurgery & Psychiatry*, 78(2): 134–140, 2007.

[370] Terry Ellis, Cees J De Goede, Robert G Feldman, Erik C Wolters, Gert Kwakkel, and Robert C Wagenaar. Efficacy of a physical therapy program in patients with parkinson's disease: a randomized controlled trial. *Archives of physical medicine and rehabilitation*, 86(4):626–632, 2005.

[371] Domenico Buongiorno, Giacomo Donato Cascarano, Antonio Brunetti, Irio De Feudis, and Vitoantonio Bevilacqua. A Survey on Deep Learning in Electromyographic Signal Analysis. In *Lecture Notes in Computer Science (including subseries Lecture Notes in Artificial Intelligence and Lecture Notes in Bioinformatics)*, volume 11645 LNAI, pages 751–761. Springer, Cham, CH, 2019. ISBN 9783030267650. doi: 10.1007/978-3-030-26766-7_68. URL http://link.springer.com/10.1007/978-3-030-26766-7{_}68.

[372] Domenico Buongiorno, Giacomo Donato Cascarano, Irio De Feudis, Antonio Brunetti, Leonarda Carnimeo, Giovanni Dimauro, and Vitoantonio Bevilacqua. Deep learning for processing electromyographic signals: A taxonomy-based survey. *Neurocomputing*, 2020. ISSN 0925-2312. doi: 10.1016/j.neucom.2020.06.139. URL http://www.sciencedirect.com/science/article/pii/S0925231220319020.

[373] D. Buongiorno, C. Camardella, G. D. Cascarano, L. Pelaez Murciego, M. Barsotti, I. De Feudis, A. Frisoli, and V. Bevilacqua. An undercomplete autoencoder to extract muscle synergies for motor intention detection. In *2019 International Joint Conference on Neural Networks (IJCNN)*, pages 1–8, July 2019. doi: 10.1109/IJCNN.2019.8851975.

[374] Domenico Buongiorno, Giacomo Donato Cascarano, Cristian Camardella, Irio De Feudis, Antonio Frisoli, and Vitoantonio Bevilacqua. Task-oriented muscle synergy extraction using an autoencoder-based neural model. *Information*, 11(4):219, 2020. doi: 10.3390/info11040219.

[375] Antonio Frisoli, Fabrizio Rocchi, Simone Marcheschi, Andrea Dettori, Fabio Salsedo, and Massimo Bergamasco. A new force-feedback arm exoskeleton for haptic interaction

in virtual environments. In *First Joint Eurohaptics Conference and Symposium on Haptic Interfaces for Virtual Environment and Teleoperator Systems. World Haptics Conference*, pages 195–201. IEEE, 2005.

[376] Denise J. Berger and Andrea d'Avella. Effective force control by muscle synergies. *Frontiers in Computational Neuroscience*, 8:46, 2014. ISSN 1662-5188. doi: 10.3389/fncom.2014.00046. URL https://www.frontiersin.org/article/10.3389/fncom.2014.00046.

[377] Domenico Buongiorno, Francesco Barone, Denise J. Berger, Benedetta Cesqui, Vitoantonio Bevilacqua, Andrea d'Avella, and Antonio Frisoli. Evaluation of a pose-shared synergy-based isometric model for hand force estimation: Towards myocontrol. In Jaime Ibáñez, José González-Vargas, José María Azorín, Metin Akay, and José Luis Pons, editors, *Converging Clinical and Engineering Research on Neurorehabilitation II*, pages 953–958, Cham, 2017. Springer International Publishing. ISBN 978-3-319-46669-9. doi: 10.1007/978-3-319-46669-9_154.

[378] Ian Goodfellow, Yoshua Bengio, and Aaron Courville. *Deep learning*. MIT press, 2016.

[379] Andrea d'Avella, Alessandro Portone, Laure Fernandez, and Francesco Lacquaniti. Control of fast-reaching movements by muscle synergy combinations. *Journal of Neuroscience*, 26(30):7791–7810, 2006. ISSN 0270-6474. doi: 10.1523/JNEUROSCI.0830-06.2006. URL http://www.jneurosci.org/content/26/30/7791.

[380] Cristiano Alessandro, Ioannis Delis, Francesco Nori, Stefano Panzeri, and Bastien Berret. Muscle synergies in neuroscience and robotics: from input-space to task-space perspectives. *Frontiers in Computational Neuroscience*, 7:43, 2013. ISSN 1662-5188. doi: 10.3389/fncom.2013.00043. URL https://www.frontiersin.org/article/10.3389/fncom.2013.00043.

[381] Matthew C Tresch, Vincent CK Cheung, and Andrea d'Avella. Matrix factorization algorithms for the identification of muscle synergies: evaluation on simulated and experimental data sets. *Journal of neurophysiology*, 95(4):2199–2212, 2006.

[382] Stacie A Chvatal, Gelsy Torres-Oviedo, Seyed A Safavynia, and Lena H Ting. Common muscle synergies for control of center of mass and force in nonstepping and stepping postural behaviors. *Journal of neurophysiology*, 106(2):999–1015, 2011.

[383] Victor R Barradas, Jason J Kutch, Toshihiro Kawase, Yasuharu Koike, and Nicolas Schweighofer. When 90% of the variance is not enough: residual emg from muscle synergy extraction influences task performance. *BioRxiv*, page 634758, 2019.

[384] Ivan Vujaklija, Vahid Shalchyan, Ernest N. Kamavuako, Ning Jiang, Hamid R. Marateb, and Dario Farina. Online mapping of emg signals into kinematics by autoencoding. *Journal of NeuroEngineering and Rehabilitation*, 15(1):21, Mar 2018. ISSN 1743-0003. doi: 10.1186/s12984-018-0363-1. URL https://doi.org/10.1186/s12984-018-0363-1.

[385] Domenico Buongiorno, Michele Barsotti, Francesco Barone, Vitoantonio Bevilacqua, and Antonio Frisoli. A linear approach to optimize an emg-driven neuromusculoskeletal model for movement intention detection in myo-control: A case study on shoulder and elbow joints. *Frontiers in Neurorobotics*, 12:74, 2018. ISSN 1662-5218. doi: 10.3389/fnbot.2018.00074. URL https://www.frontiersin.org/article/10.3389/fnbot.2018.00074.

[386] National Collaborating Centre for Chronic Conditions et al. Parkinson's disease: diagnosis and management in primary and secondary care. *National Institute for Clinical Excellence. London, National Institute for Clinical Excellence*, 2006.

[387] Janice M Beitz et al. Parkinson's disease: a review. *Front Biosci (Schol Ed)*, 6(6): 65–74, 2014.

[388] Giovanni Dimauro, Vincenzo Di Nicola, Vitoantonio Bevilacqua, Danilo Caivano, and Francesco Girardi. Assessment of speech intelligibility in parkinson's disease using a speech-to-text system. *IEEE Access*, 5:22199–22208, 2017.

[389] Giacomo Donato Cascarano, Claudio Loconsole, Antonio Brunetti, Antonio Lattarulo, Domenico Buongiorno, Giacomo Losavio, Eugenio Di Sciascio, and Vitoantonio Bevilacqua. Biometric handwriting analysis to support parkinson's disease assessment and grading. *BMC Medical Informatics and Decision Making*, 19(9):1–11, 2019.

[390] Ilaria Bortone, Marco Giuseppe Quercia, Nicola Ieva, Giacomo Donato Cascarano, Gianpaolo Francesco Trotta, Sabina Ilaria Tatò, and Vitoantonio Bevilacqua. Recognition and severity rating of parkinson's disease from postural and kinematic features during gait analysis with microsoft kinect. In *International Conference on Intelligent Computing*, pages 613–618. Springer, 2018.

[391] J Gómez-González, P Martín-Casas, and R Cano-de-la Cuerda. Effects of auditory cues on gait initiation and turning in patients with parkinson's disease. *Neurología (English Edition)*, 34(6):396–407, 2019.

[392] Shashank Ghai, Ishan Ghai, Gerd Schmitz, and Alfred O Effenberg. Effect of rhythmic auditory cueing on parkinsonian gait: a systematic review and meta-analysis. *Scientific reports*, 8(1):1–19, 2018.

[393] Roberta Marchese, Manuela Diverio, Francesca Zucchi, Carmelo Lentino, and Giovanni Abbruzzese. The role of sensory cues in the rehabilitation of parkinsonian patients: a comparison of two physical therapy protocols. *Movement Disorders*, 15(5):879–883, 2000.

[394] Jorge Cancela, Eugenio M Moreno, Maria T Arredondo, and Paolo Bonato. Designing auditory cues for parkinson's disease gait rehabilitation. In *2014 36th Annual International Conference of the IEEE Engineering in Medicine and Biology Society*, pages 5852–5855. IEEE, 2014.

My Publications

[1] Sara Invitto, Giulia Piraino, Arianna Mignozzi, Simona Capone, Giovanni Montagna, Pietro Aleardo Siciliano, Andrea Mazzatenta, Gianbattista Rocco, Irio De Feudis, Gianpaolo F Trotta, et al. Smell and meaning: an oerp study. In *Multidisciplinary Approaches to Neural Computing*, pages 289–300. Springer, 2018.

[2] Ilaria Bortone, Gianpaolo Francesco Trotta, Giacomo Donato Cascarano, Paola Regina, Antonio Brunetti, Irio De Feudis, Domenico Buongiorno, Claudio Loconsole, and Vitoantonio Bevilacqua. A supervised approach to classify the status of bone mineral density in post-menopausal women through static and dynamic baropodometry. In *2018 International Joint Conference on Neural Networks (IJCNN)*, pages 1–7. IEEE, 2018.

[3] Claudio Loconsole, Giacomo Donato Cascarano, Antonio Lattarulo, Antonio Brunetti, Gianpaolo Francesco Trotta, Domenico Buongiorno, Ilaria Bortone, Irio De Feudis, Giacomo Losavio, Vitoantonio Bevilacqua, et al. A comparison between ann and svm classifiers for parkinson's disease by using a model-free computer-assisted handwriting analysis based on biometric signals. In *2018 International Joint Conference on Neural Networks (IJCNN)*, pages 1–8. IEEE, 2018.

[4] Vitoantonio Bevilacqua, Gianpaolo Francesco Trotta, Claudio Loconsole, Antonio Brunetti, Nicholas Caporusso, Giuseppe Maria Bellantuono, Irio De Feudis, Donato Patruno, Domenico De Marco, Andrea Venneri, et al. A rgb-d sensor based tool for assessment and rating of movement disorders. In *International Conference on Applied Human Factors and Ergonomics*, pages 110–118. Springer, 2017.

[5] Sara Invitto, Antonio Calcagnì, Arianna Mignozzi, Rosanna Scardino, Giulia Piraino, Daniele Turchi, Irio De Feudis, Antonio Brunetti, Vitoantonio Bevilacqua, and Marina de Tommaso. Face recognition, musical appraisal, and emotional crossmodal bias. *Frontiers in behavioral neuroscience*, 11:144, 2017.

[6] Sara Invitto, Arianna Mignozzi, Giulia Piraino, Gianbattista Rocco, Irio De Feudis, Antonio Brunetti, and Vitoantonio Bevilacqua. Artificial neural network analysis and erp in intimate partner violence. In *Multidisciplinary Approaches to Neural Computing*, pages 247–257. Springer, 2018.

[7] Domenico Buongiorno, Cristian Camardella, Giacomo Donato Cascarano, Luis Pelaez Murciego, Michele Barsotti, Irio De Feudis, Antonio Frisoli, and Vitoantonio Bevilacqua. An undercomplete autoencoder to extract muscle synergies for motor intention detection. In *2019 International Joint Conference on Neural Networks (IJCNN)*, pages 1–8. IEEE, 2019.

[8] Antonio Brunetti, Giacomo Donato Cascarano, Irio De Feudis, Marco Moschetta, Loreto Gesualdo, and Vitoantonio Bevilacqua. Detection and segmentation of kidneys from magnetic resonance images in patients with autosomal dominant polycystic kidney disease. In *International Conference on Intelligent Computing*, pages 639–650. Springer, 2019.

[9] Giacomo Donato Cascarano, Francesco Saverio Debitonto, Ruggero Lemma, Antonio Brunetti, Domenico Buongiorno, Irio De Feudis, Andrea Guerriero, Michele Rossini, Francesco Pesce, Loreto Gesualdo, et al. An innovative neural network framework for glomerulus classification based on morphological and texture features evaluated in histological images of kidney biopsy. In *International Conference on Intelligent Computing*, pages 727–738. Springer, 2019.

[10] Domenico Buongiorno, Giacomo Donato Cascarano, Antonio Brunetti, Irio De Feudis, and Vitoantonio Bevilacqua. A survey on deep learning in electromyographic signal analysis. In *International Conference on Intelligent Computing*, pages 751–761. Springer, 2019.

[11] Domenico Buongiorno, Giacomo Donato Cascarano, Cristian Camardella, Irio De Feudis, Antonio Frisoli, and Vitoantonio Bevilacqua. Task-oriented muscle synergy extraction using an autoencoder-based neural model. *Information*, 11(4):219, 2020.

[12] Irio De Feudis, Domenico Buongiorno, Giacomo Donato Cascarano, Antonio Brunetti, Donato Micele, and Vitoantonio Bevilacqua. A nonlinear autoencoder for kinematic synergy extraction from movement data acquired with htc vive trackers. In *Progresses in Artificial Intelligence and Neural Systems*, pages 231–241. Springer, Singapore, 2021.

[13] Giacomo Losavio, Bernadette Tamma, Angelo Abbattista, Ilaria Sabina Tatò, Domenico Buongiorno, Giacomo Donato Cascarano, Antonio Brunetti, Irio De Feudis, and Vitoantonio Bevilacqua. On the analysis of the relationship between alkaline water usage and muscle fatigue recovery. In *International Conference on Applied Human Factors and Ergonomics*, pages 26–31. Springer, 2020.

[14] Nicola Altini, Giacomo Donato Cascarano, Antonio Brunetti, Irio De Feudis, Domenico Buongiorno, Michele Rossini, Francesco Pesce, Loreto Gesualdo, and Vitoantonio Bevilacqua. A deep learning instance segmentation approach for global glomerulosclerosis assessment in donor kidney biopsies. *Electronics*, 9(11):1768, 2020.

[15] Domenico Buongiorno, Giacomo Donato Cascarano, Irio De Feudis, Antonio Brunetti, Leonarda Carnimeo, Giovanni Dimauro, and Vitoantonio Bevilacqua. Deep learning for processing electromyographic signals: A taxonomy-based survey. *Neurocomputing*, 452:549–565, 2021.

[16] Giacomo Donato Cascarano, Francesco Saverio Debitonto, Ruggero Lemma, Antonio Brunetti, Domenico Buongiorno, Irio De Feudis, Andrea Guerriero, Umberto Venere, Silvia Matino, Maria Teresa Rocchetti, et al. A neural network for glomerulus classification based on histological images of kidney biopsy. *BMC medical informatics and decision making*, 21(1):1–14, 2021.

[17] Irio De Feudis, Domenico Buongiorno, Stefano Grossi, Gianluca Losito, Antonio Brunetti, Nicola Longo, Giovanni Di Stefano, and Vitoantonio Bevilacqua. Evaluation of vision-based hand tool tracking methods for quality assessment and training in human-centered industry 4.0. *Applied Sciences*, 12(4):1796, 2022.